N64-22425

CODE-1 CAT. 16

NASA CR-56470

VIDYA REPORT NO. 119
December 30, 1963

AUSCULTATORY VERSUS DIRECT PRESSURE MEASUREMENTS FOR NEWTONIAN FLUIDS AND FOR BLOOD IN SIMULATED ARTERIES

by
A. H. Sacks
K. R. Raman
J. A. Burnell
E. G. Tickner

prepared for
NATIONAL AERONAUTICS AND SPACE ADMINISTRATION
AMES RESEARCH CENTER

Contract No. NAS2-1137
Vidya Project No. 9162

OTS PRICE

XEROX $ 9.60 ph

MICROFILM $ none

VIDYA

RESEARCH DEVELOPMENT

1450 PAGE MILL ROAD, PALO ALTO, CALIFORNIA

7759

A DIVISION OF Itek CORPORATION

व VIDYA

The word Vidya, taken from the Vedanta philosophy of the Hindus, means knowledge. The symbol used to denote the Vidya organization is the letter "V" from Sanskrit, the ancient language of India.

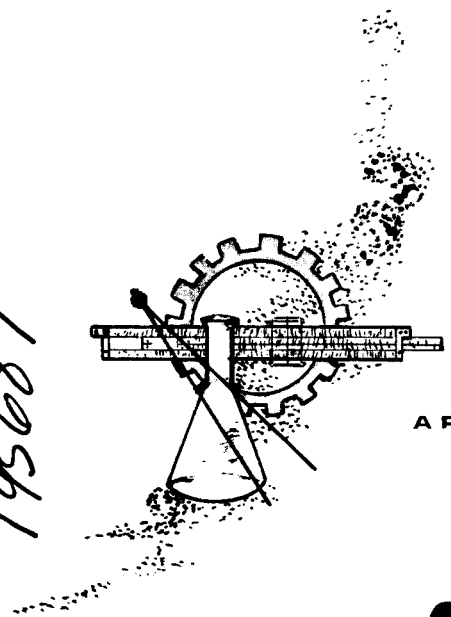

APPLIED MECHANICS . . . . PHYSICS . . . . ANALYSES

195687

CASE FILE COPY

VIDYA COPY NO. 10

VIDYA REPORT NO. 119

December 30, 1963

AUSCULATORY VERSUS DIRECT PRESSURE MEASUREMENTS FOR NEWTONIAN FLUIDS AND FOR BLOOD IN SIMULATED ARTERIES

by

A. H. Sacks
K. R. Raman
J. A. Burnell
E. G. Tickner

prepared for
NATIONAL AERONAUTICS AND SPACE ADMINISTRATION
AMES RESEARCH CENTER

Contract No. NAS 2-1137

Vidya Project No. 9162

VIDYA

A DIVISION OF Itek CORPORATION

1450 PAGE MILL ROAD • PALO ALTO, CALIFORNIA
TEL: DAVENPORT 1-2455 TWX: 415 492-9270

~~2759~~

FOREWORD

The experiments described herein were carried out during the first year of a comprehensive 3-year program sponsored by the Ames Research Center of NASA. Under this program, an attempt is being made at a fundamental understanding of blood flow and blood pressure, including the effects of acceleration. In order to insure the validity and general usefulness of the present experiments, close coordination between the engineering and physiological aspects of the problem has been maintained through the consulting services of Dr. David L. Bruns, a specialist in cardiovascular medicine.

SUMMARY

Experiments have been performed in a large-scale simulated arterial flow system to investigate the relationship between auscultatory and direct measurements of arterial blood pressure under carefully controlled conditions. Efforts were made to simulate the living system as closely as possible, and comparisons were made over a wide range of pulse rate, pulse amplitude, and mean pressure level, using various mixtures of water and glycerol, and finally whole blood as the fluid. The simulated arteries were of gum rubber or latex tubing of 1-inch diameter, 10 feet long, with wall thicknesses of 1/16 and 1/8 inch. The oscillatory intra-arterial pressures were recorded by pressure transducers attached to internal pressure probes, and auscultatory readings were accomplished with a stethoscope and a specially designed pressure chamber.

The results indicate that both the auscultatory systolic and diastolic pressure readings as determined with a sphygmomanometer are generally higher than the corresponding maximum and minimum of the oscillatory intra-arterial pressures. The error in both readings appears to depend primarily on the elastic behavior of the vessel itself and is generally greater than the buckling pressure but less than the collapsing pressure for the arterial wall. Thus, either thickening or stiffening of the arterial wall increases the error in both auscultatory readings.

The process of occluding the artery for auscultation was generally found to amplify the oncoming pulse wave just proximal to (i.e., just ahead of) the pressure cuff and to alter completely the form of the pulse wave as it passes through the cuff during the production of Korotkoff sounds. In some cases, longitudinal rupture of the simulated artery occurred in the cuff area after repeated auscultations.

In studying the simulation of the blood fluid, it was found that whole blood behaves as a combination of a pseudoplastic and a Bingham fluid. That is, it has a nonlinear pressure-flow diagram, depending primarily upon the concentration of hematocytes, and requires an initial pressure to start the flow. The value of this initial stress, however, is extremely small and depends upon the concentration of fibrinogen present.

TABLE OF CONTENTS

	Page No.
FOREWORD	ii
SUMMARY	iii
LIST OF FIGURES	vii
LIST OF SYMBOLS	ix
1. INTRODUCTION	1
2. THE AUSCULTATORY TECHNIQUE	2
3. MATCHING THE HUMAN SYSTEM	5
3.1 Elastic Properties of Living Vessels	5
3.2 Viscous Behavior of Whole Blood	8
3.3 The Idealized Model	16
3.3.1 The arterial wall	16
3.3.2 The blood fluid	18
3.4 Dynamic Similarity	18
4. EXPERIMENTAL APPARATUS	19
4.1 General Description	19
4.2 Simulated Artery	20
4.3 Pressure Pulse Generator	22
4.4 Pressure Chamber	23
4.5 Bypass System	24
4.6 Reservoir	24
4.7 Circulation Pump	25
5. INSTRUMENTATION	26
5.1 Pressure Transducers	26
5.2 Pressure Probes	27
5.3 Timing Photocell	27
5.4 Ohmmeter Setup for Static Tube Calibration	28
5.5 Aneroid Manometer	29
5.6 Stethoscope	29
5.7 Viscometer, Thermometer, and Hydrometer	29
6. CALIBRATION OF TRANSDUCERS, PROBES, AND TUBES	29

	Page No.
6.1 Pressure Transducer Calibration	29
6.2 Calibration of Probes	30
6.3 Static Tube Calibration	31
7. TESTS WITH NEWTONIAN FLUIDS	31
7.1 Test Procedure	32
7.2 Data Reduction and Accuracy	34
7.3 Experimental Results and Discussion	36
8. TESTS WITH BEEF BLOOD	44
8.1 Modification of Apparatus and Preliminary Test Results	45
8.2 Preparation and Handling of Blood and Sterilization of Equipment	47
8.3 Test Procedure	49
8.4 Experimental Results and Discussion	50
9. CONCLUSIONS	52
REFERENCES	55
TABLE I.- SUMMARY OF VISCOSITY DATA	57
TABLE II.- SUMMARY OF EXPERIMENTAL DATA	58
FIGURES 1 THROUGH 31	
APPENDIX A.- USE OF A CAPILLARY VISCOMETER AS A MEANS FOR DETERMINING VISCOSITY CHARACTERISTICS OF A PSEUDOPLASTIC FLUID	

LIST OF FIGURES

1.- Static elastic behavior of an excised human femoral artery (from Ref. 6).

2.- Dynamic elastic behavior of various excised human arteries (from Ref. 7).

3.- Relative viscosity of suspensions of human erythrocytes in ACD solution.

4.- Flow characteristics of blood and its constituents.

5.- Flow characteristics of bovine blood.

6.- Pseudoplastic exponents for whole blood.

7.- Variation of the consistency index for three blood species.

8.- Variation of viscosity coefficient with shear rate for human, canine, and bovine blood.

9.- Schematic sketch of experimental apparatus.

10.- Apparatus for auscultatory and direct blood pressure measurements on simulated artery.

11.- Sketch of pressure pulse generator piston and diaphragm.

12.- Pressure pulse generator.

13.- Exploded view of pressure chamber.

14.- Pressure transducer assembly.

15.- Dimensions and locations of pressure probes in simulated artery.

16.- Calibration rig for pressure probes.

17.- Static elastic behavior of simulated arteries.

18.- Effect of artery occlusion on the amplitude of the pressure input by the pulse generator.

19.- Variation of pressure amplitude with frequency inside the simulated artery (newtonian fluids).

20.- Auscultatory versus direct pressure measurements for Newtonian fluids in 1/16-inch wall gum rubber tubing.

21.- Auscultatory versus direct pressure measurements for water in 1/8-inch wall gum rubber tubing.

22.- Auscultatory versus direct pressure measurements for Newtonian fluids in 1/16-inch wall latex tubing.

23.- Summary of auscultatory versus direct pressure measurements for Newtonian fluids in simulated arteries. (a) 1/16-inch wall gum rubber tubing.

(b) Continued. 1/8-inch wall gum rubber tubing.

(c) Concluded. 1/16-inch wall latex tubing.

24.- 1/16-inch wall gum rubber tube showing longitudinal rupture.

25.- Oscillograph record of static (lateral) pressure just distal to pressure chamber during decompression.

26.- Upstream end of 1-inch plastic tube showing blood inlet and balloon diaphragm.

27.- Sterilization chamber.

28.- Auscultatory versus direct pressure measurements for steer blood in 1/16-inch wall gum rubber tubing.

29.- Variation of pressure amplitude with frequency inside the simulated artery (steer blood).

30.- Microphotograph of steer blood red cells (taken after use in tests). Magnification: 728 X

31.- Variation of viscosity for blood in oscillatory flow.

LIST OF SYMBOLS

A	input pressure pulse amplitude (measured in the 4-inch pipe ahead of the bifurcation)
a	capillary tube radius
E	Young's modulus of elasticity for arterial wall
E'	visco-elastic modulus for arterial wall
E_{dyn}	$E^2 + (\omega E^1)^2$
h	arterial wall thickness
H	percent hematocytes (blood cells) by volume
K	pseudoplastic consistency index, $\tau/\dot{\gamma}^n$
L	length of capillary tube between pressure taps
n	pseudoplastic exponent defined by $\tau = K\dot{\gamma}^n$
p	oscillatory static or lateral pressure inside the unobstructed simulated artery
p_d	auscultatory diastolic pressure reading
p_s	auscultatory systolic pressure reading
PA	pressure amplitude, $\frac{p_{max} - p_{min}}{2}$
ΔP	pressure drop along capillary tube over length L
Q	rate of flow through capillary tube
R	radius of test artery
t	time
$\dot{\gamma}$	fluid shear (strain) rate or radial velocity gradient
μ	coefficient of viscosity for a Newtonian fluid
μ_a	apparent coefficient of viscosity for a non-Newtonian fluid, $\tau/\dot{\gamma}$
μ_p	plastic coefficient of viscosity for a Bingham plastic, $(\tau - \tau_y)/\dot{\gamma}$

μ_{rel}	ratio of viscosity of suspension to viscosity of suspending fluid
ν	kinematic viscosity for a Newtonian fluid, μ/ρ
ν_w	value of ν for water
ρ	fluid mass density
σ	Poisson's ratio for arterial wall
τ	fluid shear stress
τ_w	shear stress at the wall
τ_y	initial or yield value of shear stress for a Bingham plastic
ϕ	phase difference between pressure change and radius change
ω	pulse rate or frequency of oscillation

Subscripts

max	maximum value over a cycle
min	minimum value over a cycle
o	undisturbed or mean value over a cycle (artery open)
c	value with chamber pressurized (artery closed)

AUSCULTATORY VERSUS DIRECT PRESSURE MEASUREMENTS FOR NEWTONIAN FLUIDS AND FOR BLOOD IN SIMULATED ARTERIES

1. INTRODUCTION

The use of the sphygmomanometer in determining the blood pressure of human subjects dates back to 1896 and is still the subject of considerable discussion as to proper technique and interpretation. Since the discovery by Korotkoff, in 1905, that more consistent readings could be taken by using the stethoscope in conjunction with the sphygmomanometer and listening to the sounds produced in the brachial artery during cuff decompression, the technique now known as the "auscultatory" technique has become common in medical practice. However, the exact cause of the Korotkoff sounds is to this day not fully understood, and the precise meaning of the systolic and diastolic blood pressure readings obtained by the auscultatory technique is still not clear insofar as what the readings tell the observer about the actual oscillatory pressure and flow within the vessel itself. It is at this latter question that the present experimental investigation is aimed.

In order to clarify the relationship between the systolic and diastolic pressure readings and the oscillatory pressures within the vessel which are clearly defined in fluid mechanics, one must be able to perform controlled experiments in which the pertinent parameters can be varied one at a time in a prescribed manner and can be accurately measured. The present experimental investigation was undertaken to fulfill this requirement and thereby furnish a direct comparison of auscultatory and direct blood pressures over a wide range of controlled conditions. Because of the intricate interrelationships of many of the parameters in the living system, and because of the resulting difficulty of varying the individual parameters, a simulated system was selected for the present study.

Inasmuch as we are concerned here only with a precise interpretation of the systolic and diastolic pressure readings in a fluid flow system, no attempt was made to simulate such factors as heart-valve function, muscle tissue, bone, vasoconstriction, etc. Rather, an intensive effort has been made to produce a known and controllable pulsating flow in a flexible tube of known properties. With such a system, sphygmomanometer readings can be related to known quantities which can be varied systematically over the desired ranges. Such data should greatly enhance the possibilities of data correlation and of a mathematical analysis of the physical phenomena involved. This is indeed the ultimate aim of the present study, and such a mathematical analysis will be undertaken in a later phase of the program, since only when this is accomplished can we fully understand blood pressure measurements made by the various techniques. The present tests are intended to provide an experimental comparison between auscultatory and direct pressure measurements, and have been carried out both with a Newtonian fluid (water and glycerol) and with fresh, whole steer blood.

2. THE AUSCULTATORY TECHNIQUE

In determining the blood pressure of a human subject, the physician first wraps a pneumatic cuff around the patient's upper arm and inflates the cuff by means of a hand pump until there is no pulse in the radial artery at the wrist. (This indicates that the brachial artery is completely occluded at the cuff.) He then gradually releases the pressure in the cuff and applies the stethoscope to the brachial artery just below the cuff. At some pressure level, he begins to hear a faint tapping sound (the first phase of the Korotkoff sounds) and he records the corresponding cuff pressure as the systolic pressure reading. As the cuff pressure is reduced further, the sound changes in character (second phase), becomes clearer and increases in intensity (third phase), then fades rather suddenly (fourth phase), and finally

disappears (fifth phase). This latter point is usually recorded as the diastolic pressure reading, although some physicians use the fourth phase (at which the sound fades suddenly) as an indication of diastolic pressure.

From the standpoint of the actual oscillatory pressure within the vessel being monitored (the brachial artery), the meaning of the systolic and diastolic pressure readings obtained in the above manner is not at all clear. It is immediately evident that the same flow in a stiffer or thicker artery will produce higher readings since a higher pressure would be required to close the stiffer vessel, even if it were devoid of fluid. A preliminary analysis of this "occluding" pressure was developed in Reference 1 for oscillatory flow in a flexible tube, and it was found that, for a pressure cuff of sufficient length[1], the occluding pressure is given approximately by

$$p_{occl} \approx p_{max} + \frac{5}{3} E \left(\frac{h}{R_o}\right)^3 \tag{1}$$

where p_{max} is the peak oscillatory pressure within the unobstructed vessel (i.e., before occlusion), R_o is the undisturbed vessel radius, and E and h are the elastic modulus and the wall thickness of the artery in question. The second term represents the collapsing or occluding pressure for a thin-walled elastic tube devoid of fluid, and is approximately five times the critical buckling pressure. This latter pressure is defined as that pressure difference (external minus internal) at which the tube is initially deformed from a circular to an elliptic cross section. In any event, it is clear that the occluding pressure depends not only upon the peak oscillatory pressure within the vessel but also upon the stiffness and thickness of the arterial wall.

---

[1]If the cuff length is too short, the large curvature of the vessel wall in the axial direction will require an additional pressure which depends upon the length of the cuff.

It should be emphasized that the cuff pressure given by Equation (1) is the occluding pressure, which must be higher than the auscultatory systolic pressure reading. That is, there can be no sounds heard in the stethoscope if the flow has been stopped in the artery. Rather, the cuff pressure must be reduced to such a level that some fluid passes through on each pulse, and further to such a level that the intermittent sounds produced become sufficiently intense to be audible through the stethoscope.

The experimental data of Reference 1 showed that in all cases the systolic pressure reading fell below the theoretical occluding pressure given by Equation (1). Furthermore, it was observed in Reference 1 that flow occurred downstream from (i.e., distal to) the pressure chamber before any Korotkoff sounds could be heard in the stethoscope. Since the auscultatory technique involves listening to these sounds, one would expect that the systolic and diastolic pressure readings should depend not only upon the parameters appearing in Equation (1) but also upon those which affect such phenomena as sound production and sound attenuation and absorption. These phenomena in turn depend upon the properties of the fluid as well as on the properties of the artery and the pressure cuff. Thus, the precise interpretation of auscultatory blood pressure readings is a complex problem involving a number of related physical phenomena and is a subject which requires scientific investigation.

The experiments described in the present report are intended to provide a direct experimental comparison between the auscultatory systolic and diastolic pressure readings and the corresponding maximum and minimum of the oscillatory pressure wave which existed in the unobstructed artery <u>before</u> the pressure cuff is applied. The actual cause of the Korotkoff sounds (i.e., the mechanism of their production) and the associated motions of the fluid and the arterial wall will be studied in a later phase of the present program, and the results will be presented in a subsequent report.

3. MATCHING THE HUMAN SYSTEM

Since auscultatory blood pressure determinations are nearly always made on the brachial artery, we shall, for purposes of the present investigation, confine our attention to that vessel and the pulsating flow within it. Furthermore, the results of theoretical analysis (Refs. 2 and 3) indicate that the effects of surrounding tissues are probably small. The problem of matching the physiological situation is thus reduced to that of matching the physical and elastic properties of the blood fluid and the brachial artery itself. In this section of the report, we shall concern ourselves with what these properties are and how we shall go about matching them in the simulated system.

3.1 Elastic Properties of Living Vessels

The physical structure of the arterial wall actually varies throughout the arterial tree, and detailed information on the human brachial artery is virtually nonexistent. However, histological evidence has been accumulated on various arteries (particularly the thoracic and the abdominal aorta, the femoral, and the carotid arteries) which indicates that the arterial wall is composed of essentially three layers of different materials, namely elastin, collagen, and smooth muscle. The geometrical structure and arrangement of each of these is somewhat unclear, although available micro-photographs show that the arterial wall is roughly approximated by an inner layer of elastin, a middle layer of smooth muscle, and an outer layer of collagen. The elastic modulus of elastin has been measured and found to be roughly 3×10^6 dynes per cm^2 or 43 psi (Ref. 4). Collagen is found to be much stiffer ($E \approx 10^9$ dynes/cm^2 or 14,500 psi) and is believed to form a restraining net of fibres surrounding both the elastin and smooth muscle. The available experimental stress-strain diagrams for both axial and circumferential extension of excised arterial specimens are quite nonlinear, and the data are rather incomplete and inconsistent. Generally speaking, however,

the stiffness of the arterial wall seems to increase with internal pressure. It is believed that at small strains the elastic behavior is dominated by the elastin, which is quite linear, but that at larger strains the stiffer collagen fibres become stretched and tend to increase the elastic resistance.

The question of how to determine experimentally the elastic properties of living tissues at once gives rise to a dilemma. The customary engineering techniques require that a sample of the material to be tested be placed in a machine with which various known loads or stresses can be applied and the corresponding changes in dimensions (i.e., the strains) can be measured. However, if a sample of the physiological material is removed from the body, it is no longer a "living tissue." Furthermore, the natural constraints under which a blood vessel normally operates inside the body have been removed. How these effects alter the elastic behavior of the vessel is unknown.

An obvious alternative to the above technique is to make stress and strain measurements on blood vessels in vivo (i.e., in the living body). This technique, although apparently more direct, is not without its problems. The static pressure within an artery can be measured by means of a wall tap, and the strain can be measured with instruments attached to the arterial wall, but this requires surgery, which could alter the surrounding tissues. A more serious limitation is that any attempt to raise the stress levels in the artery by administering drugs to raise the blood pressure leads to the possibility of simultaneous chemical or other changes in either the physical properties of the blood or the elastic properties of the arterial wall, as well as possible changes in pulse rate, which in turn would alter any frequency-dependent elastic behavior. Furthermore, the equations which must be used to extract the elastic constants from the measured stress and strain involve certain assumptions whose validity for the living system is unknown.

A third technique for dtermining the elastic modulus of blood vessels lies in the use of the relationship between the elastic modulus and the pulse wave velocity in flexible tubes. Here, however, we have two basic shortcomings: that of dealing with an excised vessel and that of the mathematical assumptions leading to the above relationship. In addition, of course, there is the problem of avoiding wave reflections from the juncture between the flexible vessel being tested and the rigid tubes to which the vessel is attached.

Perhaps the most comprehensive study of the elastic behavior of excised arterial strips was carried out in 1880 by Roy (Ref. 5), who even then observed that arteries exhibit the visco-elastic and thermoelastic properties of that class of materials now referred to as "elastomers." These rubber-like materials are characterized by the following four properties:

(a) A large elastic range (i.e., large elongations with subsequent return).

(b) A nonlinear stress-strain relation (E varies with the strain ϵ).

(c) A relaxation time (i.e., strain under constant stress varies with time).

(d) Anomalous thermal behavior (material contracts when exposed to heat while under tension).

More recently, Bergel (Ref. 6) published more precise data which indicate that the static Young's modulus E for excised arteries varied almost linearly with pressure level in the normal range of mean pressures. The variation of vessel radius with pressure is shown for the femoral artery in Figure 1, which is reproduced from Reference 6. Bergel also found that the values of E differed considerably from one vessel to another. At a pressure of 100 mm Hg the values range from about 4×10^6 dynes/cm^2 (60 psi) for the thoracic aorta to about 7×10^6 dynes/cm^2 (100 psi) for the carotid artery. Later, in Reference 7, Bergel presented

the results of dynamic tests on excised arteries, and these are reproduced in Figure 2 in terms of the magnitude of the dynamic modulus and the phase lag between stress and strain. It can be seen that the phase lag is only of the order of 5° in the normal range of pulse rate and does not exceed 10° even at high frequencies. On the other hand, the visco-elastic property of the arterial wall may be important in determining the magnitude of the oscillatory displacements, as indicated by the rather large values of the ratio E_{dyn}/E.

A detailed analysis of all available data on arteries, and possibly some additional experiments, will be undertaken in a later phase of the present overall program. In particular, an attempt will be made to ascertain the detailed physical and elastic properties of the human brachial artery.

3.2 Viscous Behavior of Whole Blood

Whole blood is actually an extremely complex fluid composed of several types of living cells suspended in a clear solution, called plasma, which itself contains salts and organic compounds (see Ref. 8). In normal human blood, about 44 percent of the volume is occupied by a heterogenous mixture of blood cells called hematocytes. The two most common types of hematocytes are the red and white corpuscles. The red corpuscles (erythrocytes) are flexible biconcave disks, about 8 microns in diameter and 2 microns thick, and these constitute over 99 percent of the total number of blood cells. The white corpuscles (leukocytes) comprise less than one-half of 1 percent of the total number of cells. Removal of all blood cells leaves the blood plasma, which is considered to be nearly a Newtonian fluid. (A Newtonian fluid is any liquid or gas whose viscosity coefficient μ is independent of the rate of shear.) However, whole blood shows a decreasing coefficient of viscosity with increasing shear rate. This departure from Newtonian behavior becomes more pronounced with increasing hematocyte concentrations.

The development of a mathematical model for the viscosity characteristics of whole blood would indeed be a formidable task, because the model must account for a suspension of flexible, non-spheroidal blood cells which have some kind of affinity for one another. However, an approximate analysis for the viscosity of a suspension of solid neutral spheres in a Newtonian fluid has been advanced by Einstein (Ref. 9). That analysis showed that the viscosity coefficient was a function of particle concentration as described by the equation:

$$\mu_{rel} = 1 + 0.025H \tag{2}$$

where μ_{rel} is the relative viscosity coefficient, defined as the ratio of the viscosity of the mixture to that of the suspending fluid, and H is the percentage of hematocytes (spheres) by volume. Equation (2) has been checked against some experimental blood flow data taken by Haynes and Burton (Ref. 10) and is plotted in Figure 3.

The experimental data shown in Figure 3 indicate a higher viscosity than would be predicted by Einstein's equation for most values of the strain rate $\dot{\gamma}$. However, the data do evidently converge upon Equation (1) with decreasing particle concentration and with increasing shear rates so that, for volumetric concentrations less than 19 percent, the experimental data and Einstein's analysis are in good agreement for high rates of shear. The lack of agreement at the higher particle concentrations is not surprising because the assumption of non-interacting, rigid particles, is clearly unjustified for normal whole blood. Nevertheless, Equation (2) is useful for approximating the viscous effects at the lower particle concentrations and for identifying one of the important parameters (H) which will be used to correlate the blood-flow data.

In addition to the suspended hematocytes, whole blood also contains in the plasma an organic compound, called fibrinogen,

which, if allowed to remain in a collected blood sample, is believed to affect another type of non-Newtonian characteristic, namely, the ability to support an initial shear stress. But since fibrinogen also contributes to the blood clotting process (Ref. 11), workers investigating the viscosity characteristics of blood generally add anticoagulants to the sample to inhibit the formation of the fibrous blood clot. The most commonly used anticoagulants are heparin, citrate, and oxalate. Cokelet (Ref. 12) has pointed out that the addition of such anticoagulants alters the ability of the blood to support an initial shear stress, or nullifies it completely.

The variable viscosity coefficient of a non-Newtonian fluid is better understood by discussing fluid flow in terms of the shear stress τ and strain rate $\dot{\gamma}$ where

$$\tau = f(\dot{\gamma}) \tag{3}$$

This relationship is generally displayed on a "flow curve," which is a plot of the shear stress against the rate of strain. Examples of flow curves for three basic classes of fluids which are discussed throughout this section are shown below.

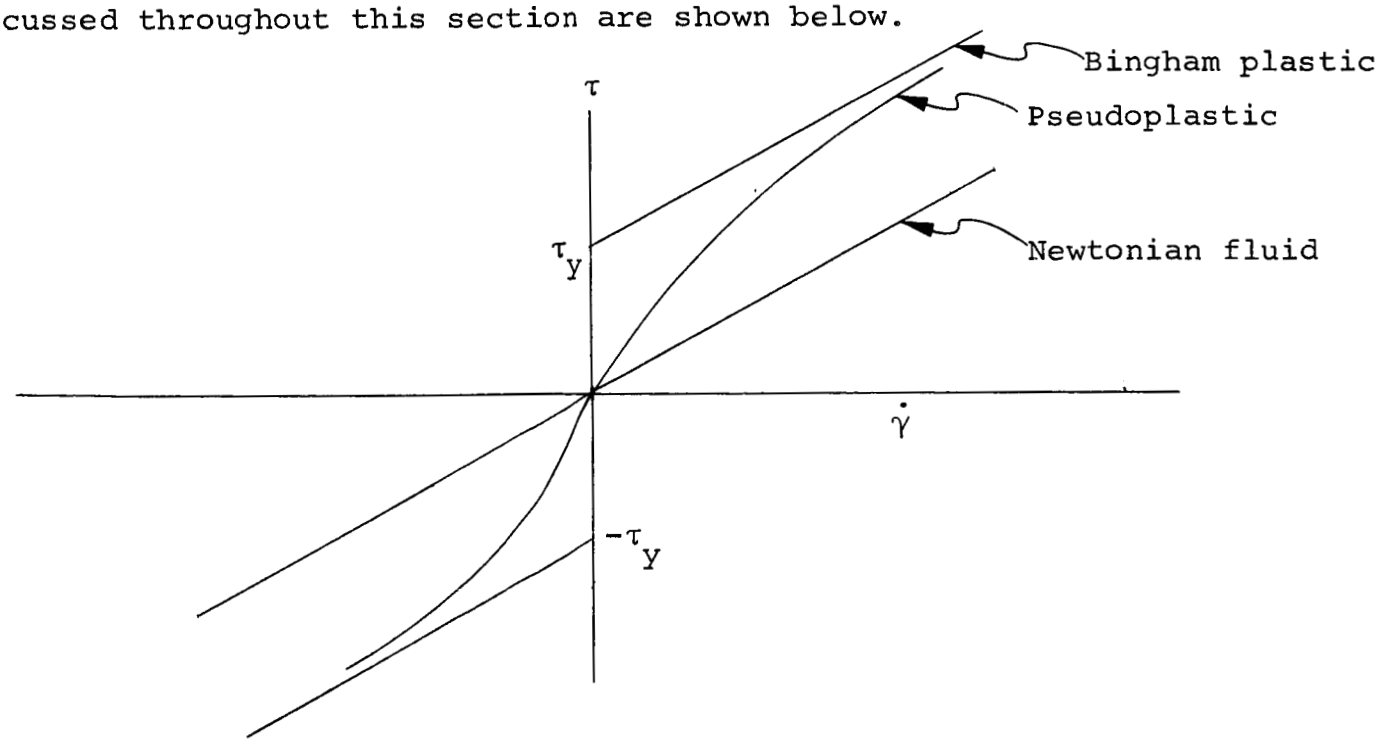

These three fluids are represented mathematically as follows (see Ref. 24):

Newtonian fluid

$$\tau = \mu\dot{\gamma} \tag{4}$$

Bingham Plastic

$$\tau - \tau_y = \mu_p\dot{\gamma} \quad \text{for} \quad |\tau| > |\tau_y| \tag{5}$$

Pseudoplastic

$$\tau = K\dot{\gamma}^n \quad \text{for} \quad n < 1 \tag{6}$$

where

μ is the Newtonian coefficient of viscosity

μ_p is the plastic coefficient of viscosity

K is the pseudoplastic consistency index

n is the pseudoplastic exponent

The so-called "apparent" viscosity coefficient for such fluids is defined as

$$\mu_a = \frac{\tau}{\dot{\gamma}} = \frac{f(\dot{\gamma})}{\dot{\gamma}} \tag{7}$$

Thus, unless the fluid is Newtonian, μ_a will vary with shear rate. For a pseudoplastic fluid, substitution of Equation (6) into Equation (7) shows that the coefficient of viscosity decreases with increasing shear rate according to the relation

$$\mu_a = \frac{K}{\dot{\gamma}^{1-n}} \quad \text{for} \quad n < 1 \tag{8}$$

An analysis based upon the data from Reference 10 and References 12 through 19 indicates that whole blood is and remains a

pseudoplastic fluid over a very wide range of shear rates. A brief summary of some of the pertinent technical information from each of these references (such as type of blood, anticoagulant added, and viscometer used) is presented in Table I.

The flow curves for human and canine blood plasma, blood serum (the fluid remaining after coagulation), and whole blood at normal cell concentrations (42 to 44 percent) are presented in Figure 4. Also plotted on the same graph for comparitive purposes is the flow curve for water. It can be seen that normal blood without the protein fibrinogen[2] is much more viscous than water; that is, the blood has a higher shear stress for a given shear rate as seen from the specific viscosity coefficient (ratio of shear stress of fluid in question to that of water at any fixed shear rate). The specific viscosity of whole blood without fibrinogen decreases from 19 to 2.8 as $\dot{\gamma}$ increases from 10^{-2} to 10 sec^{-1}, while for the blood plasma and serum, the specific viscosity remains at a constant value (1.7) over all the aforementioned shear rates. Since the slope of the curves for plasma and serum is nearly 1.0, the flow characteristics of plasma and serum are seen to be nearly Newtonian. Another significant observation made from Figure 4 is that human and canine blood appear to be nearly identical in viscous behavior.

The data from which the flow curves of Figure 4 were constructed were obtained with various types of viscometers (capillary[3] and rotational), and in general gave similar results.

Figure 5 displays the flow characteristics of bovine blood for various hematocyte concentrations. It can be seen that the slope of these logarithmic stress-strain curves is constant for each hematocyte concentration. Hence, bovine blood is seen to be

---

[2]We shall consider the influence of fibrinogen separately.

[3]The shear stresses and rates were determined by employing the analyses presented in Appendix A.

a pseudoplastic fluid (Eq. (6)), and the slope of each curve yields the value of the pseudoplastic exponent n.

One will also note in Figure 5 that there is a dependence of the pseudoplastic exponent upon the hematocyte concentration H. This type of dependence is evidently also characteristic of human and canine blood.

Figure 6 is a plot of the pseudoplastic exponent as a function of particle concentration for human, canine, and bovine blood. The linear curve drawn through the human blood data was determined by a least squares fit through the data of Haynes and Burton (Ref. 10). Haynes and Burton's data were chosen because they appeared to be more consistent and covered a wider range of cell concentrations (8.8 percent to 82.5 percent by volume) than any others. The least mean square curve calculated for the bovine blood utilized all the bovine data points. The plots in Figure 6 indicate that the pseudoplastic exponent is roughly a linear function of cell concentration which can be expressed as

$$n(H) = 1.00 - C_1 H \tag{9}$$

where H is the percentage of hematocytes by volume and C_1 is an empirical constant which is dependent upon the species of the animal blood.

The value of the coefficient C_1 was determined by the least squares method and found to be

$$\left.\begin{aligned} C_1 &= 4.5\times10^{-3} \quad \text{for human and canine blood} \\ C_1 &= 1.7\times10^{-3} \quad \text{for bovine blood} \end{aligned}\right\} \tag{10}$$

Now in order to define completely the pseudoplastic characteristics of whole blood (with no fibrinogen), the dependence of the consistency index (K) upon the volumetric concentration of cells must be determined. K was determined from the original flow curves by observing the shear stress at $\dot{\gamma} = 1.0$, because K

and τ are equal at that condition (see Eq. (6)). The consistency indices for all three species (human, canine, and bovine) are plotted in Figure 7 as functions of hematocyte concentration. The linear curve was determined by a least squares fit through the experimental data of Haynes and Burton (Ref. 10), and Coulter and Pappenheimer (Ref. 17). This curve indicates that K increases as an exponential function of cell concentration, given by

$$K(H) = C_2 e^{C_3 H} \tag{11}$$

and the constants were determined to be

$$C_2 = 1.05\times10^{-2}; \quad C_3 = 5.4\times10^{-2} \tag{12}$$

for human, canine, and bovine blood.

Having approximated the pseudoplastic characteristics of whole blood, one can now develop the viscosity coefficient by substituting Equations (9) through (12) into Equation (8). The calculated viscosity coefficients, assuming a normal cell count (or 43 percent), are plotted in Figure 8 as a function of shear rate. The plots again show that bovine blood is much more nearly Newtonian (but generally more viscous) than are human and canine blood. The near-Newtonian behavior of the bovine blood can be seen from the flatness of the curve, since a constant coefficient of viscosity is characteristic of a Newtonian fluid. In general, the calculated curves show that the coefficients of viscosity for whole blood decrease with increasing shear rate, particularly at low shear rates, which is typical of pseudoplastic fluids.

It will be recalled from Figure 4 that whole blood has the ability to sustain an initial shear stress τ_y, which is typically characteristic of a Bingham plastic (see Eq. (5)). The ability to sustain an initial yield stress was attributed by Cokelet (Ref. 12) to the presence of the protein fibrinogen. Cokelet found that, when the fibrinogen was removed, the fluid became pseudoplastic

over the entire range of shear rates investigated. The changes in the flow curves for normal human blood produced by different amounts of fibrinogen are shown in Figure 4.

There is only a meager amount of experimental data available to evaluate the relationships between the initial shear stress and the other parameters. Thus, the information which is available does not warrant an analytic relationship at this time. It does appear from Figure 4 that τ_y increases with the percentage by volume of fibrinogen.

In view of the rather small values of τ_y indicated in Figure 4, a question remains as to whether the initial shear stress effect in real blood is at all significant. This question can be partially answered by comparing the relative magnitudes of a typical shear stress τ in an artery to the value of this yield stress, τ_y.

Haynes and Burton (Ref. 10) suggest a value of shear stress of 60 dynes/cm^2 as typical of flow in the larger arteries, and Cokelet found the yield stress to be 0.03 dynes/cm^2 in normal blood. Hence, τ_y is of the order of 0.05 percent of the probable value of τ, and consequently τ_y is probably negligible. However, in an oscillatory flow that has a zero mean velocity, the fluid shear stress becomes equal to or less than τ_y each time the velocity passes through zero. In such a case, the fluid must be said to behave as a Bingham plastic, at least over part of the cycle. Whether or not this Bingham plastic effect, experienced during oscillatory flow, can be neglected must therefore await further examination.

Analysis of the available blood flow data for human and animal blood has indicated that the presence of blood cells and the protein fibrinogen in whole blood causes the blood to behave as a combination of a Bingham plastic and a pseudoplastic fluid. The accumulated information appears to be sufficiently complete to warrant the following approximate equations for the shear stress and the apparent viscosity coefficient of blood:

$$\tau - \tau_y = 0.0105\ e^{0.054H}\ \dot{\gamma}^{(1-C_1H)} \qquad \text{for} \quad |\tau| > |\tau_y| \tag{13}$$

where τ_y is extremely small, so that

$$\mu_a \approx \frac{1.05\times10^{-2}e^{0.054H}}{\dot{\gamma}^{C_1H}} \qquad \text{for} \quad |\tau| > |\tau_y| \tag{14}$$

The constant C_1 and the small initial stress τ_y are dependent upon the species of the animal.

In summary, whole blood appears to behave essentially as a pseudoplastic fluid, having a decreasing coefficient of viscosity with increasing shear rate. The small initial shear or yield stress seems to be caused by the protein fibrinogen, so that, when the fibrinogen is removed, the yield effect vanishes. Human and canine blood evidently possess very nearly identical non-Newtonian characteristics, but bovine blood, as represented by steer blood, is much more nearly Newtonian, although more viscous. Lastly, Einstein's Equation (2) seems to furnish reasonable viscosity estimates for the smaller particle concentrations (0 to 10 percent by volume) and higher shear rates ($\dot{\gamma} > 100\ \text{sec}^{-1}$), but does not predict the non-Newtonian behavior.

All of the blood-flow data analyzed herein were taken in glass capillary tubes or rotating viscometers. Corresponding "in vivo" data do not appear to be available at this time.

3.3 The Idealized Model

3.3.1 The arterial wall

In attempting to match the human system for the purpose of the present investigation, we shall first idealize both the artery in question (the brachial) and the fluid contained therein (the blood), so that we can characterize the problem by a number of non-dimensional parameters which can then be controlled for the experiments. For this purpose, we shall consider the artery

itself to be a Kelvin-Voigt solid, which behaves like a spring and viscous damper arranged in parallel (see sketch)

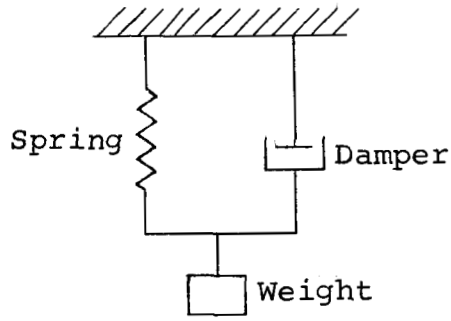

The stress-strain relation for such a material can be expressed in the form

$$\delta = E\epsilon + E'\dot{\epsilon} \tag{15}$$

where

δ = stress

ϵ = strain

$\dot{\epsilon}$ = rate of strain

E = static Young's modulus

E' = visco-elastic modulus

Now, for a purely sinusoidal strain, we have

$$\epsilon = \epsilon_o e^{-i\omega t} \tag{16}$$

and Equation (15) yields

$$\delta = E\epsilon_o\left(1 - \frac{i\omega E'}{E}\right) \tag{17}$$

Hence, the idealized artery can be characterized for the present problem by the static Young's modulus E and the dimensionless ratio $\omega E'/E$.

3.3.2 The blood fluid

Inasmuch as whole blood is a rather complicated non-Newtonian fluid whose actual composition is not fully understood, we shall not attempt to match the non-Newtonian behavior of the fluid for the present tests. Rather, we shall first knowingly over-simplify the fluid to the point of using a homogeneous Newtonian fluid of variable viscosity and then proceed to check our experimental results by making tests with whole blood. Hence, the initial test fluid is characterized by its mass density and its kinematic viscosity. This approach seems justified, since we are concerned here with one of the larger arteries (the brachial) in which the shear rates are generally high and the non-Newtonian viscous behavior seems relatively unimportant in determining the fluid pressures. On the other hand, the check with real blood is essential, since the production, attenuation, and absorption of the Korotkoff sounds may well be influenced by other factors in the blood fluid, regardless of scale.

3.4 Dynamic Similarity

Rather than attempting to match each parameter of the physiological system (some of which are not accurately known), it will be convenient here to scale up the entire system to a size which will simplify the instrumentation problem (and improve the experimental accuracy) and to vary the parameters over a wide range. In order to scale the problem properly, of course, one must be certain that all of the non-dimensional parameters of the flow problem are matched to insure dynamic similarity. For the problem of an oscillatory viscous flow in an elastic tube, these parameters involve the physical and elastic properties of the fluid and the vessel wall, as well as the quantities which describe the pulsating flow. For a simple sinusoidal pressure wave (which we shall employ in the experiments), the linearized mathematical analysis of References 2 and 3 indicates that for small displacements, the appropriate non-dimensional quantities can be written in the following form:

$$\frac{h}{R_o}, \quad \sigma, \quad \frac{\rho V_o^2}{E}, \quad \frac{R_o^2\omega}{\nu}, \quad \frac{R_o V_o}{\nu}, \quad \frac{\omega E'}{E} \tag{18}$$

where h, R_o, and σ are the thickness, radius, and Poisson's ratio of the arterial wall, V_o is the mean velocity, ω is the pulse frequency, and ν is the fluid kinematic viscosity. The quantity $R_o V_o/\nu$ is recognized as the Reynolds number based on the mean velocity, and the quantity $R_o^2\omega/\nu$ is the corresponding unsteady Reynolds number based on the frequency of oscillation. In addition, since the present problem of partial occlusion involves large displacements, we may have to add to the above list the parameters

$$\frac{p_o}{E} \quad \text{and} \quad \frac{PA}{p_o}$$

where p_o is the mean pressure level and PA is the pulse amplitude.

The physical and elastic properties of the simulated artery are determined by the selection of the material and dimensions of the flexible tubing. The fluid viscosity will be varied by using varying concentrations of glycerol in water, and the flow conditions are to be adjusted by means of the experimental apparatus. In view of the rather wide normal variation and uncertainty of the above parameters for the physiological problem, the approach here will be to cover a range which brackets the known normal physiological range and is sufficiently wide to establish any significant trends.

4. EXPERIMENTAL APPARATUS

4.1 General Description

The "blood pressure" measurements in the simulated artery were taken by use of a fluid flow apparatus which was designed to simulate the human brachial artery, including the pulsating fluid

flow therein. The apparatus is capable of producing wide ranges of mean pressure level, pulse amplitude, pulse frequency, and mean flow rates. Other variables include artery wall physical characteristics and fluid viscosity. The pulse wave shape in the unobstructed vessel was essentially sinusoidal in all cases.

An enlarged version of a sphygmomanometer was used to enable "blood pressure" measurements to be taken by the clinical auscultatory method of occluding the artery. Pressure probes inserted into the artery were used to measure the corresponding intra-arterial pressure directly.

The experimental apparatus is shown schematically in Figure 9. The apparatus is a closed-loop system in which the test fluid is fed from the reservoir through the circulation pump to the pressure pulse generator. With the pulse generator operating, periodic pressure pulses are imparted to the liquid which then divides into two sections. A part of the pulsating flow passes into the 1-inch diameter section containing the simulated artery; the rest travels through the bypass system. The test section and bypass have independent return lines to the reservoir in order to avoid any mutual interaction between the traveling waves of each branch. The major components of the apparatus are discussed in detail in the following paragraphs.

4.2 Simulated Artery

The simulated arteries used in the present tests had the following nominal dimensions:

inside diameter	1 inch
wall thickness	1/16 inch or 1/8 inch
natural length	120 inches
installed length	141.5 inches

Because of the general lack of information on elastic properties of physiological materials (particularly the human brachial artery), and since one cannot specify the elastic constants when buying

commerically available rubber compounds, it was necessary to choose rubber tubing which could be purchased in the size and shape required for the simulated artery and then measure the elastic properties of those materials. Numerous elastomeric materials were investigated for possible use to simulate arteries. Natural gum rubber and latex were finally selected because of availability in the diameter, wall thickness, length and general elastic range required for the present investigation. These materials were chosen to fulfill two basic requirements. First, the simulated artery should model the physiological artery as far as the general range of elastic properties and the ratio of wall thickness to radius are concerned; and second, the diameter and length of the simulated artery are governed by the requirement of measuring internal static (or lateral) and total (or stagnation) pressures at various positions. That is, the simulated artery must be (1) large enough so that the presence of the pressure probes does not appreciably alter the flow characteristics within the tube, and (2) large enough to permit radial positioning of the probes at various distances off the axis of symmetry (to determine radial distribution).

Several precautions were taken in order to obtain accurate and reproducible data. It was required first that the rubber tubes be manufactured in such a manner as to produce tubes of nearly circular cross section to provide nearly symmetrical wall displacements during each pulse. End effects were kept to a minimum by (1) having a long test artery (approximately 12 feet), (2) installing 10-foot lengths of 1-inch I.D. rigid clear plastic tubing both upstream and downstream of the test section, and (3) tapering the junctions between the rigid and flexible tubing. The rubber tubing was maintained straight and level by placing it on a rigid plastic channel of semi-circular cross section. The channel diameter was slightly larger than the rubber tube outer diameter so that the expansion of the rubber tube was not restricted during a pulse. The channel did not extend through the pressure chamber.

Two small (1/8-inch diameter) holes were made in the underside of the simulated artery slightly downstream of the pressure chamber. These holes were used for inserting the static and total pressure probes into the flexible tube. This installation is shown in Figure 10 and is discussed in Sections 5 and 6.

4.3 Pressure Pulse Generator

The pulsating flow in the simulated arterial system is produced by a positive-displacement piston actuated by a variable-speed motor and is provided with an adjustable throw to provide sinusoidal pressure oscillations of variable amplitude and frequency.

The 4-inch I.D. pulse generator cylinder and piston are made of clear acrylic plastic in order to permit visual observation of the fluid motion and to reduce the number of metallic parts which may produce and transmit extraneous noises. In order to avoid the scraping noises associated with piston rings, the seal between the piston and cylinder wall is obtained by using a Bellofram rolling diaphragm. This type of diaphragm rolls itself out along the piston and cylinder wall (see Fig. 11).

A sinusoidal piston motion was produced by making the connecting rod between the piston and the rotating crank mechanism with a length more than four times the largest eccentricity of the crank mechanism (Ref. 20). The crank mechanism is adjustable to provide piston strokes from approximately 3/4 to 3-1/2 inches, in 8 increments.

A second rubber diaphragm was installed across the downstream end of the pump cylinder to form a 20-inch long air chamber between the piston and the working fluid, as shown in Figure 11. With this arrangement, it was possible (by varying the pressure in the air chamber) to produce sinusoidal pulse waves of reasonable amplitude at the test section with small volumetric displacements.

A rubber timing-belt drive system is used to transmit the power from the variable-speed motor to the crank mechanism (see Fig. 12). This type of drive tends to damp out noise and vibrations which might otherwise be transmitted from the motor to the

pump. The combination of the drive motor speed adjustment and one change of drive pulleys is sufficient to vary the pulse frequency from 0.2 to 3 cycles per second (12 to 180 beats per minute).

4.4 Pressure Chamber

The design of the pressure chamber used to occlude the simulated artery is based on the findings of Erlanger (Ref. 21); that is, the volume of air in the chamber must be above a certain minimum value relative to the size of the artery, and the membrane used in the chamber to compress the artery must be sufficiently flexible to permit a pressure pulse to pass through the artery at appropriate chamber pressures. In addition, the pressure chamber must not impose any artificial constraints on the artery at the ends of the chamber.

An exploded view of the pressure chamber is shown in Figure 13 where only the parts of the lower section of the chamber are identified, since the upper and lower sections are identical. The top and bottom parts of the pressure chamber are essentially open hardwood boxes whose outside dimensions are 18 by 12 by 2 inches. A rubber gasket is embedded in each box wall to seal the chamber. A thin rubber membrane covers the opening of each box, and a plastic frame 1-inch thick is placed over each membrane as shown in the figure. The plastic frames each have semi-circular openings in their opposite ends to permit the artery to pass freely through the pressure chamber in such a way that the chamber does not exert any artificial "end effects" when the artery is sandwiched between the upper and lower halves of the chamber. This requirement was considered essential in order to avoid any extraneous effects on the Korotkoff sounds by local constraints on the artery. When the upper and lower sections of the pressure chamber are clamped tightly together, the rubber gaskets ("O" rings) and the membranes seal the upper and lower chambers between the box and the membrane. Thus, when compressed gas is fed into the upper and lower chambers, the membranes expand symmetrically onto the enclosed artery. As the pressure behind the membranes increases,

the membranes expand further and flatten the artery evenly until the artery is completely occluded. An aneroid-type pressure gage from a standard clinical sphygmomanometer is used to measure the chamber pressure.

4.5 Bypass System

The bypass system simulates that part of the human circulatory system which is not closed off when the sphygmomanometer occludes the brachial artery during auscultatory measurements. The bypass is a 4-inch-diameter plastic pipe which branches from the main system between the pulse generator and the contraction to the test section. It is scaled to the simulated artery so as to match approximately the ratio of the cross-sectional area of the brachial artery to that of the aorta close to the heart, through which latter vessel the entire output from the heart is initially transported. (This ratio is about 16 to 1 in human beings.) A valve is provided in the bypass system to permit control of the flow through the bypass. The first several feet of the bypass is constructed of clear plastic pipe to permit observation of the local flow conditions and to see whether air bubbles are present in the system. The bypass flow is returned directly to the reservoir by a separate pipeline in order to prevent any feedback of flow or pressure pulsations to the test section.

4.6 Reservoir

A 240 gallon capacity reservoir is used to provide an adjustable mean pressure head of the test fluid. Of dimensions 4 by 4 by 2 feet, it is constructed of plywood with an angle iron frame and is lined with galvanized steel.

The large free surface area of the reservoir allows the pressure pulsations induced in the system by the pulse generator to damp quickly. Also, the variation of fluid mass due to the displacement of the pulse piston (which is approximately 4 inches in diameter) has no significant effect on the fluid level of the much larger surface area in the reservoir.

The reservoir can be raised approximately 13-1/2 feet above the floor level by means of an electrically powered cable hoist which is remotely operated from the control panel near the test section. An electrical meter at the control panel provides an approximate indication of the reservoir height. By adjusting the reservoir height, one can vary the mean pressure in the test section from 0 to 225 mm Hg.

Two openings are provided in the bottom of the reservoir, one for the inlet line to the pulse generator section, the other for the test section and bypass return lines. These lines are flexible 2-inch-diameter gum rubber tubes with internal stainless steel coils to prevent the tubes from collapsing when the reservoir is lowered. The tubes coil beneath the reservoir when it is lowered and uncoil as the reservoir is raised. The flexible tubes are connected at the floor level to plastic pipes which lead to the inlet and the outlets of the blood flow apparatus. These inlet and outlet lines all have quick-closing valves near the control panel so that the flow from the reservoir can be stopped in the event of a break in the test section area.

The reservoir is installed in a separate enclosure in an area which affords higher overhead clearance than does the 8-foot ceiling of the hemodynamics laboratory. This close-fitting enclosure acts as a shield to reduce temperature variations and also protects nearby personnel from the remotely-controlled hoist and its load.

4.7 Circulation Pump

A 50-gallon-per-minute centrifugal pump is mounted in the inlet line from the reservoir to the pulse generator section for the purpose of providing a mean flow rate in the system when desired. A throttling valve in parallel with the pump is used to control the magnitude of the mean flow rate. With this arrangement, a maximum mean velocity of 10 feet per second can be obtained in the test section with the bypass fully open. The higher rates

of circulation through the system are also available for driving trapped air bubbles to the various air traps in the system. Several small valves are located throughout the apparatus for the purpose of bleeding off the trapped air.

5. INSTRUMENTATION

5.1 Pressure Transducers

All pressure measurements of the pulsating flow within the simulated artery were obtained with unbonded strain-gage-type pressure transducers, CEC model 4-312, with a range of ± 15 psid. The pressure measured by the differential transducer is gage pressure since one side of the transducer was vented to the atmosphere. The output signal from the transducer was fed into a CEC 7-339 galvanometer in the CEC recording oscillograph. The excitation voltage for each differential transducer was supplied by a 6-volt battery.

The pressure sensing side of the transducer was fitted to a plexiglas reservoir which served three purposes: (1) to transmit fluid pressure from pressure probe to transducer, (2) to afford protection of the delicate diaphragm of the transducer, and (3) to permit collection and removal of entrained air from the system. The clear cylindrical reservoir was made to close tolerance for each transducer used in the test and, after an application of vacuum grease on the mating surfaces, was bolted in place to provide a leak-proof assembly (see Fig. 14). This rigid assembly permits each transducer to measure the fluid pressure felt at each probe without introducing additional errors. A 1/8-inch bleed hole was provided on top of the transducer reservoir, which facilitated the removal of the air bubbles collected within the pressure measurement system by passing a mean flow through it. The remainder of the probe-transducer assembly consists of a teflon valve and plexiglas adapter. The valve provides protection for the transducer, particularly during the times when sudden transient pressure pulses might exist within the simulated artery.

Also, during the transducer calibration phase, it becomes necessary to vent the chamber to the atmosphere to obtain a datum pressure, namely atmospheric pressure. The plexiglas adapter permits a lead-proof union of the probe and valve.

5.2 Pressure Probes

Two pressure probes were mounted within the simulated artery. The probes were installed several inches downstream from the pressure chamber and entered the flexible tube from the bottom. They were so oriented that their longitudinal axis was approximately coincident with the centerline of the tube, since earlier measurements (Ref. 1) indicated no radial pressure variation across the tube. Figure 15 shows a section view of this arrangement and the relative locations of the important components.

The two probes were designed to measure total (stagnation) and static (lateral) pressures within the fluid. Both pressure probes used in the experiments were made of 1/16-inch O.D. brass tubing with a wall thickness of about 0.01 inch. For the total pressure probe, the end of the brass tube was cut normal to the axis and carefully smoothed square and free of burrs. For the static probe, the open end of the tube was sealed with silver solder and rounded, and four small holes (0.025-in. diameter) were drilled symmetrically around the circumference 0.25 inch from the probe tip. The static and total probes were designed so that the distance from the pressure hole to the probe support was the same in each case (1.75 in.).

5.3 Timing Photocell

The frequency of the piston-type pulse generator was monitored with a cadmium-type photocell, Clariex 505L, whose output was fed into a recording oscillograph. The photocell was excited by a light beam which was periodically interrupted by the piston. The resulting time-reference blip was recorded simultaneously with the other data.

5.4 Ohmmeter Setup for Static Tube Calibration

In order to determine the elastic properties of the flexible tube used to represent the artery in each case, measurements were made of the change in outer tube radius with each change in internal static pressure. This was done in place by raising and lowering the reservoir and measuring the tube diameter.

A relatively simple technique was devised which made it possible to avoid any flattening of the tube by the measurement instrument. The sketch below shows the physical arrangement employed in this technique, and the procedure was as follows:

(1) One lead from an ohmmeter was connected to a fine wire of known diameter which was glued onto the top of the flexible tube.

(2) The second lead from the meter was attached to a vernier height gage which was placed as shown in the sketch.

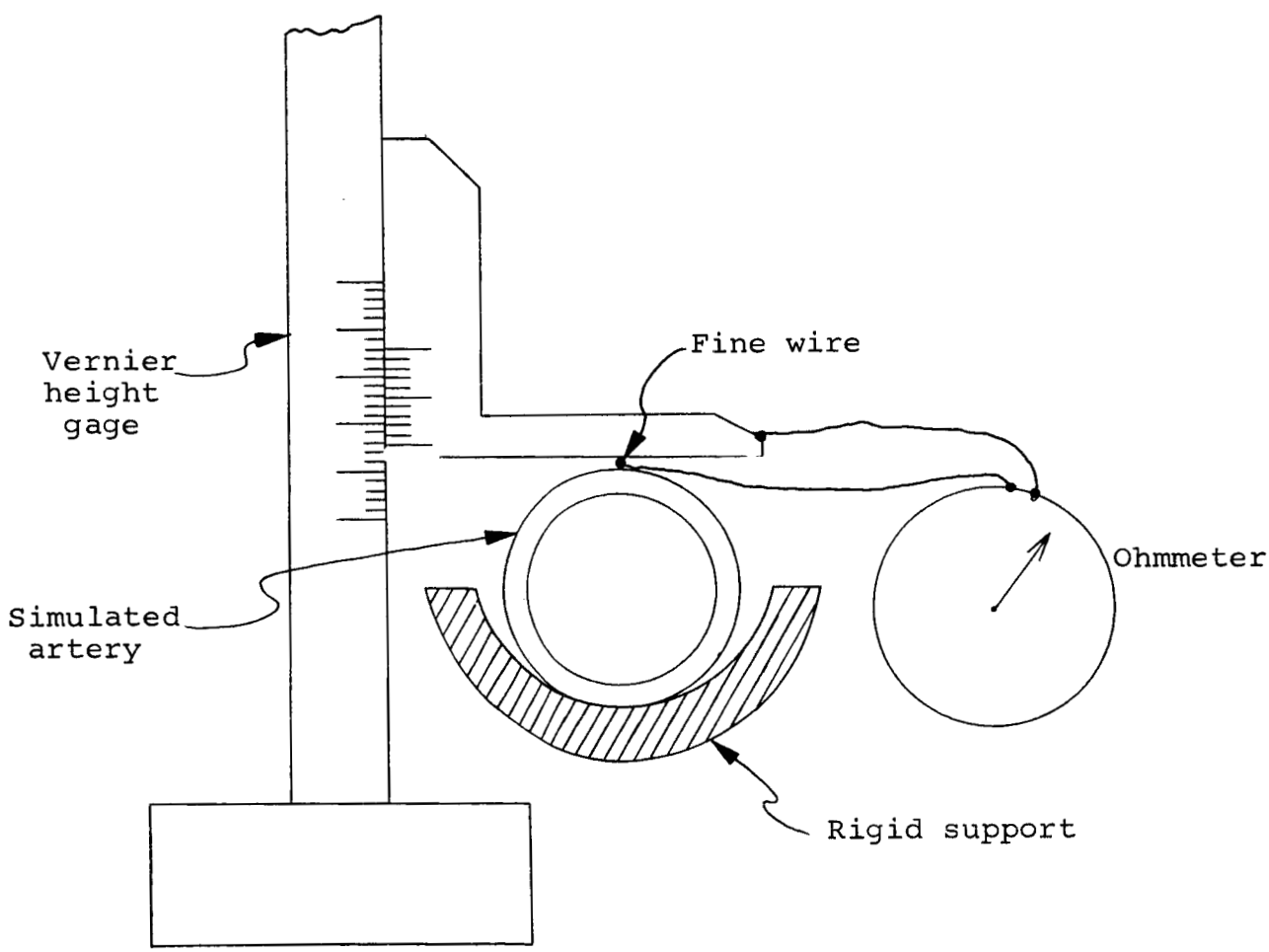

(3) The arm of the height gage was lowered until it touched the wire, thereby completing the electrical circuit, which causes an ohmmeter needle deflection. The gage reading then gives the total of the tube diameter plus the wire thickness.

5.5 Aneroid Manometer

The pressure in the pressure chamber representing the cuff of the sphygmomanometer was monitored with a standard medical Tycos Aneroid Manometer.

5.6 Stethoscope

The stethoscope employed for the purpose of monitoring the Korotkoff sounds during auscultatory tests was a Littman Stethoscope made by the Cardiosonics Company. The stethoscope was held in one place on top of the simulated artery by an ordinary rubber band (see Fig. 10) and was pressed down on the artery by hand as required during auscultation.

5.7 Viscometer, Thermometer, and Hydrometer

The viscosity of the fluid in the simulated artery was determined with an ASTM-300, Ostwald type, viscometer. The viscometer was calibrated with a set of standard viscometer calibration fluids supplied by the Cannon Company and was used to ascertain the specific viscosity of each sample of fluid drawn from the test section. A 20° to 88° F ($\pm 0.2^{\circ}$ F) precision thermometer was placed in the test fluid and used to monitor the fluid temperature throughout the experiments and the viscosity measurements. An ASTM 1000-1220 hydrometer served to measure the various specific gravities of the test fluids.

6. CALIBRATION OF TRANSDUCERS, PROBES, AND TUBES

6.1 Pressure Transducer Calibration

Initially, the pressure transducers were calibrated statically against a column of mercury over the entire working range of each transducer, and all transducers exhibited a linear pressure-displacement

(displacement on the recorder trace) relationship and were found to be accurate within the ± 1 percent specified by the manufacturer. Since the linearity of each pressure transducer was verified, all subsequent calibrations were performed with the probes in place, varying the mean pressure by raising and lowering the reservoir. The static pressure was determined by measuring the height that a column of fluid rose above the probes in a 1/4-inch glass tube. The open tube was connected to the test section by a valve and extended vertically upwards. The height of the liquid level was measured after opening the valve and allowing the transient oscillations of the fluid in the column to damp completely.

6.2 Calibration of Probes

Because of possible probe errors due to the oscillatory flow and the extremely low Reynolds numbers of the present experiments, the total and static pressure probes were calibrated by rotating each probe in an annular tank filled with the test fluid. The submerged probe is rotated at a constant depth with its axis normal to the axis of rotation, as shown in Figure 16. A range of velocities and accelerations is obtained by a simple pulley and weight arrangement. The indicated pressure readings are measured by the pressure transducer and the velocity and acceleration of the probe determined by means of a photocell arrangement as shown in the figure.

It can be shown that, for a total pressure probe moving in a circular path, the pressure measured by a transducer located at the center of rotation is simply the pressure correction of the probe (see Ref. 1). The static probe analysis is not quite as direct, but the correction factors can easily be evaluated using the analysis presented in Reference 1. The results of this calibration indicated a maximum error of ± 1 mm Hg for either probe experiencing both forward and reverse flow in the range of Reynolds numbers and accelerations covered by the present tests.

Since the fluid total and static pressure measurements in the test artery were actually taken at locations 14 and 19.25 inches (respectively) downstream from the center of the pressure chamber, the pressure amplitude changes over these distances were checked experimentally over the frequency range of the present tests. The present tests do not require a knowledge of the phase lag caused by the displacement of the probes, but only of the mean pressure level and the amplitude of the pressure pulses. The static probe measurements at the downstream position were found to be within $\pm$ 2 percent of those at the center of the chamber, whereas the downstream total probe was accurate within $\pm$ 5 percent.

6.3 Static Tube Calibration

Each tube used as the test artery was calibrated statically for elastic properties by determining the outside tube diameter as a function of internal pressure. But since flattening of the tube may occur at reduced internal pressures, the necessary measurements were made by two methods. The first method was the ohmmeter technique discussed in Section 5.4 whereby the tube's vertical diameter is determined from the micrometer readings, and the second method was a simple measurement of the tube outer circumference with a thin, taut piece of paper wrapped around it. Both measurements were performed simultaneously at various static pressures, and the tube diameter calculated. Figure 17 shows a plot of the results of both techniques and it can be seen that the two measurements agree within the experimental scatter, indicating that the flattening of the tube is negligible for the materials and wall thicknesses tested.

7. TESTS WITH NEWTONIAN FLUIDS

As pointed out earlier, the initial experiments were performed using a Newtonian fluid consisting of various concentrations of water and glycerol. This was done in order to isolate the influence of the fluid viscosity. But since whole blood is a

complex, non-Newtonian fluid (see Section 3.2) whose properties might affect the auscultatory pressure readings, later tests were performed using fresh steer blood, and those tests will be discussed in Section 8.

7.1 Test Procedure

The present experiments involve setting up several basic parameters at the start of each run and holding these parameters fixed during the test while the blood pressures (systolic and diastolic pressures) are measured by auscultation and while the instantaneous fluid pressures in the pulsating flow are recorded. Several of these fixed parameters were measured just before the actual tests. These included the physical and elastic properties of the simulated artery and the physical properties of the fluid in the artery. The details of the test procedure are outlined below:

(1) The simulated artery is installed on the apparatus with care to avoid any twisting of the tube.

(2) The pressure chamber is assembled around the simulated artery, and the leads from the aneroid pressure gage and the compressed air bottle are connected to the pressure chamber.

(3) The total and static pressure probes are installed in the artery just downstream of the pressure chamber.

(4) The temperature of the test fluid is measured and recorded.

(5) The specific gravity of the test fluid is measured and recorded.

(6) The viscosity of the test fluid is measured and recorded.

(7) The reservoir is raised above the longitudinal axis of the test "artery" about 3 feet and the liquid is allowed to fill the experimental apparatus. The water pump in the feed line from the reservoir is turned on (during this phase only) to establish a mean flow and thus transport the air bubbles to the air traps for subsequent removal from the system.

(8) The power for the recording oscillograph is turned on. The pressure transducers are connected to the 6-volt (d.c.) supply and the timing photocell is connected to the 1.5-volt (d.c.) supply.

(9) The bleed hole screw in each of the clear plastic transducer adapters is removed and each of the pressure-probe-transducer-adapter systems is bled as a unit until all the entrapped air is removed. The valves provided in the pressure lines connecting the probes to the transducer adapters are closed. A record of outputs of the transducers is made, and this corresponds to atmospheric pressure. Now, the valves in the pressure lines connecting the probes to the transducer adapters are opened and the bleed screws put in place.

(10) The transducers for the pressure probes are calibrated in place at several reservoir heights.

(11) During Setp (10), the outside circumference and the vertical outside diameter of the artery are also measured for several internal pressures (i.e., several reservoir levels).

(12) The reservoir height is adjusted to yield the selected mean pressure level for the tests. This pressure is easily monitored by observing the transducer outputs on the oscillograph. Once the reservoir height is fixed, a record of the pressure outputs from the transducers is made.

(13) The frequency and the stroke of the piston in the pulse generator are selected. The air pressure in the chamber between the 4-inch-diameter diaphragm and the piston (see Section 4.3) is adjusted in such a way that the pulse wave at the test section remains essentially sinusoidal at all frequencies. This generally requires that the diaphragm not be permitted to buckle during any part of the cycle.

(14) With the pulse generator operating, the pressure chamber is pressurized and the systolic and diastolic pressures determined by the auscultatory technique. These measurements are made independently by two observers, and the readings recorded on the data sheet.

(15) With the pressure chamber vented to atmospheric pressure (i.e., no constriction of the test artery), the oscillatory pressure outputs from the transducers are recorded along with the timing marks on the oscillograph.

Completion of these various steps constitutes the initial test run of the day, and for a subsequent run with a different test condition (for the same simulated artery) only Steps (12) to (15) have to be repeated. Steps (4) to (6) are repeated several times during the day. The singificance of the steps in the procedure outlined above are as follows:

(1) Steps (1) to (3) are installation of the "artery" and various instruments.

(2) Steps (4) to (6) give the physical properties of the test liquid.

(3) Steps (7) and (8) bring the test apparatus to operable condition.

(4) Steps (9) and (10) calibrate the transducers.

(5) Step (11) yields the elastic properties of the simulated artery.

(6) Steps (12) to (15) set the test conditions and yield the experimental data.

7.2 Data Reduction and Accuracy

All of the experimental data in the present investigation were reduced using the Vidya IBM 1620 computer, and the reduced data are presented either directly in terms of pressures (mm Hg) or in the form of pressure ratios. All of the independent variables required for the data reduction, namely ω, ν, ρ, and T were measured directly as described in Section 7.1

Since the present experiments involve oscillatory flows of a viscous fluid over the pressure probes, the effects of viscosity and acceleration on the probe accuracy had to be determined by means of a calibration tank, as explained in Section 6.2. However, the uncorrected pressures were found to be within + 1 mm Hg

of the actual pressures and are therefore well within the accuracy with which determination of the blood pressures could be made by the auscultatory technique.

Radial pressure traverses made over a wide range of test conditions indicated that the pressure output (either total or static) at any given time of the cycle was the same for all radial locations within the accuracy of the pressure transducers. This does not imply a flat velocity profile, but rather that the variation of dynamic pressure across the tube is negligble compared with the static pressure level within the tube (see Ref. 1).

The intra-arterial pressure measurements were actually made downstream from the pressure chamber (see Fig. 15 for exact locations). However, the mean pressure level measured at that location was found to be identical with that at the center of the chamber, and the amplitude of the pressure pulse for the static (lateral) pressure probe was found to be within $\pm$ 2 percent of the corresponding pressure oscillation at the center of the pressure chamber. The amplitude for the total (stagnation) of the pressure oscillation within $\pm$ 5 percent of that at the center of the pressure chamber. Therefore, the static (lateral) probe data were used exclusively, and no correction was applied.

The cross-sectional area of the pressure probes never exceeded 0.5 percent of the internal cross-sectional area of the simulated artery. Hence, no blockage correction is made to account for the presence of the pressure probe in the flow.

Both the pressure transducers and the aneroid manometer used with the pressure chamber were calibrated against a known column of mercury. The transducers were found to be accurate within the $\pm$ 1 percent specified by the manufacturer, and the aneroid was correct within 2 mm Hg at a full-scale deflection of 300 mm Hg.

The pressure required in the empty pressure chamber to bring the two rubber diaphragms into contact with one another was measured and found to be less than 2 mm Hg.

In summary, no corrections were applied to any of the measurements made herein. All probe pressure measurements are accurate within ± 1 mm Hg, and the auscultatory readings are accurate within 5 mm Hg as customary in medical practice.

In the auscultatory technique used in obtaining the systolic and diastolic pressure readings, the auditory acuity of the individual observer becomes an important factor. For this reason, the individual observers for the present experiments were trained by Vidya's medical consultant, Dr. Bruns[4], in recognizing and distinguishing the various phases of the Korotkoff sounds for determining the systolic and diastolic pressures. These readings were made independently by at least two observers whose readings agreed within 5 mm Hg in all cases, and the disappearance of sounds (the fifth phase) was used throughout as an indication of diastolic pressure.

7.3 Experimental Results and Discussion

All of the experiments described herein were performed with a sinusoidal pulse wave in the unobstructed artery (i.e., before auscultation). That is, the input wave to the system is essentially sinusoidal in all cases, although the pulse wave may be distorted in producing the Korotkoff sounds during partial occlusion. Also, since the mean flow rate in the brachial artery is believed to be small compared with the oscillatory component, all tests were performed with zero mean flow rate in the system. That is, the circulation pump was off during all runs, and the pulsating flow is that produced by the pressure pulse generator alone (see Fig. 9). A few preliminary check runs indicated that the effect of a mean flow rate on the experimental results discussed herein is negligible, provided that the intra-arterial oscillatory pressures are

---

[4]Dr. Bruns is a cardiovascular specialist and is Associate Clinical Professor of Medicine at the University of California Medical School in San Francisco.

taken as those measured by the static (lateral) pressure probe. This was done in all cases.

The data obtained during the present investigation are summarized for all test conditions in Table II. Runs in which the Korotkoff sounds were difficult to hear, or in which agreement on the systolic and diastolic pressure readings could not be reached between the two observers within an accuracy of 5 mm Hg, have been eliminated. Likewise, runs in which the pulse wave shape was clearly nonsinusoidal in the unobstructed artery have also been eliminated. All auscultatory readings appearing in Table II were obtained by averaging the individual readings of the two observers.

The tests covered a range of frequencies from about 1/3 cycle per second (20 beats per minute) to about 2.5 cycles per second (150 beats per minute). The mean pressure levels ranged from about 100 to 150 mm Hg and the fluid viscosity from that of water to about 12 times that value. In addition, three simulated arteries were tested.

During the present experimental investigation, it was noticed that the oscillatory wall displacements just proximal to (i.e., upstream of) the pressure chamber become amplified during occlusion, indicating an amplification of the oncoming pressure wave. This finding raises the question of whether the process of occluding the artery in the simulated system actually changes the pulse wave put into the system by the pressure pulse generator. Therefore, the pressure in the 4-inch section just proximal to the bifurcation was monitored with a pressure transducer, and it was found that the input wave was altered considerably at low frequencies. The values of amplitude ratio produced at the pump by occlusion of the simulated artery are listed in Table II and are plotted in Figure 18 as a function of frequency. In the human circulatory system being simulated, a ratio much different from unity would mean that applying the sphygmomanometer to the brachial artery produces a sizeable change in the pressure wave put out by the heart. Such an effect seems unlikely and, moreover, would tend to obscure the results of

the present investigation, which is intended to compare the indirect and direct pressure measurements for a constant input to the system. Therefore, although all of the data are included in Table II, runs for which the amplitude ratio A_o/A_c differed from unity by more than 5 percent have been omitted from the plotted results. It is worth noting that the amplitude ratio remained essentially equal to unity for frequencies above about 1 cycle per second, as seen in Figure 18.

Inasmuch as the auscultatory systolic and diastolic pressure readings are commonly thought to be indicative of the maximum and minimum of the corresponding oscillatory intra-arterial pressures in the unobstructed artery, the results of the present experiments are presented in the form of

$$p_s \quad \text{versus} \quad p_{max}$$

and

$$p_d \quad \text{versus} \quad p_{min}$$

where p_{max} and p_{min} are the maximum and minimum oscillatory static (lateral) pressures which existed inside the test artery <u>before</u> the pressure chamber was activated for auscultation. Experimental data have been taken over a wide range of pulse rates and mean pressures, using various concentrations of glycerol and water as the working fluid. The corresponding variation of pulse amplitude with frequency for a fixed piston stroke is shown in Figure 19.

The experimental results are presented in Figures 20 to 22 in the form p_s versus p_{max} and p_d versus p_{min}. It can be seen from Figures 20 to 22 that the auscultatory systolic pressure reading generally exceeds the maximum oscillatory intra-arterial pressure p_{max} by nearly a constant pressure for each simulated artery, independent of frequency, viscosity, or mean pressure level. Furthermore, since there was a sizeable variation in

amplitude with frequency (for a fixed piston stroke), as shown in Figure 19, the difference between p_s and p_{max} appears to be relatively independent of amplitude as well. The scatter appears to be greatest for the lowest mean pressure.

The diastolic data show considerably more scatter, which is not surprising since the diastolic reading is considerably more difficult to obtain by the auscultatory technique. However, except for the latex tubing (Fig. 22), the same general trend can be noted for the diastolic reading. That is, it generally exceeds the minimum oscillatory intra-arterial pressure by roughly a constant pressure for each tube. Furthermore, this difference (for both the systolic and diastolic pressures) is considerably larger for a thick-walled tube (Fig. 21) than for a thin-walled tube (Fig. 20) of the same material. It will be noted that the scatter is considerably larger for the latex tube (Fig. 22) and that the diastolic pressure reading therein is sometimes <u>less</u> than the corresponding minimum intra-arterial pressure, particularly at the lowest mean pressure. However, it should be mentioned that the latex tube proved to be the most difficult on which to perform auscultations, because many extraneous sounds appeared, presumably because of the acoustical properties of the tube.

All in all, with few exceptions, it would appear from Figures 20 to 22 that both the auscultatory systolic and diastolic pressure readings generally exceed the corresponding maximum and minimum intra-arterial pressures, respectively, by an amount which depends primarily upon the characteristics of the vessel itself rather than uppn the oscillatory flow inside it. This would suggest that the critical buckling pressure of the vessel may be of primary importance in the production of the Korotkoff sounds during partial occlusion. This buckling pressure is the pressure difference (external minus internal) at which the tube initially buckles from a circular into an elliptical cross section. Once this happens to the arterial wall, the reduction in cross-sectional area of the vessel causes a reduction of the fluid pressure because of the velocity through

the resulting orifice (the Bernoulli effect). This produces a further decrease in cross section, and the vessel collapses. The intermittent phenomenon which produces the Korotkoff sounds would then be initiated when the oncoming pressure wave becomes amplified ahead of the occlusion and forces the vessel to open. The pressure then drops again and the process repeats itself.

The critical buckling pressure for a thin-walled elastic tube is given by the expression (Ref. 22)

$$p_{cr} = \frac{E}{4(1 - \sigma^2)} \left(\frac{h}{R_o}\right)^3 \tag{19}$$

where E is the elastic modulus, σ is Poisson's ratio, and h and R_o are the wall thickness and radius of the tube. This expression can be evaluated for any given vessel by making use of the pressure-diameter relation

$$\frac{dp}{dR_o} = \frac{Eh}{R_o^{\,2}} \cdot \frac{1}{1 - \sigma^2} \tag{20}$$

Thus, Equation (19) can be written in the form

$$p_{cr} = \frac{dp/dR_o}{4} \cdot \frac{h^2}{R_o} \tag{21}$$

and the critical buckling pressure is obtained in terms of the slope of the pressure-diameter curve for the vessel in question.

It can be seen from Equation (21) that, for tubes having a constant value of dp/dR_o, as in the present tests (see Fig. 17), the value of the critical buckling pressure will decrease as the internal pressure rises, since h decreases and R_o increases with internal pressure[5]. But since the wall thickness of each tube

[5]This would probably not be true of real arteries, since they evidently become stiffer as the internal pressure rises (see Fig. 1).

was found to be rather nonuniform in the circumferential direction, and since h was measured only with no fluid in the tube (i.e., at atmospheric pressure), we can calculate here only approximate values of p_{cr}. These are listed in the table below and were calculated using average values of the wall thickness at atmospheric pressure and average values of R_o over the range of mean pressures tested.

Material	Nominal wall thickness	Actual wall thickness	dp/dR_o (mm Hg/mm)	h^2/R_o (mm)	p_{cr} (mm Hg)
gum rubber	1/16 in.	0.082 in.	80.6	0.34	7
gum rubber	1/8 in.	.140 in.	262	.95	62
latex	1/16 in.	.080 in.	83.3	.31	6

The values of the buckling pressures listed in the above table are seen to be of the same order as the errors in the auscultatory readings for each tube (see Figs. 20 to 22), although the errors generally exceed the buckling pressure and show considerable scatter. It will be noted that the tabulated values of p_{cr} indicate that the auscultatory errors for the 1/8-inch wall tube should be about 9 to 10 times that for either of the 1/16-inch wall tubes. A look at Figures 20 to 22 indicates an average error of about 15 mm Hg on the auscultatory readings for the two 1/16-inch wall tubes (2 to 3 times the buckling pressure) and an average error of about 80 mm Hg for the 1/8-inch wall tube (about 1.3 times the buckling pressure), yielding a factor of about 5. It will be seen that the auscultatory errors appear to agree much more closely with the critical buckling pressure for the thicker-walled tube. This may simply be due to the poor accuracy in calculating p_{cr} for the thinner tubes because of their small values and because of a more significant variation of wall thickness with pressure, which was not measured.

It would appear from the results of Figures 20 to 22 that, except for very low viscosity fluids, the auscultatory systolic and diastolic pressure readings generally exceed the corresponding maximum and minimum oscillatory pressures inside the vessel by an amount which depends primarily upon the critical buckling pressure of the tube, although other effects are evidently also present. This seems to indicate that the Korotkoff sounds are produced only if the tube is collapsed over part of the cycle, and that the essential difference between systole and diastole is the length of time during which the tube is collapsed. Thus, at systole, the vessel is collapsed over nearly the entire cardiac cycle, opening only when the peak pressure occurs. At diastole, on the other hand, the vessel is collapsed only when the intra-arterial pressure falls to its minimum level. In either case, however, the cuff pressure exceeds the corresponding internal oscillatory pressure by an amount which depends upon the elasticity and the wall thickness of the vessel being occluded.

In order to illustrate the above conclusion, a summary plot of auscultatory versus direct pressure readings has been prepared for each simulated artery tested, and these are presented in Figure 23. The systolic and diastolic data both appear on the same plot in these figures, and the straight line through the experimental data is given in all cases by the relation

$$p_s - p_{max} = p_d - p_{min} = kp_{cr} \tag{22}$$

where k is evidently between 1.0 and 4.0. It will be recalled that $k = 5$ corresponds to the theoretical occluding pressure for the vessel devoid of fluid (see Ref. 1). The fact that k differs for each tube and is greater than unity may well be related to the amplification of the oncoming wave each time the vessel collapses. This point is now under investigation and will require a more sophisticated analysis.

Certain qualitative observations were made during the present experiments which seem to warrant some mention here, although they may not bear directly on the experimental results. Perhaps the most dramatic effect in this category was the structural failure of the simulated artery after numerous auscultations. Such failures occurred on at least three samples of gum rubber tubing of 1/16-inch wall thickness ($h/R_o \approx 1/8$) and took the form of a relatively straight rupture of the tube wall in the axial direction. A photograph of such a ruptured vessel is shown in Figure 24. It will be noted that the rupture occurred in a location which is the site of a stress concentration during occlusion in the pressure chamber. It seems likely that the rupture is a fatigue failure brought on by repeated stresses associated with the production of the Korotkoff sounds.

Although the oncoming pressure wave is amplified just proximal to the occlusion, its wave shape remains essentially unchanged. On the other hand, the wave shape just distal to (i.e, downstream from) the pressure chamber changes drastically during partial occlusion. As a matter of fact, small high-frequency components appear during decompression which seem to be associated with the Korotkoff sounds themselves. Figure 25 shows an oscillograph record of the pressures just distal to the occlusion during decompression of the pressure chamber which represents the cuff of the sphygmomanometer. The first portion of the oscillograph record shows the mean pressure level and then the oscillatory pressures in the unobstructed artery, prior to activating the pressure chamber. As we move to the right in the figure, the artery is occluded and the record then shows the gradual buildup of the pressures distal to the chamber as the chamber pressure is decreased, until finally the pressure oscillation returns to its original wave shape and amplitude. The points at which the Korotkoff sounds are first heard (first phase) and finally disappear (fifth phase) are marked as systole and diastole. It is interesting to note that diastole appears to coincide with the disappearance of one of the

higher harmonics of the pulse wave, whereas systole does not appear to show any dramatic change in wave shape.

8. TESTS WITH BEEF BLOOD

Inasmuch as the experiments described in the foregoing sections were conducted using a Newtonian fluid composed of water and glycerol, the question naturally arises as to whether such results are valid for real blood. The general characteristics of blood as a fluid were discussed in Section 3.2, and it was concluded that the apparent viscosity of whole blood is intimately related to the concentration of suspended red cells. Since it is further apparent that the presence of suspended particles might well affect the production of the Korotkoff sounds, it was considered essential that tests be performed using a fluid more closely representative of whole blood in the experimental apparatus.

A preliminary investigation was made of various plastic and glass beads which are commercially available and which might be added to a solution of water and glycerol to yield a more realistic model of living blood for the present experiments. Upon microscopic examination of the samples obtained, however, it was found that the plastic beads were quite irregular in shape, and that the glass beads (although spherical in shape) were of non-uniform diameter and had excessively high density. Furthermore, it was realized that the absorption and reflection of sound would be quite different for the rigid beads than for the actual deformable red cells they are to represent. Therefore, it was decided that a meaningful check on the present experimental results would only be obtained by using real blood. The fact that the blood cells would not then be properly scaled up in accordance with the size of the simulated artery was considered to be of no significance, since the ratio of the red-cell diameter (about 8 microns) to that of the brachial artery (about 1/4 inch) is clearly negligible.

Since it would be impractical to fill the entire apparatus (capacity 250 gallons) with blood, it was necessary to make provision

to restrict the blood to the test section area without significantly affecting the operating of the apparatus or the experimental results. This was accomplished by installing a rather slack, flexible diaphragm at either end of the test section area. The pressures generated in the remainder of the apparatus (which is filled with water) are then transmitted across the diaphragms to the blood in the test section. The diaphragms, being very slack, absorb or reflect very little of the pressure impulse. With this installation, selected test cases which had already been conducted with water and glycerol as the test fluid (Section 7) were repeated using fresh steer blood as the test fluid. These test results were then compared with the water and glycerol test data in order to evaluate the dependency of auscultatory measurements upon the type of fluid involved.

8.1 Modification of Apparatus and Preliminary Test Results

The test apparatus was modified to facilitate the testing of whole steer blood by restricting the blood to the region of the test section. The blood was contained between rubber diaphragms mounted in the 1-inch-diameter clear plastic tubes which extend on either end of the simulated artery. As shown in Figure 26, the diaphragms were installed at the extreme outer ends of the 1-inch plastic tubes in order to reduce "end effects" resulting from pressure wave reflections and to damp out secondary oscillations produced by the diaphragms. In order to facilitate installation of the diaphragms, short sections of the 1-inch plastic tubes were removed as near as practicable to their inlet and outlet connections. These sections were replaced by adapters of acrylic plastic which were machined to fit over the ends of the remaining 1-inch tubing, as shown in Figure 26. The resulting joints are sealed by "O" rings. A side opening in each of the adapters acts as an inlet and drain so that the test section can be completely filled with blood. It will be noticed in Figure 25 that an angled inlet tube is installed in each of the adapters to provide connections

for a circulation pump in the event that sedimentation might require that the blood be stirred between pressure readings.

A clinical three-way stopcock was installed in the 1-inch plastic tubes near their connections to the simulated artery. These stopcocks fit a standard medical syringe which was used to inject blood into the test section for pressurizing the test section (to equalize the pressures on either side of the diaphragm) or to withdraw blood samples for examination.

Several membranes adapted from available materials were tested to determine whether diaphragms could be obtained which would have little effect on the normal operating characteristics of the apparatus or on the test results and yet have reasonable durability. The best results were obtained using ordinary toy rubber balloons of sausage shape. These balloons were inexpensive and readily available, and were replaced frequently to avoid fatigue failure or rupture. It was found that if the balloons were inflated with air until they were near their maximum expansion, and then deflated, a very thin tubular diaphragm is formed which is slightly less than 1 inch in diameter and 4 to 5 inches long. This diaphragm is then inserted into the 1-inch plastic tube, the open end of the diaphragm folded back over the plastic tube with about an inch of overlap, and the adapter pressed into place over the folded-back section of the diaphragm. The outermost "O" ring seals the joint and holds the diaphragm in place. The remaining attachments of the test section are made as previously described in Section 7, and the test section is then ready to be filled with the desired test fluid. Approximately 5 quarts of blood are required to fill the modified test section area between the two diaphragms. With the circulation pump installed, approximately 7 quarts would be required to fill the section and the return tubing.

In order to check out the modified system, several preliminary tests were conducted using water and a 10 percent solution of glycerol as the test fluids, since the latter gives a viscosity

close to that of blood in the larger vessels. The auscultatory data from these tests were then compared with tests conducted using the same fluid throughout the system without the diaphragms installed. It was found that the installation of the diaphragms produced no noticeable effects.

A sterilization chamber was designed and built for the purpose of sterilizing those components and accessories which come into contact with the blood. Since neither the blood nor the equipment were to be used in connection with living animals or humans, it was advised that the use of ultraviolet germicidal lights would be sufficient to retard spoilage of the blood and to prevent an accumulation of bacteria growth over the duration of the testing. The sterilization chamber is of plywood construction and is 12-feet high and 2-feet square, with six tubular ultraviolet germicidal lights mounted inside, as shown in Figure 27.

8.2 Preparation and Handling of Blood and Sterilization of Equipment

Since it was flet that a considerable number of special techniques might be involved with the satisfactory and safe use of whole blood, consultations were held with members of the Stanford Medical Center staff who have been involved with the development and use of the heart-lung machine[6]. Although human blood might possibly be obtained in the quantities needed, it was not recommended for use without proper equipment and trained medical personnel, because of the slight risk of contracting hepatitis and because of the necessity of matching blood types. It was decided that beef blood would be the most practical for this experiment. Beef blood which is obtained from inspected cattle is quite safe to use, is easily obtainable in large quantities, and can be mixed without regard to type. The Medical Staff's experience with cow blood

---

[6]Drs. Charles Whitcher (M.D.) and R. C. Stofer (D.V.M.) were consulted and were quite helpful in establishing the procedures followed during the whole blood tests reported herein.

had shown, however, that the red cells therein have a high sedimentation rate; therefore, provision was made for an auxiliary pump to circulate the blood between blood pressure measurements. It was also advised that heparin be used at the anticoagulant since less than 1 percent is required. Thus, dilution is not significant when compared with the 25 percent concentration of ACD solution required to prevent coagulation.

Two medical technicians were employed to assist on this portion of the test program, and arrangements were made for obtaining fresh quantities of beef blood nearly every weekday from a nearby meat packing company. Because of the availability of fresh blood, it was decided that the blood would be discarded at the end of each day's testing and a fresh supply obtained for the following day, rather than follow the strict procedures required for sterility if the blood is to be used for 2 or more days[7]. For this reason, no special precautions were taken to maintain sterility of the blood as it was collected. It was found that the most expedient method of collection was to receive the blood in sterilized plastic, 2-quart containers as the animal was being bled. Usually, 10 to 12 quarts were collected at a time (from two animals) to provide for refilling in the event of loss of blood through a failture in the system. It was decided to use only steer blood for these tests, since steers were normally slaughtered every day. This choice proved fortuitous, since sedimentation rate tests showed that steer blood has essentially a zero sedimentation rate for the first 4 days, so that the auxiliary circulation pump was not required.

Prior to filling the test section with blood, the apparatus was disassembled and the components which come in contact with the blood were scrubbed with Haemosol and thoroughly rinsed. The

---

[7]This procedure was made possible by the cooperation of the Ferrara Meat Co., Inc., San Jose, California, which contributed all of the blood used in these experiments.

brass pressure probes were coated with silicone to prevent the formation of clots on the probes. After cleaning, these sections of the apparatus and the various blood containers were placed in the sterilization cabinet (Fig. 27) for at least 8 hours (usually overnight) to reduce the bacteria count and to allow the articles to dry thoroughly. The rubber tube test section and 1-inch-diameter plastic tubes were hung vertically to ensure drainage of the wash and rinse water. It is necessary for all components and vessels in contact with the blood to be completely free of water if hemolysis is to be avoided.

8.3 Test Procedure

The basic test procedures followed when using whole blood were identical with those previously described in Section 7.1. The only changes instituted were those connected with handling the blood, introducing the blood into the test section, maintaining a null position of the diaphragms, and making the additional measurements of the physical properties of the blood. (These were made at the Palo Alto-Stanford Hospital.)

The freshly collected blood was allowed to stand in the collection containers while final installations and adjustments were made to the test apparatus. This was done to allow the blood to approach room temperature in order to reduce the temperature variation during testing. Care was exercised to prevent the blood from foaming while it was poured and fed through the various fittings of the test apparatus. Foaming was largely prevented by first slowly pouring the blood from the collection containers into the conical glass percolator shown in Figure 26. The tube clamp on the tubing connecting the percolator to the inlet on the adapter fitting was then opened slightly to allow a small flow of blood into the test section. As the test section was filling, air was removed at the stopcocks on the 1-inch plastic tube and at the downstream adapter. When the test section was filled and the air bubbles had been removed, the clamp at the percolator was closed

and the other openings in the adapters clamped shut. Since the auxiliary circulation pump was not necessary, the pump connections in the adapters were clamped shut, as shown in Figure 26.

It had been found in the preliminary testing that the best operation of the diaphragms was obtained when the diaphragms were initially in a null position; that is, doubled up limply in a central position so that they may extend an equal distance in either direction before becoming elastically deformed during a pulse. For many test conditions, the diaphragms were never in a fully extended position, but simply moved in one direction and then the other during a pulse. In this condition, the diaphragms merely "floated" between the two liquids, having little or no effect on the imposed pressure pulse. In order to obtain this initial null position at each mean pressure head, it was necessary to inject or extract blood at the test section to accommodate the increase or decrease in diameter of the simulated artery. After the rubber diaphragms were equalized in this manner, the blood pressure tests were performed following the procedure described in Section 7.1.

Several tests were made on each supply of blood to determine its physical characteristics. The sedimentation rate was measured using a Wintrobe Blood Sedimentation Test Tube, and the hematocrit was determined using a special centrifuge at the Stanford Medical Center. The specific gravity of the blood was measured with a hydrometer.

At the conclusion of each day's testing, the test section and accessories were dismantled, scrubbed with Haemosol detergent to remove all traces of blood, rinsed well, and placed in the sterilization chamber.

8.4 Experimental Results and Discussion

The data taken during the tests using steer blood were the same as described in Section 7; namely, systolic, diastolic, and intra-arterial pressure. These data were obtained for a number

of test conditions in the same range of frequency, amplitude, and mean pressure as were tested with water and with a olution of glycerol (without diaphragms installed). It was observed by the auscultators that the Korotkoff sounds were virtually unchanged, neither easier nor more difficult to hear. This observation was shared by Dr. Bruns, who was consulted frequently during the planning and the performance of the auscultatory tests with whole blood.

The experimental results for whole blood in the 1/16-inch wall gum rubber test artery are presented in Table II and Figure 28 for a range of frequencies and mean pressure levels. It can be seen from Figure 28 that the auscultatory errors for both the systolic and diastolic pressures are again relatively constnat and approximately equal to one another. Furthermore, the values of these ratios agree almost exactly with those obtained for Newtonian fluids in the same vessel (compare Fig. 28 with Fig. 20), despite the fact that the amplitudes are generally higher with the blood in the simulated artery (see Fig. 29). Unfortunately, the amplitude ratio A_o/A_c was not measured during these tests, but a subsequent test with water in the system and a mixture of water and glycerol ($\nu = 5\nu_w$) between the rubber diaphragms indicated that A_o/A_c was equal to 1.0 for frequencies above about 10 radians per second. Hence, only those experimental data which were taken at frequencies above that value are plotted in Figure 28.

The reason for the zero sedimentation rate of steer blood is evidently not understood, although the fact that steer blood has no sedimentation rate has been verified in the literature (Ref. 23). A photograph of the steer blood red cells from the present experiments was taken through a microscope and is shown in Figure 30. The shape and size of these red cells are quite similar to those given as a normal average for humans. The hematocrit of the steer blood averaged approximately 45 percent, which is also similar to human blood. The medical technician taking the hematocrit observed that almost no hemolysis had taken place in a blood sample withdrawn from the area of the pressure chamber after a period of testing. The specific gravity of all blood samples was 1.06.

With regard to the experimental results presented in Figure 28, it is difficult to assess the influence of viscosity of whole blood, which is a non-Newtonian fluid whose viscosity depends upon the shear rate and therefore varies over each cycle. This effect is illustrated in Figure 31, which shows the variation of shear rate and apparent viscosity of blood over a cycle typical of the present tests.

9. CONCLUSIONS

The results of the present experimental investigation appear to warrant certain conclusions regarding auscultatory blood pressure determinations, despite the fact that the mechanism responsible for the production of the Korotkoff sounds is as yet not understood. In particular, the following conclusions can be drawn for sinusoidal pulse waves in elastometric tubes:[8]

(1) For blood, and for Newtonian fluids of comparable viscosity, the auscultatory systolic and diastolic pressure readings generally exceed the corresponding maximum and minimum intra-arterial pressures, respectively, by an amount which depends primarily on the thickness and stiffness of the arterial wall.

(2) The magnitude of the error in both the systolic and diastolic pressure readings is generally greater than the critical buckling pressure of the arterial wall, but less than the collapsing pressure and is independent of either frequency or mean pressure level.

(3) At low fluid viscosities and/or low mean pressure levels, these errors tend to show considerable scatter, indicating that other effects may become dominant.

(4) The oncoming pulse wave is generally amplified (but unaltered in form) just proximal to the pressure cuff when the

---

[8]The auscultatory diastolic pressure referred to here is that recorded at the disappearance of Korotkoff sounds (the fifth phase).

artery is occluded. This amplification may be one factor responsible for the discrepancies between the auscultatory errors and the calculated buckling pressures.

(5) The pulse wave just distal to the pressure cuff is altered during partial occlusion to produce high harmonics which are believed to be associated with the Korotkoff sounds themselves.

(6) In the case of the 1/16-inch wall gum rubber tubing, a longitudinal rupture of the simulated artery occurred within the cuff area after repeated auscultations. Such ruptures occurred in several samples.

(7) The diastolic pressure readings were generally more difficult to ascertain than the systolic readings and produced a larger scatter of the diastolic data.

The detailed mechanisms involved in the production of the Korotkoff sounds during partial occlusion are now under investigation under the present contract. It is hoped that theoretical and experimental information will be obtained regarding the motions of the vessel wall and the fluid and the amplification of the oncoming pressure wave ahead of the occlusion, which will permit more accurate prediction of the auscultatory systolic and diastolic blood pressures in vessels of known elastic behavior. Studies are also under way to determine the elastic behavior of the human brachial artery, on which vessel auscultatory blood pressure measurements are normally made.

The following conclusions can be drawn from the study of available data on the non-Newtonian viscous behavior of whole blood in glass capillary tubes and rotary viscometers:

(1) Whole blood behaves as a combination of a pseudoplastic and a Bingham fluid. Thus, it has a nonlinear pressure-flow diagram and requires an initial pressure to start the flow.

(2) The deviation from a linear viscous behavior depends primarily on the concentration of hematocytes or blood cells.

(3) The initial yield stress is extremely small and depends the concentration of fibrinogen present.

(4) Human and canine blood are nearly identical in viscous behavior, but bovine blood is more nearly Newtonian and generally has a higher viscosity.

(5) The Einstein equation for suspended spheres predicts the viscosity of blood quite well for very low hematocrits (below 10 percent) at high shear rates, but does not predict the non-Newtonian behavior.

REFERENCES

1. Sacks, A. H., Raman, K. R., and Abbott, D. E.: An Experimental Comparison of Auscultatory and Direct Determination of "Blood Pressure" in Simulated Arteries. Vidya Rept. No. 75, June 10, 1962.

2. Morgan, G. W. and Ferrante, W. R.: Wave Propagation in Elastic Tubes Filled with Streaming Liquid. Jour. of Acoustical Soc. of Amer., vol. 27, no. 4, July 1955, pp. 715-725.

3. Womersley, J. R.: An Elastic Tube Theory of Pulse Transmission and Oscillatory Flow in Mamilian Arteris. WADC Tech. Rept. TR 56-614, Jan. 1957.

4. Burton, A. C.: Relation of Structure to Function of the Tissue of the Walls of Blood Vessels. Physiol. Rev. 34, 1954, pp. 619-642.

5. Roy, C. S.: The Elastic Properties of the Arterial Wall. Jour. Physiol., vol. 3, Nov. 1880, pp. 125-160.

6. Bergel, D. H.: The Static Elastic Properties of the Arterial Wall. Jour. Physiol., vol. 156, 1961.

7. Bergel, D. H.: The Dynamic Elastic Properties of the Arterial Wall. Jour. of Physiol., vol. 156, 1961.

8. Altman, P. L. and Dittmer, D. S.: Blood and Other Body Fluids. Published by Federation of American Societies for Experimental Biology, 1961.

9. Einstein, A.: Eine neue Bestimmung der Molekuel Dimensionen. An Physik, 19, 289(1906), 34, 591(1911) 104.

10. Haynes, R. H. and Burton, A. C.: Role of the non-Newtonian Behavior of Blood in Hemodynamics. Amer. Jour. of Physiol., vol. 197, Nov. 1959, pp. 943-950.

11. Stafford, J. L.: Fibrinalaysis - A Fluid Situation. Proc. of the Royal Society of Medicine, Section of Experimental Medicine and Therapeutics, vol. 56, May 1963, pp. 407-418.

12. Cokelet, G. L.: The Rheology of Human Blood. Ph.D. Thesis in Dept. of Chemical Engineering, Massachusetts Institute of Technology, Jan. 1963.

13. Fahraeus, R. and Lindquist, T.: The Viscosity of the Blood in Narrow Capillary Tubes. Amer. Jour. of Physiol., vol. 96, 1931, pp. 562-568.

14. Copley, A. L. and Stainsby, G., Ed.: Flow Properties of Blood and Other Biological Systems. Pergamon Press, 1960.

15. Wells, R. E. and Merrill, E. W.: Shear Rate Dependence of the Viscosity of Whole Blood and Plasma. Sci., vol. 133, 1961, pp. 763-764.

16. Wells, R. E., Denton, R., and Merrill, E. W.: Measurement of Viscosity of Biologic Fluids by Cone Plate Viscometer. Jour. of Lab. and Clin. Med., vol. 57, 1961, pp. 646-656.

17. Coulter, N. A. and Pappenheimer, J. R.: Development of Turbulence in Flowing Blood. Amer. Jour. of Physiol., vol. 159, Nov. 1949, pp. 401-408.

18. Kumin, K.: Inaugural Dissertation der Universitat Bern. Freiburg in der Schweiz, Paulusdruckerei, 1949.

19. Bayliss, L. E.: Flow Properties of Blood and Other Biological Systems. Edited by A. Copley and G. Stainsby. Pergamon Press, 1960, pp. 29-62.

20. Den Hartog, J. P.: Mechanical Vibrations. McGraw-Hill Book Co., Inc., 3rd Edition, 1947, London and New York.

21. Erlanger, J.: Studies in Blood Pressure Estimation by Indirect Methods. II. The Mechanism of the Compression Sounds of Korotkoff. Amer. Jour. of Physiol., vol. 40, 1961, pp. 82-446.

22. Timoshenko, S.: Theory of Elastic Stability. Engineering Societies Monograph, McGraw-Hill Book Co., Inc., New York, 1936, p. 216.

23. Coffin, D. L.: Manual of Veterinary Clinical Pathology. Third Edition, Comstock Publishing Assoc., Ithaca, New York, 1953.

24. Wilkenson, W. L.: Non-Newtonian Fluids. Pergamon Press, New York, 1960.

TABLE I

SUMMARY OF VISCOSITY DATA

Ref. No.	Author	Year	Type of Blood	Additive	Anti Coagulant	Anti-Coagulant (% by volume)	Concentration of Hematocytes (% by volume)	Temp. of Blood in °C	Type of Viscometers*	Tube Diameter Annular Gap (mm)	Angle of cone (deg)	Maximum Shear Rate (sec^{-1})
10	Haynes and Burton	1959	Human	ACD	ACD	17.5 to 100	0 to 82.5	25.5	CAP	0.057 to 0.747	-	500
12	Cokelet	1963	Human	Plasma and Serum	ACD or isotonic citrate	<0.10	0 to 66	10 to 37	CYL	1.50	-	20
13	Fahraeus & Lindquist	1931	Human	-	Sodium citrate	5.0	normal ≈ 43	38	CAP	0.040 to 0.505	-	10,000
15	Wells & Merrill	1961	Human	Plasma	Potassium, Oxalate & Heparin	-	0 to 57	37	CON	-	1°33'	225
16	Wells, Denton, & Merrill	1961	Human	Plasma	None	-	33 to 57	37	CON	-	2°33'	125
17	Coulter and Pappenheimer	1949	Bovine	-	Isotonic, sodium citrate & heparin	0.10	10 to 63	15 to 37	CAP	1.26 to 3.40	-	12,000
18	Kumin	1949	Bovine	Plasma	?	-	40	?	CAP	0.029 to 2480	-	2,800
19	Bayliss	1959	Canine	Plasma	Not known	-	25 to 59	37	CAP	0.076 to 5.00	-	1,800

*CAP - Capillary Viscometer
CYL - Rotary Viscometer, Cylindrical
CON - Rotary Viscometer, Cone-Plate

Note: All viscometers used in the above references were siliconized.

TABLE II

SUMMARY OF EXPERIMENTAL DATA

SIMULATED ARTERY - GUM RUBBER 1/16 INCH WALL
FLUID - WATER - GLYCEROL MIXTURE, $\nu = 12\ \nu_w$

Run	ω	p_{max}	p_{min}	p_o	PA	p_s	p_d	$\frac{p_s}{p_{max}}$	$\frac{p_d}{p_{min}}$	$\frac{A_o}{A_c}$
2803	3.41	157.8	107.0	132.44	25.37	189.00	161.00	1.19	1.50	1.66
2804	3.89	149.6	115.2	132.44	17.20	181.00	178.00	1.20	1.54	1.23
2805	4.63	146.6	118.2	132.44	14.19	178.00	145.00	1.21	1.22	1.01
2806	5.12	144.4	120.4	132.44	12.04	178.00	140.00	1.23	1.16	0.88
2807	5.72	144.9	119.9	132.44	12.47	179.00	132.00	1.23	1.10	0.80
2808	6.28	144.9	119.9	132.44	12.47	172.00	116.00	1.18	.96	0.86
2809	6.95	143.6	121.2	132.44	11.18	160.00	152.00	1.11	1.25	0.98
2810	8.11	141.9	122.9	132.44	9.46	159.00	154.00	1.12	1.25	1.01
2811	8.85	141.0	123.8	132.44	8.60	159.00	153.00	1.12	1.23	1.00
2812	9.98	141.9	122.9	132.44	9.46	158.00	153.00	1.11	1.24	1.00
2813	11.13	144.0	120.8	132.44	11.61	158.00	153.00	1.09	1.26	1.00
2814	12.98	144.4	120.4	132.44	12.04	159.00	156.00	1.10	1.29	1.01
2902	2.49	157.8	107.0	132.44	25.37	189.00	168.00	1.19	1.57	1.34
2903	3.19	163.4	101.4	132.44	30.96	197.00	185.50	1.20	1.82	1.94
2904	3.89	152.2	112.6	132.44	19.78	187.00	176.00	1.22	1.56	1.25
2905	4.69	147.0	117.8	132.44	14.62	182.50	139.00	1.24	1.17	0.99
2906	5.12	145.3	119.5	132.44	12.90	181.50	143.50	1.24	1.20	0.89
2907	5.63	144.4	120.4	132.44	12.04	172.00	133.00	1.19	1.10	0.81
2908	6.38	144.4	120.4	132.44	12.04	165.00	143.00	1.14	1.18	0.88
2909	7.08	143.1	121.6	132.44	10.75	159.50	149.00	1.11	1.22	0.99
2910	7.79	141.9	122.9	132.44	9.46	158.00	150.50	1.11	1.22	1.01
2911	9.05	141.0	123.8	132.44	8.60	158.00	151.50	1.12	1.22	1.01
2912	9.98	141.9	122.9	132.44	9.46	158.50	152.50	1.11	1.24	1.00
2913	10.82	144.4	120.4	132.44	12.04	157.50	151.50	1.09	1.25	0.99
2914	12.98	144.9	119.9	132.44	12.47	157.50	152.50	1.08	1.27	1.00
2915	14.42	139.7	125.1	132.44	7.31	157.50	153.00	1.12	1.22	1.00
3002	3.27	155.6	109.2	132.44	23.22	176.50	144.00	1.13	1.31	1.65
3003	3.72	152.6	112.2	132.44	20.21	180.00	175.00	1.17	1.55	1.40
3004	4.63	145.3	119.5	132.44	12.90	173.50	145.00	1.19	1.21	1.06
3005	5.19	144.4	120.4	132.44	12.04	176.00	139.50	1.21	1.15	0.92
3006	5.72	144.9	119.9	132.44	12.47	174.50	129.50	1.20	1.08	0.78
3007	6.28	146.2	118.6	132.44	13.76	173.00	130.00	1.18	1.09	0.80
3008	7.09	144.9	119.9	132.44	12.47	163.00	146.00	1.12	1.21	0.97
3009	7.82	142.7	122.1	132.44	10.32	158.00	148.00	1.10	1.21	1.01
3010	9.05	141.9	122.9	132.44	9.46	159.50	151.50	1.12	1.23	1.00
3011	9.73	141.9	122.9	132.44	9.46	158.50	152.50	1.11	1.24	1.00
3012	11.13	144.0	120.8	132.44	11.61	158.00	151.50	1.09	1.25	1.00
3013	12.98	144.9	119.9	132.44	12.47	158.50	154.00	1.09	1.28	1.00
3014	14.42	139.7	125.1	132.44	7.31	158.00	153.50	1.13	1.22	1.01
3102	2.40	168.2	134.5	151.36	16.85	196.00	187.00	1.16	1.39	1.32
3103	3.19	172.6	130.0	151.36	21.32	200.50	192.50	1.16	1.48	1.66
3104	3.89	165.6	137.0	151.36	14.27	199.00	191.00	1.20	1.39	1.18
3105	4.64	163.4	139.3	151.36	12.04	193.50	165.50	1.18	1.18	1.00
3106	5.13	162.3	140.3	151.36	11.00	194.50	140.00	1.19	.99	0.84

SIMULATED ARTERY - GUM RUBBER 1/16 INCH WALL
FLUID - WATER - GLYCEROL MIXTURE, $\nu = 12\ \nu_w$

Run	ω	p_{max}	p_{min}	p_o	PA	p_s	p_d	$\frac{p_s}{p_{max}}$	$\frac{p_d}{p_{min}}$	$\frac{A_o}{A_c}$
3107	5.75	164.4	138.2	151.36	13.07	193.50	118.00	1.17	.85	0.79
3108	6.55	165.1	137.6	151.36	13.76	188.00	122.00	1.13	.88	0.92
3109	7.18	163.2	139.4	151.36	11.86	180.00	170.50	1.10	1.22	0.99
3110	8.06	161.5	141.1	151.36	10.23	178.50	170.00	1.10	1.20	1.01
3111	8.56	160.6	142.0	151.36	9.28	177.00	173.00	1.10	1.21	0.99
3112	9.72	161.9	140.7	151.36	10.57	177.50	173.00	1.09	1.22	1.00
3113	10.88	164.6	138.0	151.36	13.33	176.50	172.00	1.07	1.24	0.99
3114	12.56	162.1	140.6	151.36	10.75	178.00	174.00	1.09	1.23	1.00
3115	14.50	157.8	144.8	151.36	6.53	174.00	173.00	1.10	1.19	1.02
3203	3.27	163.8	135.4	149.64	14.19	188.00	184.00	1.14	1.35	1.33
3204	3.89	160.1	139.1	149.64	10.49	187.00	177.50	1.16	1.27	1.18
3205	4.63	159.1	140.1	149.64	9.46	187.00	168.00	1.17	1.19	1.11
3206	5.90	158.6	140.6	149.64	9.03	191.00	163.50	1.20	1.16	0.91
3207	5.74	161.9	137.3	149.64	12.29	199.50	128.00	1.23	.93	0.71
3208	6.28	166.2	133.0	149.64	16.59	193.00	120.00	1.16	.90	0.90
3209	7.22	164.2	135.0	149.64	14.62	185.00	135.00	1.12	1.00	0.98
3210	7.89	161.6	137.6	149.64	12.04	182.50	172.00	1.12	1.25	1.00
3211	8.85	160.1	139.1	149.64	10.49	181.50	173.50	1.13	1.24	1.00
3212	9.80	160.8	138.4	149.64	11.18	179.00	173.00	1.11	1.25	1.00
3213	7.05	162.9	136.3	149.64	13.33	179.00	174.00	1.09	1.27	1.00
3214	12.60	159.5	139.7	149.64	9.89	178.50	174.50	1.11	1.24	1.02
3215	14.42	154.8	144.4	149.64	5.16	176.50	174.50	1.14	1.20	1.04
3302	2.49	123.8	92.8	108.36	15.48	152.00	138.00	1.22	1.48	1.09
3303	3.17	126.7	89.9	108.36	18.40	153.00	145.50	1.20	1.61	1.51
3304	3.79	124.7	92.0	108.36	16.34	155.00	146.00	1.24	1.58	1.37
3305	4.77	119.5	97.1	108.36	11.18	143.50	127.00	1.20	1.30	1.12
3306	5.11	120.8	95.8	108.36	12.47	147.50	122.50	1.22	1.27	1.10
3307	5.72	123.2	93.4	108.36	14.87	162.00	109.00	1.31	1.16	0.82
3308	6.38	122.3	94.3	108.36	14.01	159.00	178.50	1.30	1.89	0.74
3309	7.16	122.1	94.6	108.36	13.76	144.00	87.00	1.17	.91	0.91
3310	7.85	119.5	97.1	108.36	11.18	140.50	129.50	1.17	1.33	1.01
3311	8.98	117.8	98.9	108.36	9.46	139.00	132.00	1.17	1.33	1.01
3312	9.98	117.4	99.2	108.36	9.11	138.00	131.00	1.17	1.32	1.02
3313	11.00	119.1	97.6	108.36	10.75	137.00	130.00	1.15	1.33	0.60
3314	12.64	122.3	94.3	108.36	14.01	137.00	132.50	1.12	1.40	1.75
3315	14.30	116.2	100.4	108.36	7.91	137.00	133.50	1.17	1.32	1.01
3316	5.06	120.4	96.3	108.36	12.04	148.50	121.00	1.23	1.25	1.10

SIMULATED ARTERY - GUM RUBBER 1/16 INCH WALL
FLUID - WATER - GLYCEROL MIXTURE, $\nu = 6\ \nu_w$

Run	ω	p_{max}	p_{min}	p_o	PA	p_s	p_d	$\frac{p_s}{p_{max}}$	$\frac{p_d}{p_{min}}$	$\frac{A_o}{A_c}$
3402	2.48	125.5	91.1	108.36	17.20	162.00	129.50	1.29	1.42	0.99
3403	3.23	130.2	86.5	108.36	21.84	158.50	148.00	1.21	1.71	1.54
3404	3.86	133.2	83.5	108.36	24.85	165.50	119.00	1.24	1.42	1.45
3405	4.58	120.4	96.3	108.36	12.04	157.00	128.00	1.30	1.32	1.08
3406	5.12	120.5	96.1	108.36	12.21	157.50	121.00	1.30	1.25	1.05
3407	5.76	119.7	96.9	108.36	11.43	163.50	100.00	1.36	1.03	0.78
3408	6.40	124.8	91.8	108.36	16.51	167.50	80.00	1.34	.87	0.68
3409	7.13	123.1	93.5	108.36	14.79	155.50	77.50	1.26	.82	0.90
3410	7.91	119.5	97.1	108.36	11.18	146.00	107.00	1.22	1.10	1.03
3411	9.01	118.0	98.6	108.36	9.71	143.50	122.00	1.21	1.23	1.01
3412	10.25	117.3	99.3	108.36	9.03	140.00	111.50	1.19	1.12	0.99
3413	11.19	118.6	98.0	108.36	10.32	139.50	133.50	1.17	1.36	0.99
3414	12.73	124.7	92.0	108.36	16.34	141.00	130.50	1.13	1.41	1.01
3502	2.68	139.3	70.5	104.92	34.40	174.00	111.00	1.24	1.57	1.42
3503	3.21	146.6	63.2	104.92	41.71	185.00	104.00	1.26	1.64	2.37
3504	3.88	136.9	72.9	104.92	31.99	185.50	104.50	1.35	1.43	1.57
3505	4.67	122.4	87.3	104.92	17.54	167.00	114.00	1.36	1.30	1.00
3506	5.09	120.5	89.2	104.92	15.65	166.00	100.50	1.37	1.12	0.93
3507	5.68	117.8	92.0	104.92	12.90	159.50	97.00	1.35	1.05	0.78
3508	6.49	118.0	91.7	104.92	13.15	154.00	79.50	1.30	.86	0.80
3509	7.16	117.2	92.6	104.92	12.29	141.50	86.00	1.20	.92	0.94
3510	8.00	115.8	93.9	104.92	10.92	136.00	121.00	1.17	1.28	1.02
3511	8.85	113.9	95.8	104.92	9.03	133.00	126.00	1.16	1.31	1.00
3602	2.57	170.5	135.6	153.08	17.45	203.50	189.00	1.19	1.39	1.74
3603	3.26	172.0	134.1	153.08	18.92	200.50	193.50	1.16	1.44	1.44
3604	3.78	173.9	132.1	153.08	20.89	206.00	200.50	1.18	1.51	1.36
3605	5.10	163.8	142.3	153.08	10.75	204.00	160.00	1.24	1.12	0.92
3606	5.69	164.2	141.9	153.08	11.18	188.00	161.00	1.14	1.13	1.01
3607	11.13	168.5	137.6	153.08	15.48	186.00	176.00	1.10	1.27	0.99
3702	2.78	115.2	77.4	96.32	18.92	144.00	122.00	1.25	1.57	1.41
3703	3.26	119.4	73.1	96.32	23.13	144.00	98.00	1.20	1.34	1.44
3704	3.90	122.1	70.5	96.32	25.80	144.00	98.00	1.17	1.39	1.85
3705	4.63	109.4	83.1	96.32	13.15	140.00	110.00	1.27	1.32	1.08
3706	5.26	108.4	84.1	96.32	12.12	139.00	88.00	1.28	1.04	1.10
3707	5.79	109.9	82.7	96.32	13.58	142.00	72.00	1.29	.87	0.82
3708	6.38	112.3	80.3	96.32	15.99	150.00	64.00	1.33	.79	0.66
3709	7.24	110.7	81.8	96.32	14.44	142.00	58.00	1.28	.70	0.78
3710	8.08	109.6	82.9	96.32	13.33	130.00	79.00	1.18	.95	1.00
3711	8.77	106.7	85.9	96.32	10.40	125.00	92.00	1.17	1.07	1.01
3712	10.09	105.6	87.0	96.32	9.28	122.00	90.00	1.15	1.03	1.00
3713	11.13	106.2	86.4	96.32	9.89	120.00	74.00	1.12	.85	0.99
3714	12.81	110.5	82.1	96.32	14.19	122.00	114.00	1.10	1.38	1.00
3715	14.53	109.2	83.4	96.32	12.90	126.00	118.00	1.15	1.41	1.01
3717	5.74	113.7	78.8	96.32	17.45	170.00	70.00	1.49	.88	0.75

SIMULATED ARTERY - GUM RUBBER 1/16 INCH WALL
FLUID - WATER.

Run	ω	p_{max}	p_{min}	p_o	PA	p_s	p_d	$\frac{p_s}{p_{max}}$	$\frac{p_d}{p_{min}}$	$\frac{A_o}{A_c}$
3802	2.48	141.2	115.6	128.48	12.81	174.50	148.50	1.23	1.28	0.49
3803	3.24	142.6	114.6	128.65	14.01	169.50	160.00	1.18	1.39	2.35
3804	3.91	144.9	107.1	126.07	18.92	171.00	130.50	1.18	1.21	2.18
3805	4.71	141.0	115.9	128.48	12.55	173.50	137.00	1.23	1.18	1.18
3806	5.20	138.3	119.9	129.17	9.20	163.50	132.50	1.18	1.10	1.18
3807	5.77	136.0	118.8	127.45	8.60	171.00	120.50	1.25	1.01	0.94
3808	6.40	136.9	113.4	125.21	11.78	176.00	109.50	1.28	.96	0.80
3809	7.24	135.8	108.0	121.94	13.93	178.00	72.00	1.31	.66	0.61
3810	7.95	142.1	113.7	127.96	14.19	163.00	110.00	1.14	.96	1.09
3811	8.89	137.8	119.7	128.82	9.03	161.50	139.50	1.17	1.16	1.04
3812	9.98	136.8	121.8	129.34	7.48	161.00	131.00	1.17	1.07	1.01
3813	11.19	137.8	121.5	129.68	8.17	161.50	118.50	1.17	.97	1.00
3814	12.98	142.0	116.9	129.51	12.55	160.50	143.50	1.13	1.22	0.98
3815	14.98	141.9	114.6	128.31	13.67	161.50	140.50	1.13	1.22	1.02
3904	3.99	141.7	48.8	95.28	46.44	180.00	58.00	1.27	1.18	2.79
3905	4.72	128.0	72.8	100.44	27.60	182.50	143.00	1.42	1.96	1.17
3906	5.15	120.1	80.4	100.27	19.86	172.00	100.00	1.43	1.24	1.03
3908	3.17	116.1	86.7	101.48	14.70	142.50	118.00	1.22	1.36	1.81
3909	3.91	121.4	79.8	100.62	20.81	142.50	98.00	1.17	1.22	2.00
3910	4.75	117.4	85.1	101.30	16.16	150.50	111.50	1.28	1.31	1.28
3911	5.09	111.9	90.9	101.48	10.49	141.00	112.00	1.26	1.23	1.13
3912	5.76	110.0	89.7	99.93	10.14	140.50	111.00	1.27	1.23	1.15
3913	6.42	109.2	88.9	99.07	10.14	141.00	98.00	1.29	1.10	0.93
3914	7.16	112.4	89.5	100.96	11.43	155.00	64.50	1.37	.72	0.60
3915	8.01	111.1	83.5	97.35	13.76	140.00	55.00	1.26	.65	0.85
3916	8.89	111.4	92.5	101.99	9.46	131.50	110.50	1.18	1.19	1.07
3917	10.04	108.7	94.1	101.48	7.31	133.50	107.00	1.22	1.13	1.01
3918	11.25	104.4	90.2	97.35	7.13	138.00	96.50	1.32	1.06	1.02
3919	12.56	109.8	91.7	100.79	9.03	134.00	117.50	1.22	1.28	0.98
3920	14.75	121.0	80.8	100.96	20.12	133.00	117.00	1.09	1.44	1.01
4002	2.55	153.8	136.4	145.16	8.68	175.50	171.50	1.14	1.25	0.86
4003	3.21	152.5	134.6	143.62	8.94	175.50	171.00	1.15	1.27	1.86
4004	3.85	153.7	124.8	139.32	14.44	177.50	154.50	1.15	1.23	1.63
4005	4.79	149.6	133.4	141.55	8.08	177.50	151.50	1.18	1.13	1.12
4006	5.22	147.4	135.0	141.21	6.19	174.00	148.00	1.18	1.09	1.20
4007	5.86	146.0	133.6	139.83	6.19	178.00	141.50	1.21	1.05	0.97
4008	6.47	149.9	131.4	140.69	9.28	194.00	121.50	1.29	.92	0.60
4009	7.13	154.1	117.9	136.05	18.06	194.50	85.50	1.26	.72	0.75
4010	7.91	156.3	124.7	140.52	15.82	181.00	120.50	1.15	.96	1.08
4011	9.14	150.7	130.9	140.86	9.89	174.50	152.00	1.15	1.16	1.04
4012	10.14	149.1	132.6	140.86	8.25	177.50	143.50	1.19	1.08	1.01
4013	11.13	150.8	133.3	142.07	8.77	173.50	132.00	1.15	.99	1.00
4014	12.73	156.7	125.9	141.38	15.39	173.00	158.00	1.10	1.25	0.98
4015	14.53	149.8	131.9	140.86	8.94	174.00	163.00	1.16	1.23	1.00

SIMULATED ARTERY - GUM RUBBER 1/8 INCH WALL
FLUID - WATER.

Run	ω	p_{max}	p_{min}	p_o	PA	p_s	p_d	$\frac{p_s}{p_{max}}$	$\frac{p_d}{p_{min}}$	$\frac{A_o}{A_c}$
4402	2.66	163.3	56.1	109.73	53.57	234.50	139.00	1.43	2.47	1.00
4403	3.24	183.5	12.2	97.86	85.65	247.50	166.00	1.34	13.60	0.83
4404	3.89	157.6	36.0	96.83	60.80	221.00	143.50	1.40	3.98	0.42
4410	8.93	130.2	77.2	103.71	26.48	191.00	173.50	1.46	2.24	0.95
4411	10.09	112.1	93.9	103.02	9.11	207.00	172.50	1.84	1.83	0.97
4412	11.19	109.8	94.5	102.16	7.65	202.00	173.00	1.83	1.83	0.96
4414	14.53	112.4	98.7	105.60	6.88	192.50	171.50	1.71	1.73	1.03

SIMULATED ARTERY - LATEX 1/16 INCH WALL
FLUID - WATER - GLYCEROL MIXTURE, $\nu = 6\ \nu_w$

Run	ω	p_{max}	p_{min}	p_o	PA	p_s	p_d	$\frac{p_d}{p_{max}}$	$\frac{p_d}{p_{min}}$	$\frac{A_o}{A_c}$
4502	2.71	143.7	123.1	133.45	10.26	154.00	148.00	1.07	1.20	1.39
4503	3.26	144.4	118.9	131.68	12.74	153.50	142.00	1.06	1.19	1.58
4504	3.77	148.0	116.0	132.04	16.01	155.50	144.50	1.05	1.24	1.13
4505	4.75	142.1	124.0	133.10	9.02	152.00	144.50	1.06	1.16	1.08
4506	5.13	143.6	124.3	133.98	9.64	151.00	142.00	1.05	1.14	1.07
4507	5.79	147.8	117.9	132.92	14.95	157.50	138.50	1.06	1.17	1.05
4508	6.40	149.3	112.9	131.15	18.23	161.50	118.50	1.08	1.04	0.83
4509	7.17	143.9	120.4	132.21	11.77	157.00	114.50	1.09	.95	0.74
4510	7.87	140.2	122.7	131.51	8.76	151.50	142.50	1.08	1.16	0.96
4511	8.98	139.1	127.7	133.45	5.66	151.00	145.50	1.08	1.13	1.02
4512	9.77	138.8	128.0	133.45	5.39	150.00	143.50	1.08	1.12	1.01
4513	11.31	139.1	127.0	133.10	6.01	149.00	145.50	1.07	1.14	1.00
4514	12.52	141.5	124.3	132.92	8.58	148.00	146.00	1.04	1.17	1.00
4515	13.34	145.7	120.4	133.10	12.65	148.50	147.00	1.01	1.22	1.00
4602	2.57	149.7	101.1	125.49	24.29	172.50	133.00	1.15	1.31	1.26
4603	3.24	157.5	88.8	123.17	34.35	171.50	127.50	1.08	1.43	1.56
4604	3.82	162.3	91.4	126.91	35.42	175.50	126.00	1.08	1.37	1.38
4605	4.69	153.5	109.9	131.72	21.80	163.00	137.50	1.06	1.25	1.05
4606	5.19	155.0	106.2	130.65	24.38	167.00	111.50	1.07	1.04	0.99
4607	5.76	156.9	99.6	128.33	28.65	175.00	99.00	1.11	.99	0.89
4608	6.42	153.3	105.1	129.22	24.11	174.00	99.50	1.13	.94	0.80
4609	7.17	146.8	112.3	129.58	17.26	160.00	91.00	1.08	.81	0.84
4610	7.94	141.7	119.1	130.47	11.30	154.00	102.00	1.08	.85	1.00
4611	8.94	140.5	124.3	132.43	8.09	153.00	117.50	1.08	.94	0.99
4612	9.97	140.5	124.6	132.61	7.92	152.00	121.00	1.08	.97	1.01
4613	11.26	141.6	122.8	132.25	9.43	150.50	101.50	1.06	.82	1.00
4614	12.64	144.3	114.8	129.58	14.77	150.50	135.50	1.04	1.18	1.00
4615	14.32	145.7	112.6	129.22	16.55	151.50	129.50	1.03	1.15	1.00

SIMULATED ARTERY - LATEX 1/16 INCH WALL
FLUID - WATER.

Run	ω	p_{max}	p_{min}	p_o	PA	p_s	p_d	$\frac{p_s}{p_{max}}$	$\frac{p_d}{p_{min}}$	$\frac{A_o}{A_c}$
4102	2.61	132.9	72.7	102.85	30.10	138.50	102.50	1.04	1.40	0.60
4104	4.03	114.8	90.4	102.68	12.21	134.00	117.50	1.16	1.29	1.61
4105	4.64	122.2	83.0	102.68	19.60	146.50	110.00	1.19	1.32	1.51
4106	5.16	121.8	85.9	103.88	17.97	141.50	109.00	1.16	1.26	1.32
4107	5.81	124.7	79.2	101.99	22.79	153.50	89.00	1.23	1.12	1.34
4108	6.44	123.8	77.7	100.79	23.04	173.50	87.00	1.40	1.11	0.80
4109	7.24	115.7	88.5	102.16	13.58	150.50	77.00	1.30	.87	0.70
4110	7.91	110.3	91.9	101.13	9.20	137.00	53.50	1.24	.58	0.75
4111	9.50	112.8	98.0	105.43	7.39	132.00	104.50	1.17	1.06	1.07
4112	9.93	113.0	99.5	106.29	6.79	130.50	109.00	1.15	1.09	1.02
4113	11.39	112.9	99.6	106.29	6.62	132.00	96.00	1.16	.96	1.01
4114	12.73	113.7	98.4	106.12	7.65	131.00	79.00	1.15	.80	1.00
4115	14.75	130.2	83.7	106.98	23.22	130.50	111.00	1.00	1.32	0.99
4202	2.60	147.0	112.6	129.86	17.20	164.50	144.50	1.11	1.28	0.35
4203	3.22	146.9	112.7	129.86	17.11	166.50	143.50	1.13	1.27	1.90
4204	3.91	147.4	102.2	124.87	22.61	167.50	100.00	1.13	.97	1.96
4205	4.77	149.5	103.6	126.59	22.96	166.00	140.50	1.11	1.35	1.22
4206	5.18	139.4	114.4	126.93	12.47	162.00	140.00	1.16	1.22	1.22
4207	5.71	137.7	110.9	124.35	13.41	170.50	120.50	1.23	1.08	1.16
4208	6.49	138.6	105.9	122.29	16.34	176.50	119.00	1.27	1.12	0.84
4209	7.35	141.7	105.6	123.66	18.06	184.00	83.50	1.29	.79	0.62
4210	9.88	133.9	108.6	121.26	12.64	165.50	63.50	1.23	.58	0.87
4211	10.14	135.1	121.4	128.31	6.88	158.50	136.50	1.17	1.12	1.02
4212	11.06	134.7	121.5	128.14	6.62	160.00	121.50	1.18	1.00	1.01
4213	14.86	157.8	97.6	127.79	30.10	157.50	142.50	.99	1.46	1.04
4302	2.68	126.8	76.4	101.65	25.19	187.50	112.00	1.47	1.46	0.25
4305	4.65	135.4	67.5	101.48	33.97	172.00	108.00	1.27	1.60	1.45
4306	5.11	129.6	78.4	104.06	25.62	176.50	105.00	1.36	1.33	1.15
4307	5.84	124.7	82.9	103.88	20.89	182.50	94.50	1.46	1.13	0.99
4308	6.47	120.7	81.5	101.13	19.60	175.50	85.00	1.45	1.04	0.81
4311	9.01	116.1	93.3	104.74	11.35	134.50	84.00	1.15	.90	1.10
4312	10.14	114.3	95.4	104.92	9.46	137.50	82.50	1.20	.86	1.02
4313	11.39	114.9	96.2	105.60	9.37	134.50	91.50	1.17	.95	1.01
4314	12.81	117.3	95.5	106.46	10.92	137.50	72.00	1.17	.75	0.99
4315	14.64	128.9	82.3	105.60	23.30	133.00	109.50	1.03	1.33	1.00

SIMULATED ARTERY - GUM RUBBER 1/16 INCH WALL
FLUID - STEER BLOOD

Run	ω	p_{max}	p_{min}	p_o	PA	p_s	p_d	$\frac{p_s}{p_{max}}$	$\frac{p_d}{p_{min}}$
2231	5.23	97.0	40.5	68.80	28.27	140.00	58.50	1.44	1.44
2232	5.32	93.4	50.5	72.00	21.46	142.00	55.00	1.52	1.08
2233	4.18	93.8	49.0	71.47	22.40	138.50	39.50	1.47	.80
2234	4.07	92.5	52.0	72.27	20.26	134.00	40.00	1.44	.76
2236	3.97	104.8	60.5	82.67	22.13	139.30	44.30	1.32	.73
2237	3.92	93.3	56.0	74.67	18.66	137.00	53.50	1.38	1.86
2355	2.41	93.9	56.3	75.17	18.79	142.00	130.50	1.51	2.31
2356	2.47	96.3	54.7	75.53	20.78	143.00	80.50	1.48	1.47
2357	2.57	99.7	51.3	75.53	24.21	143.30	61.30	1.43	1.19
2359	5.32	94.6	49.8	72.28	22.40	136.30	81.70	1.43	1.63
2360	3.45	154.8	114.0	134.44	20.41	206.30	127.30	1.33	1.11
2401	6.04	158.8	126.6	142.75	16.08	222.00	78.00	1.39	.61
2402	5.92	156.4	132.6	144.56	11.92	218.00	85.00	1.39	.64
2403	3.34	175.0	117.6	146.36	28.73	223.50	148.50	1.27	1.26
2483	3.14	171.1	131.7	151.42	19.69	220.00	150.50	1.28	1.51
2484	3.49	179.8	138.1	159.01	20.87	214.50	142.50	1.19	1.03
2485	2.49	168.7	131.9	150.34	18.43	219.50	199.00	1.30	1.50
2486	6.28	156.8	132.9	144.92	11.92	213.70	87.30	1.36	.65
2487	6.68	159.6	129.8	144.74	14.90	209.30	87.00	1.31	.67
2488	4.16	168.7	119.9	144.37	24.39	218.00	147.00	1.29	1.22
2491	6.28	159.7	139.5	149.61	10.11	216.00	98.50	1.35	.70
2492	6.41	161.7	134.2	147.99	13.73	216.00	88.50	1.33	.65
2494	11.42	178.3	132.8	155.58	22.76	205.50	158.50	1.15	1.19
2495	8.72	171.2	137.4	154.31	16.89	208.50	164.00	1.21	1.19
2496	7.75	168.9	134.6	151.78	17.16	210.00	132.00	1.24	.98
2497	7.85	170.4	133.8	152.14	18.25	211.00	125.00	1.23	.93
2498	7.39	170.2	126.4	148.35	21.86	214.00	102.50	1.25	.81
2504	4.75	119.0	71.2	95.12	23.88	167.50	104.00	1.40	1.46
2505	3.65	119.7	79.2	099.50	20.29	140.50	95.50	1.17	1.20
2509	13.96	122.7	76.2	099.50	23.28	141.00	98.00	1.14	1.28
2510	8.26	110.7	078.7	094.72	16.01	142.00	54.70	1.28	.69
2511	7.85	109.0	74.0	91.54	17.51	143.30	38.30	1.31	.51
2512	9.51	111.8	077.6	094.72	17.11	143.30	48.00	1.28	.61
2513	8.97	112.4	75.0	093.72	18.70	143.50	36.50	1.27	.48
2514	3.07	125.7	61.6	93.72	32.03	162.00	91.50	1.28	1.48
2515	3.34	121.7	69.2	95.52	26.26	165.30	88.70	1.35	1.28

SIMULATED ARTERY - GUM RUBBER 1/16 INCH WALL
FLUID - STEER BLOOD

Run	ω	p_{max}	p_{min}	p_o	PA	p_s	p_d	$\frac{p_s}{p_{max}}$	$\frac{p_d}{p_{min}}$
2603	12.56	157.2	107.0	132.13	25.07	178.00	130.00	1.13	1.21
2604	12.56	159.3	107.2	133.33	26.06	178.00	131.50	1.11	1.22
2605	8.72	151.0	112.4	131.73	19.30	183.00	83.00	1.21	.73
2606	8.05	150.2	108.8	129.54	20.69	185.00	78.50	1.23	.72
2607	7.66	146.4	100.2	123.38	23.08	184.50	63.50	1.26	.63
2608	7.66	146.2	101.2	123.77	22.48	184.50	63.50	1.26	.62
2609	6.28	136.9	98.3	117.60	19.30	186.00	60.00	1.35	.61
2610	4.61	152.6	94.1	123.38	29.25	200.00	110.50	1.31	1.17
2612	4.48	159.5	83.1	121.39	38.20	210.00	114.50	1.31	1.37
2613	4.61	157.0	89.7	123.38	33.63	210.00	113.50	1.33	1.26

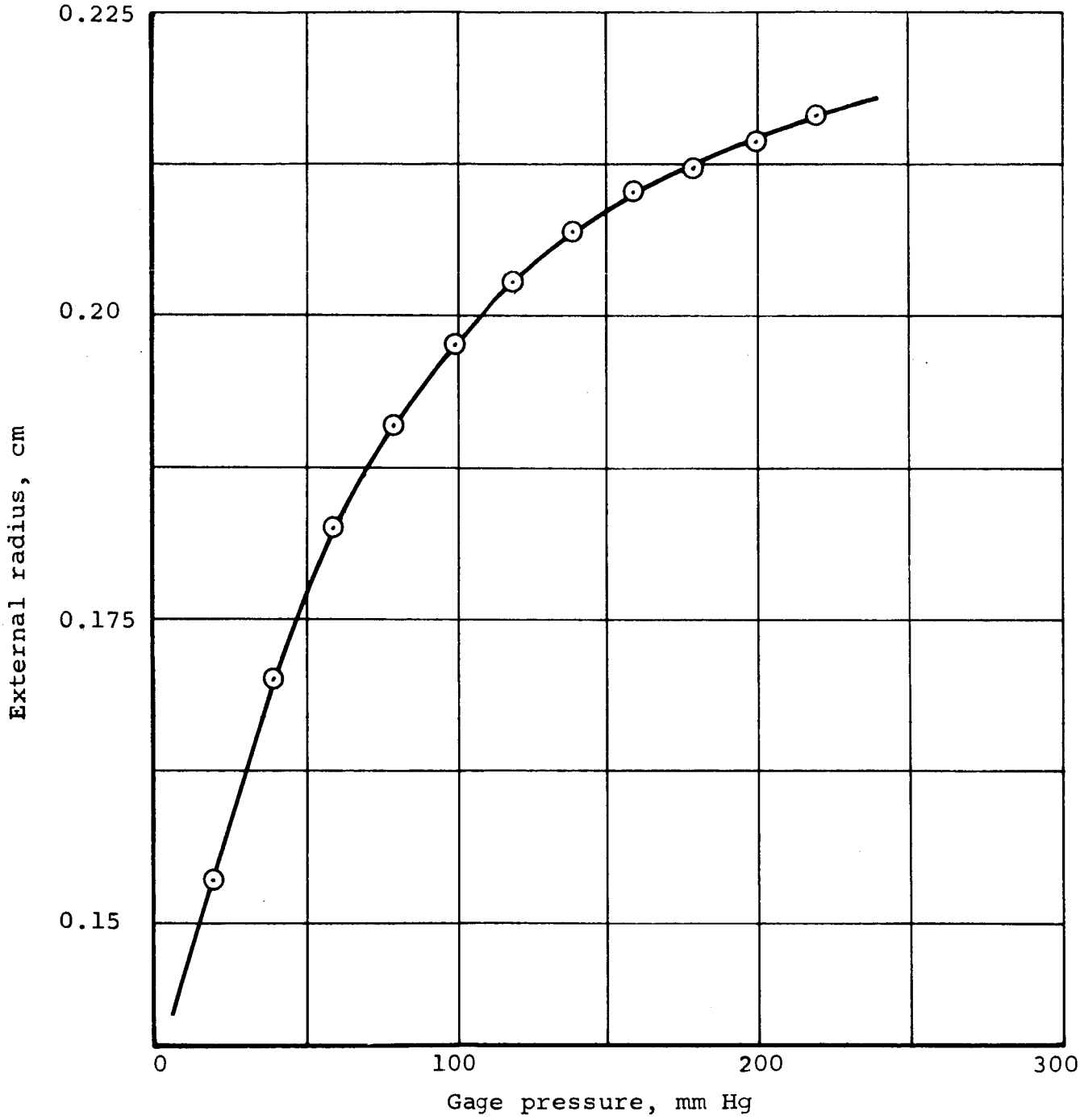

Figure 1.- Static elastic behavior of an excised human femoral artery (from Ref. 6).

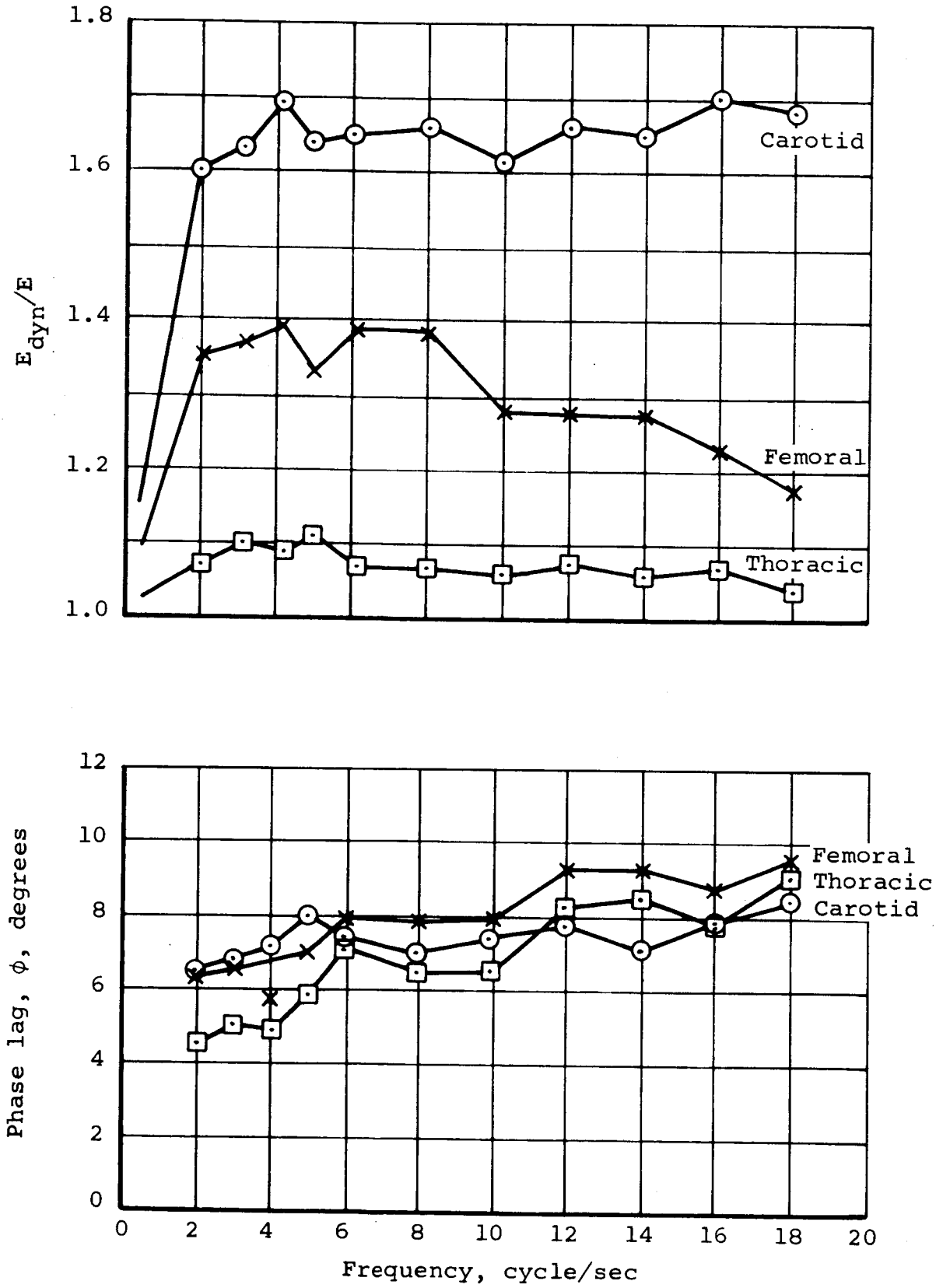

Figure 2.- Dynamic elastic behavior of various excised human arteries (from Ref. 7).

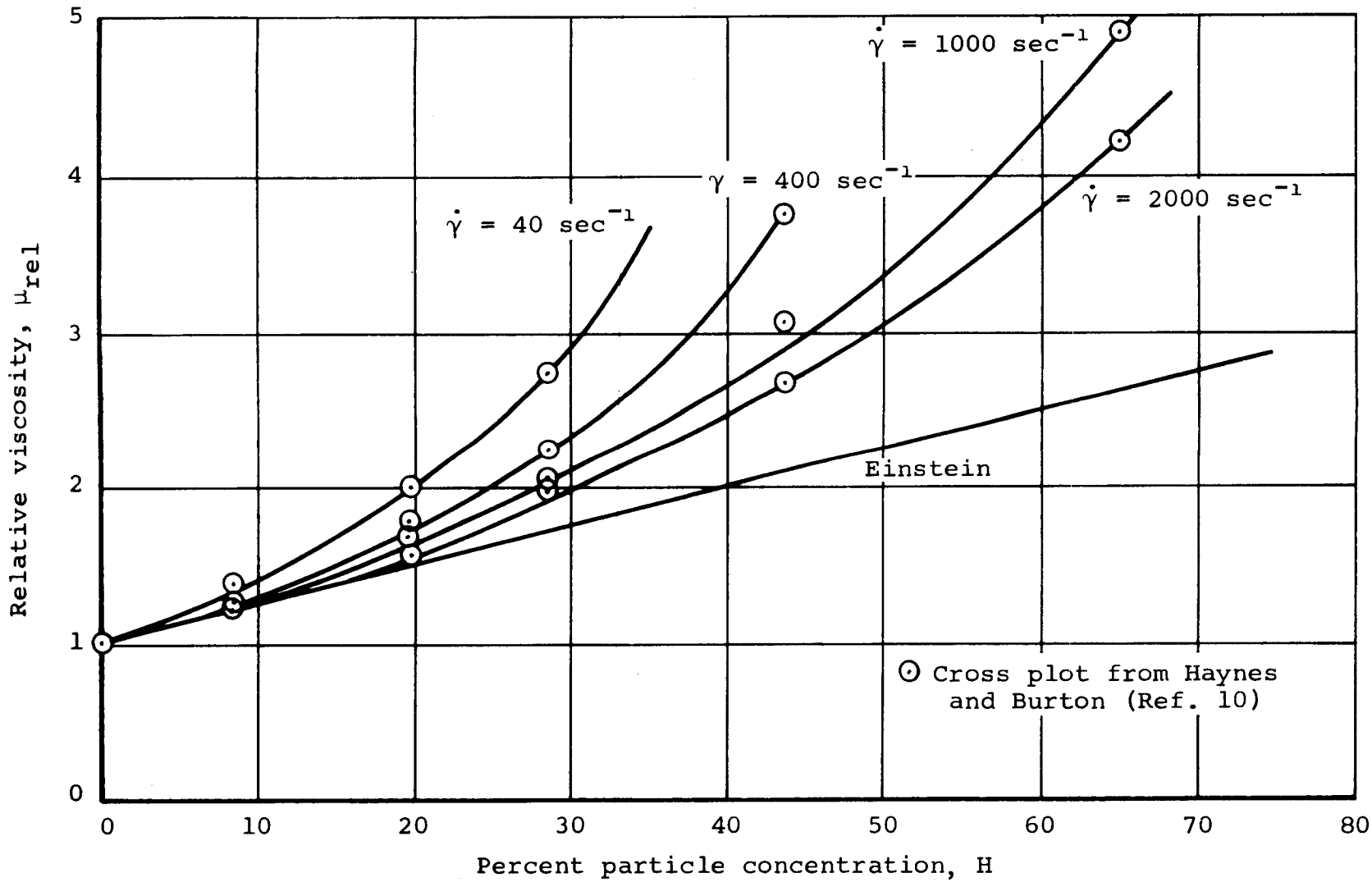

Figure 3.- Relative viscosity of suspensions of human erythrocytes in ACD solution.

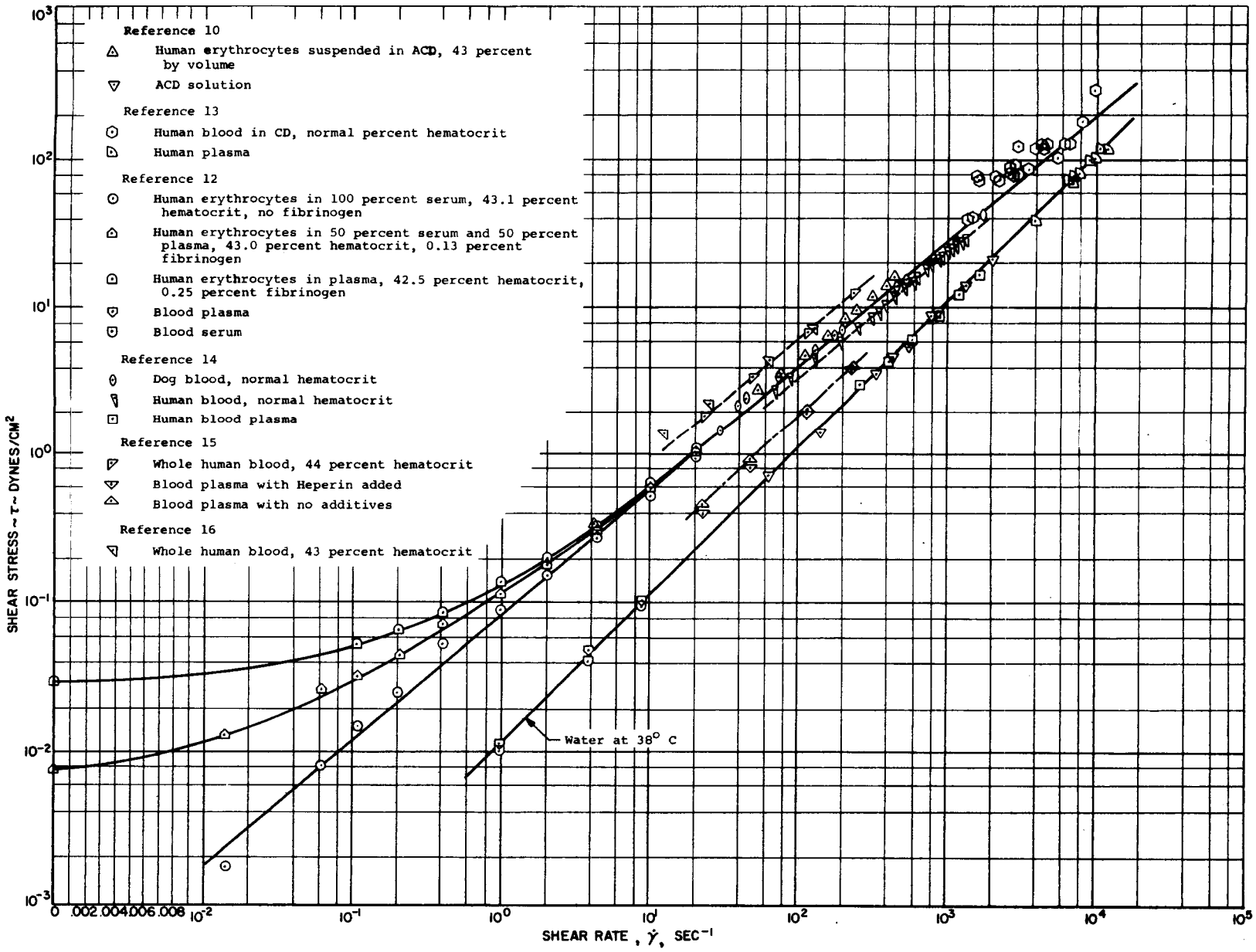

FIGURE 4.- FLOW CHARACTERISTICS OF BLOOD AND ITS CONSTITUENTS

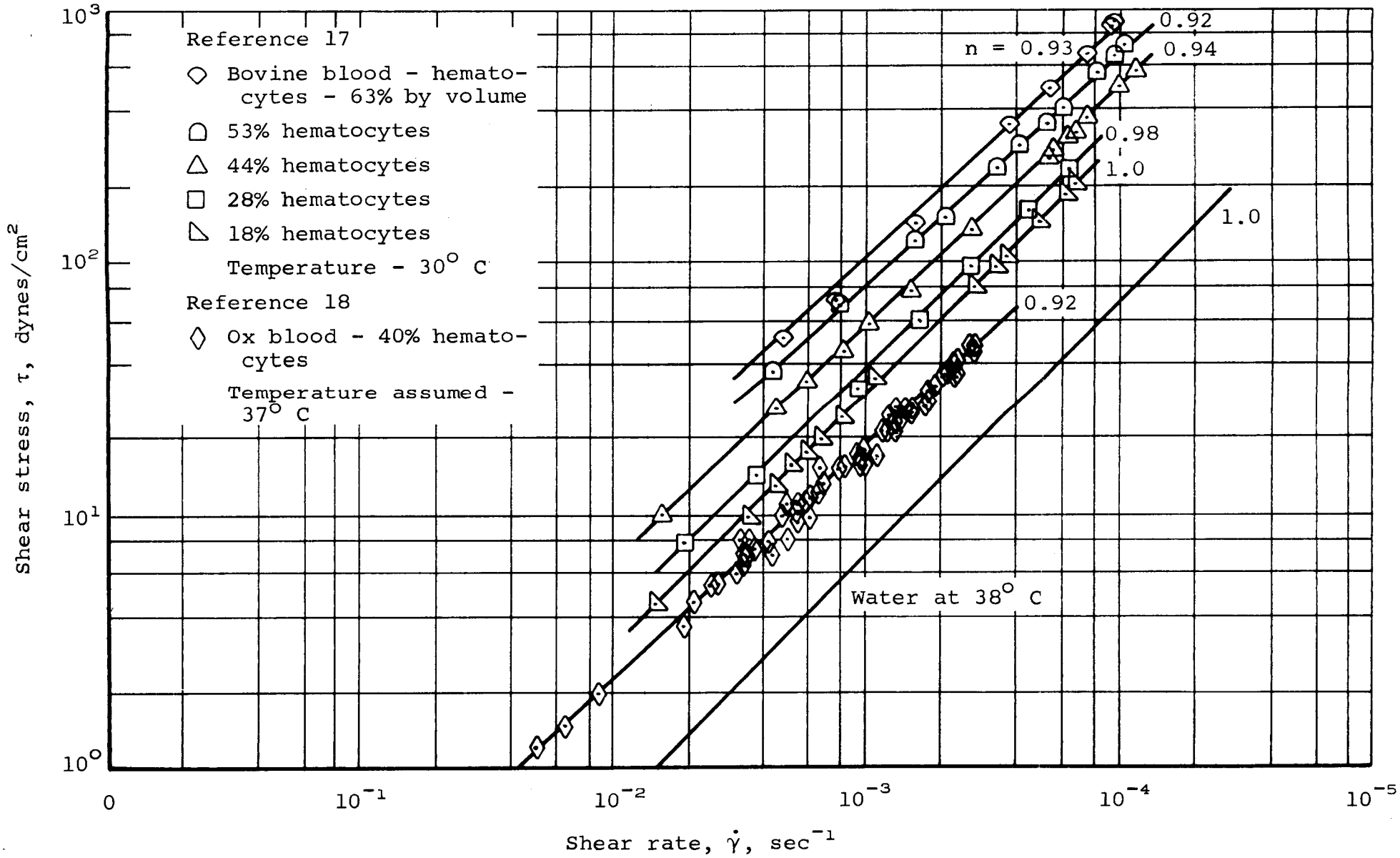

Figure 5.- Flow characteristics of bovine blood.

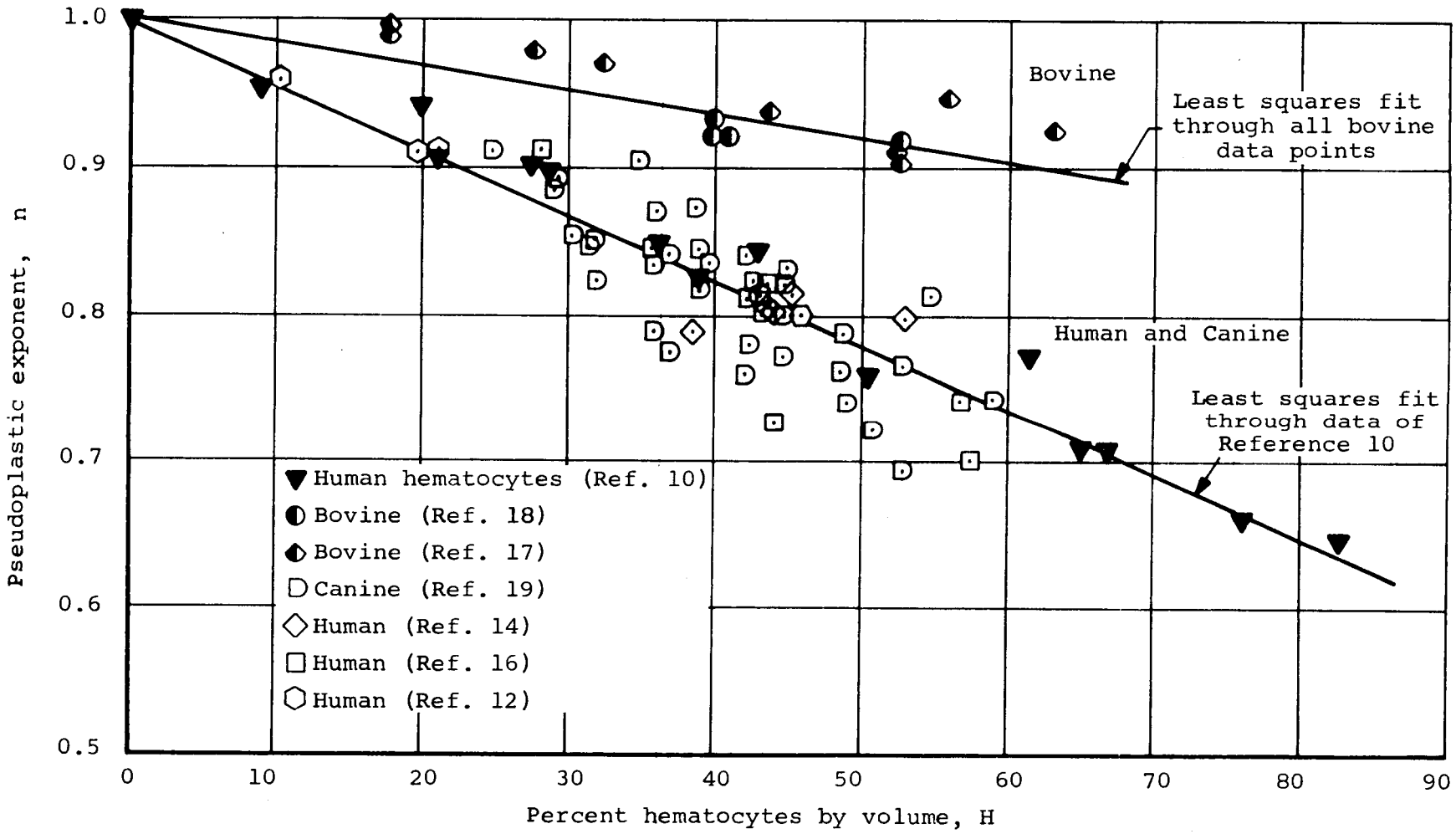

Figure 6.- Pseudoplastic exponents for whole blood.

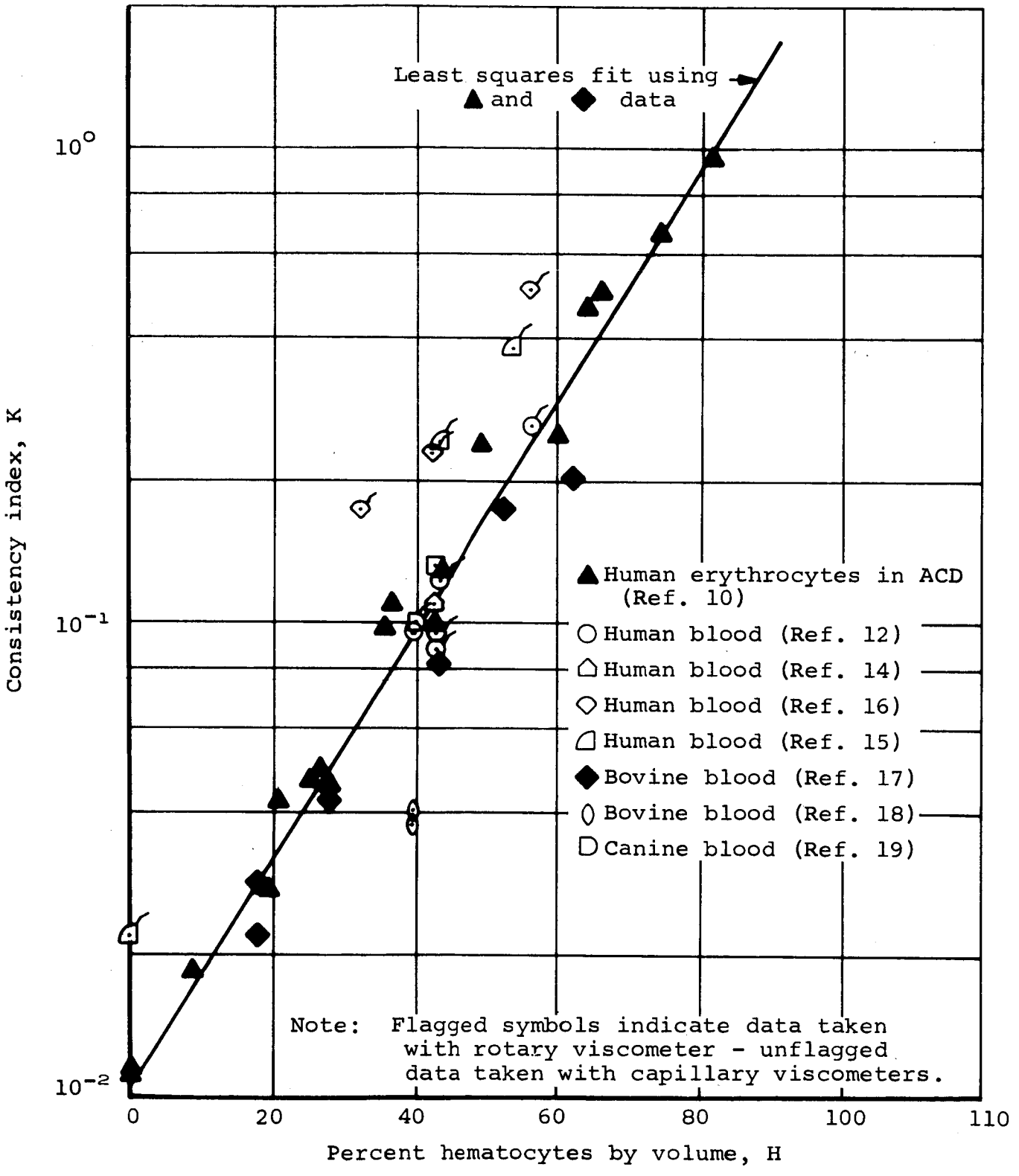

Figure 7.- Variation of the consistency index for three blood species.

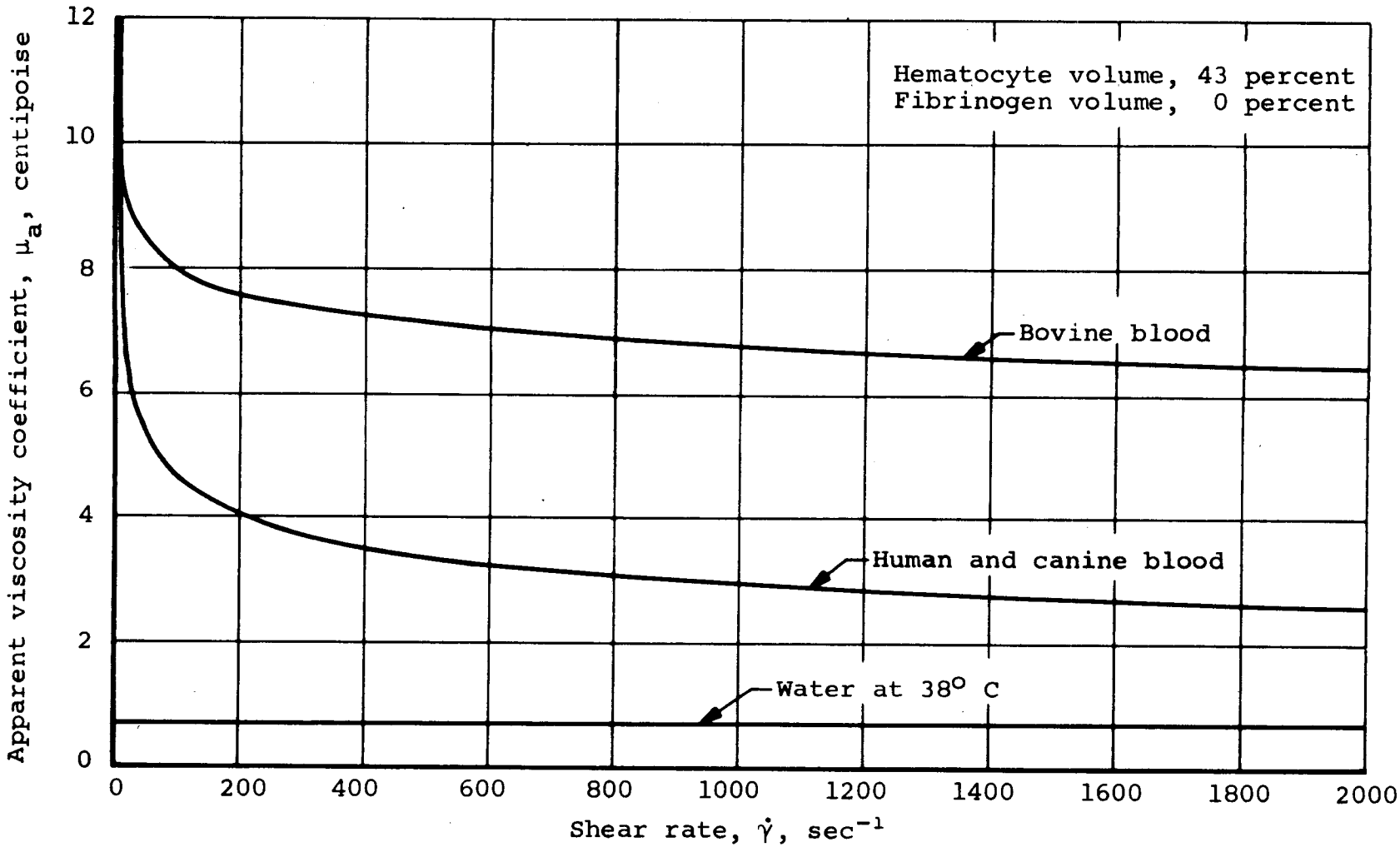

Figure 8.- Variation of viscosity coefficient with shear rate for human, canine, and bovine blood.

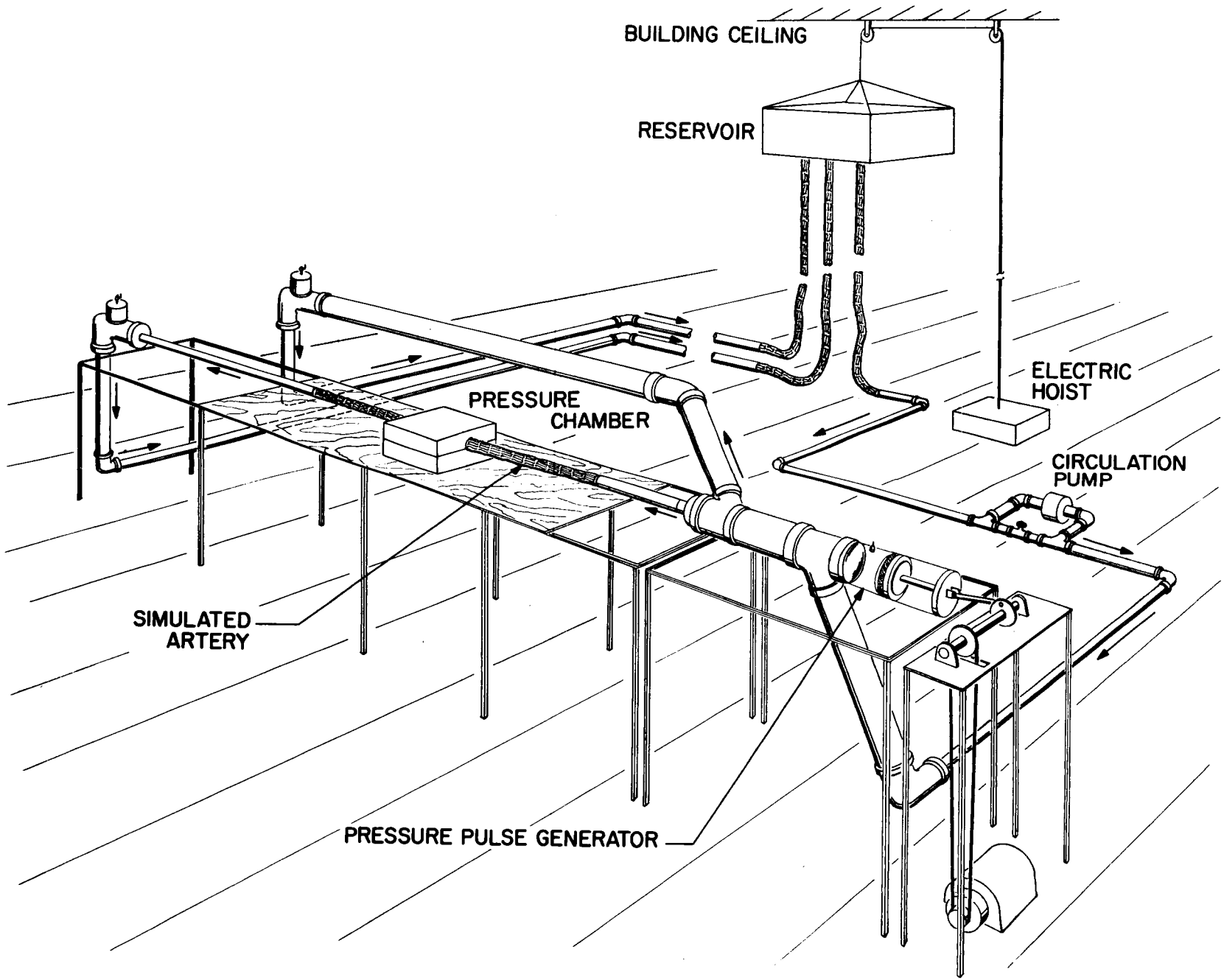

Figure 9.- Schematic sketch of experimental apparatus.

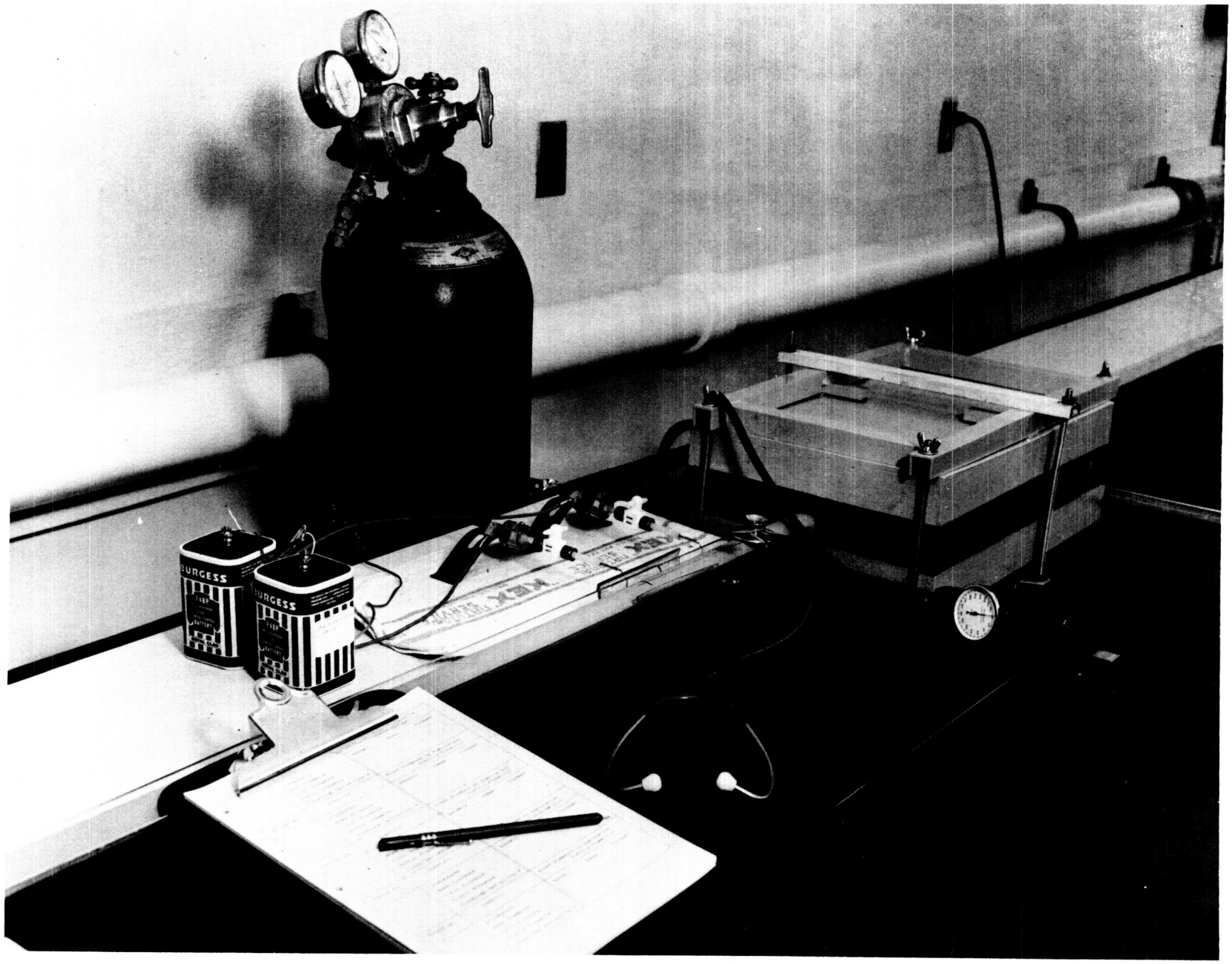

Figure 10.- Apparatus for auscultatory and direct blood pressure measurements on simulated artery.

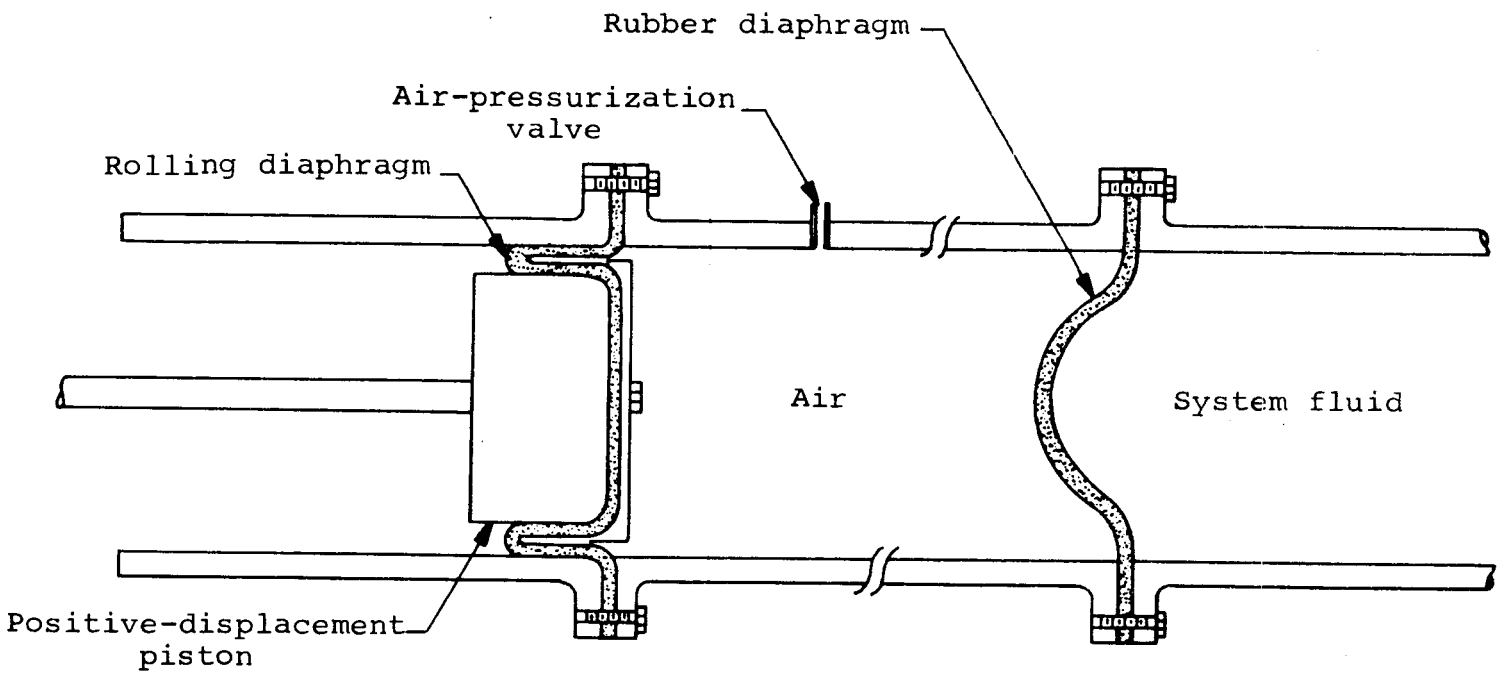

Figure 11.- Sketch of pressure pulse generator piston and diaphragm.

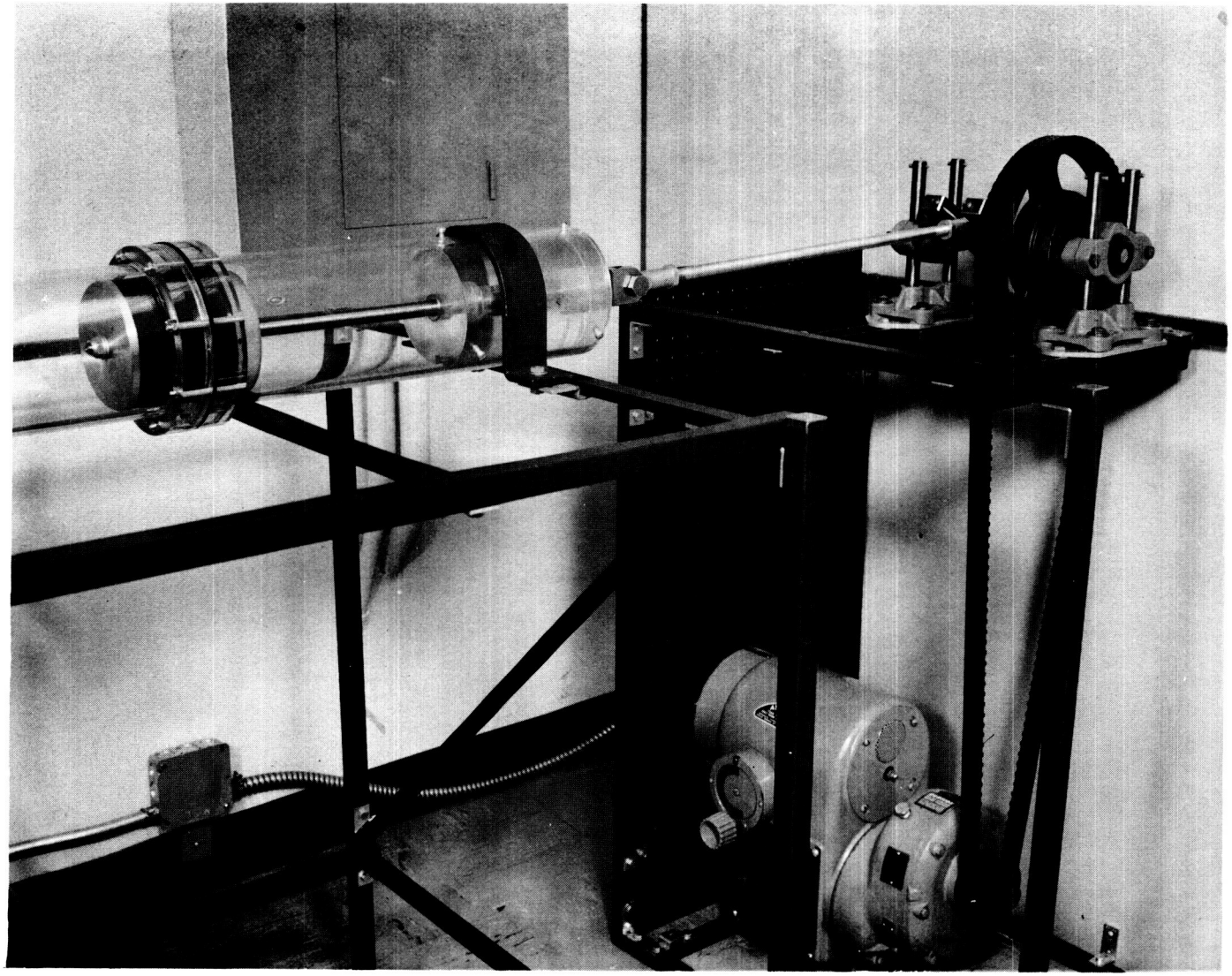

Figure 12.- Pressure pulse generator.

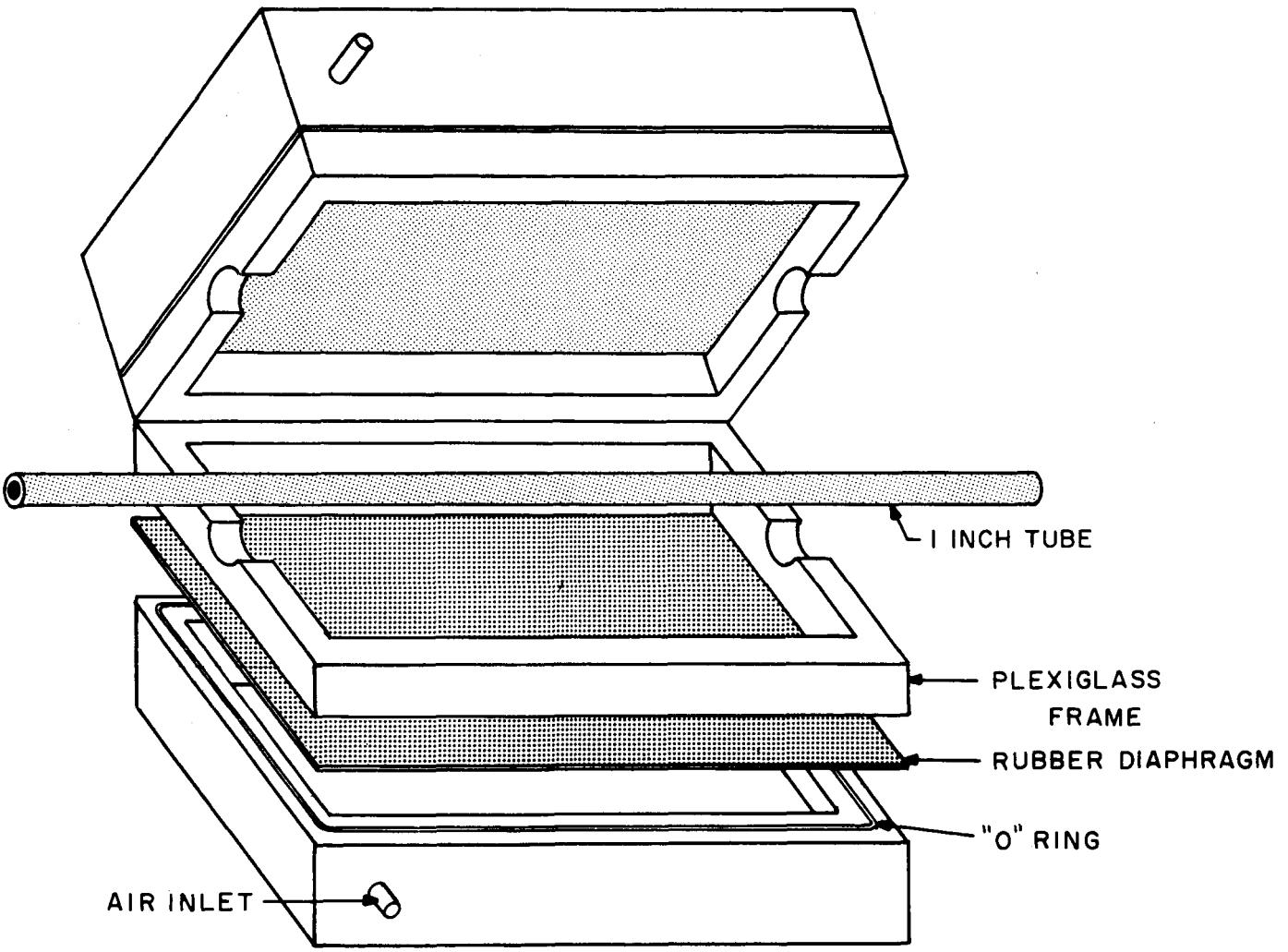

Figure 13.- Exploded view of pressure chamber.

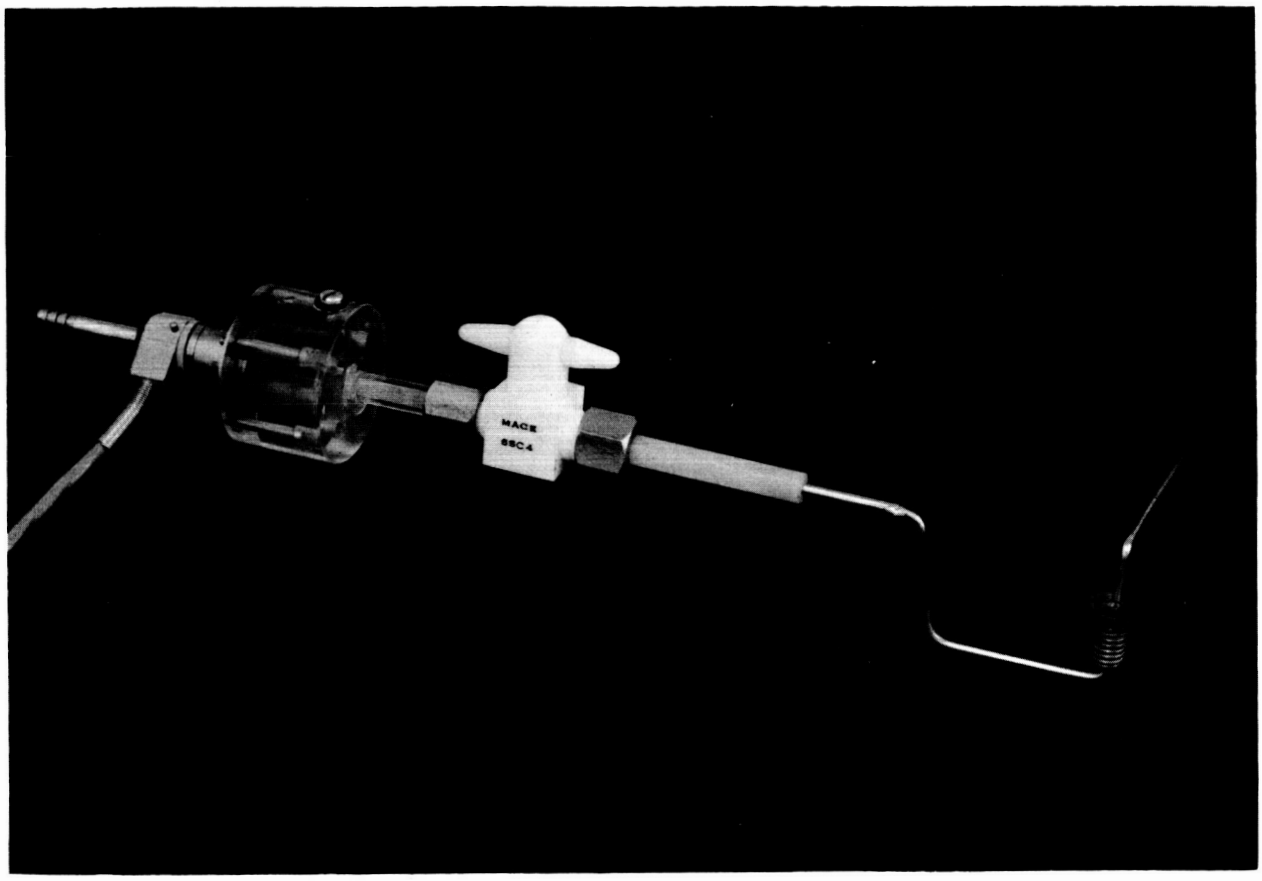

Figure 14.- Pressure transducer assembly.

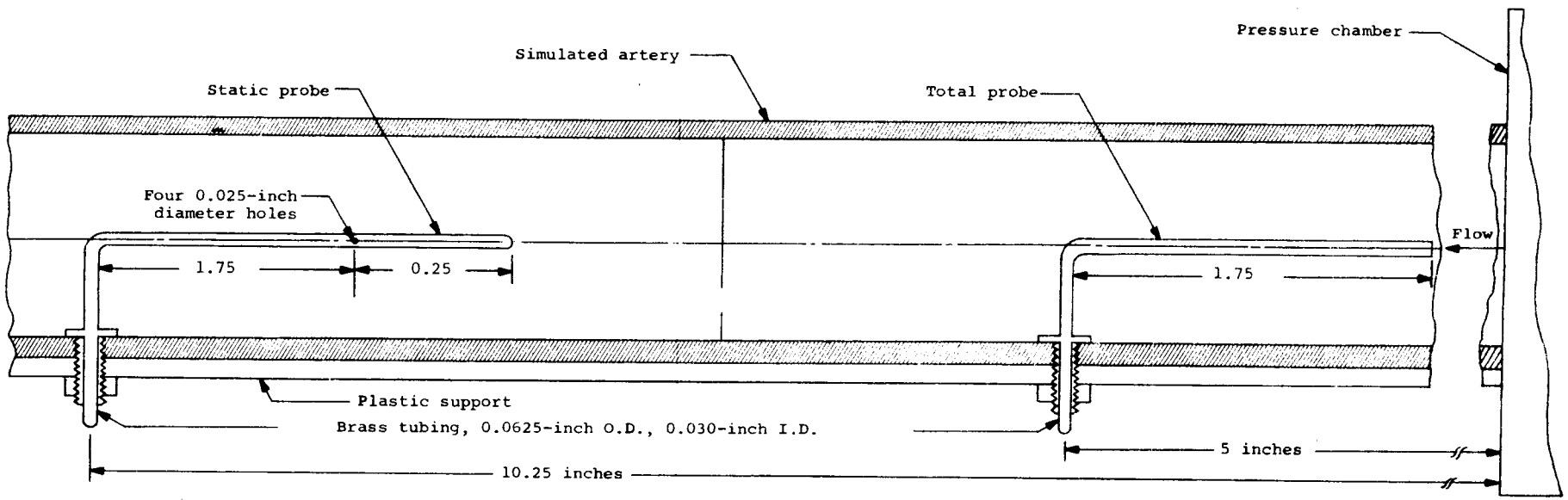

Figure 15. - Dimensions and locations of pressure probes in simulated artery.

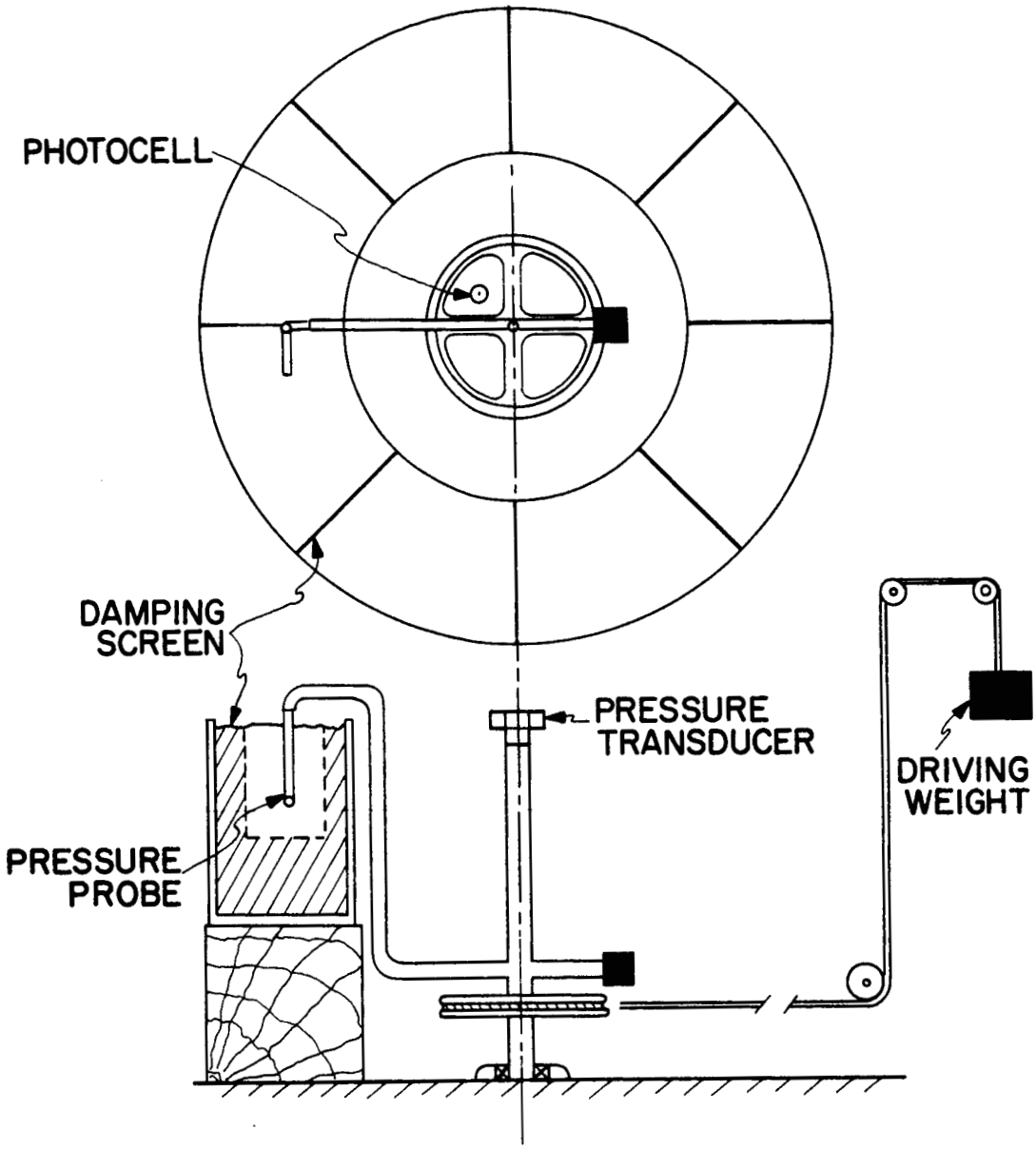

Figure 16.- Calibration rig for pressure probes.

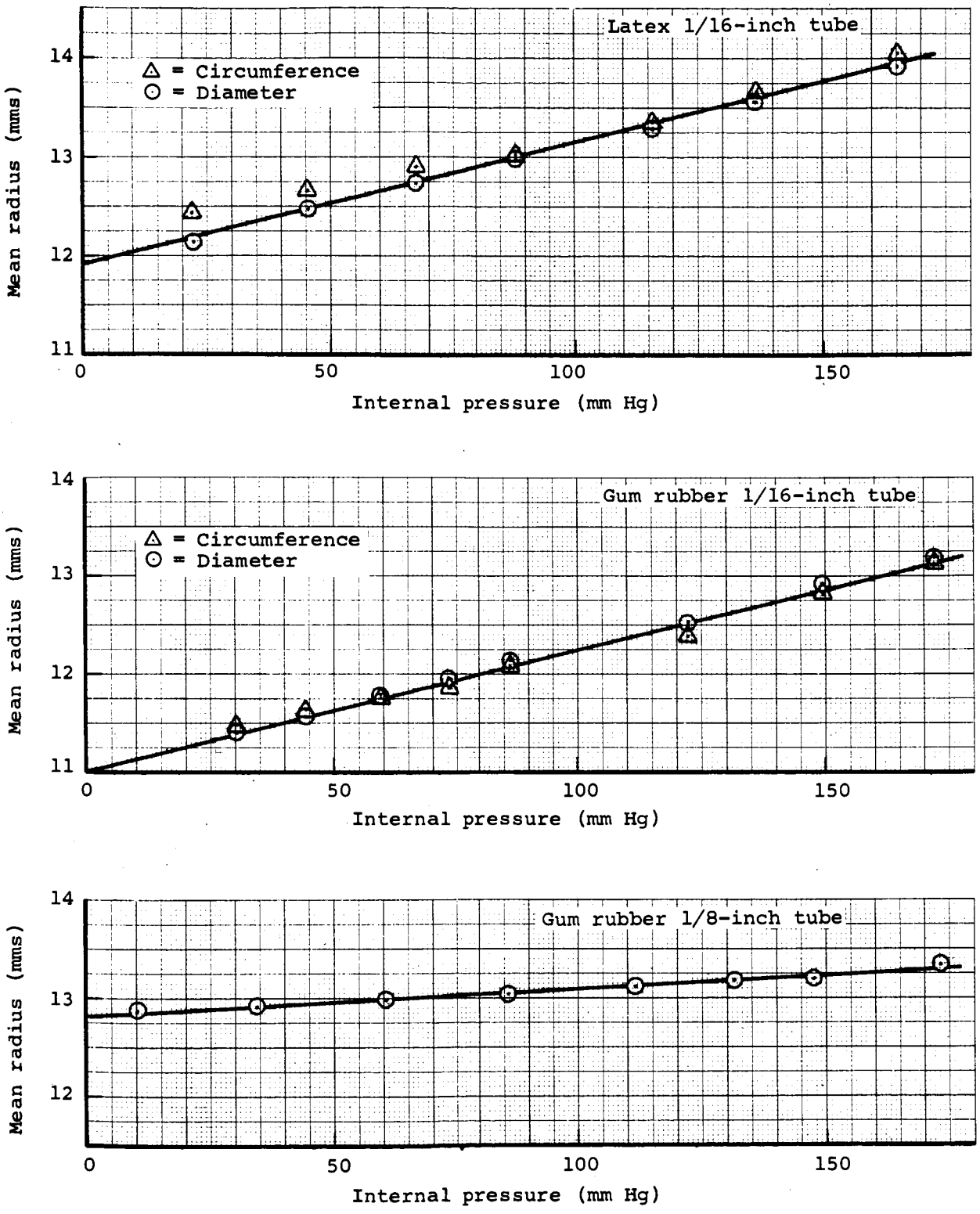

Figure 17.- Static elastic behavior of simulated arteries.

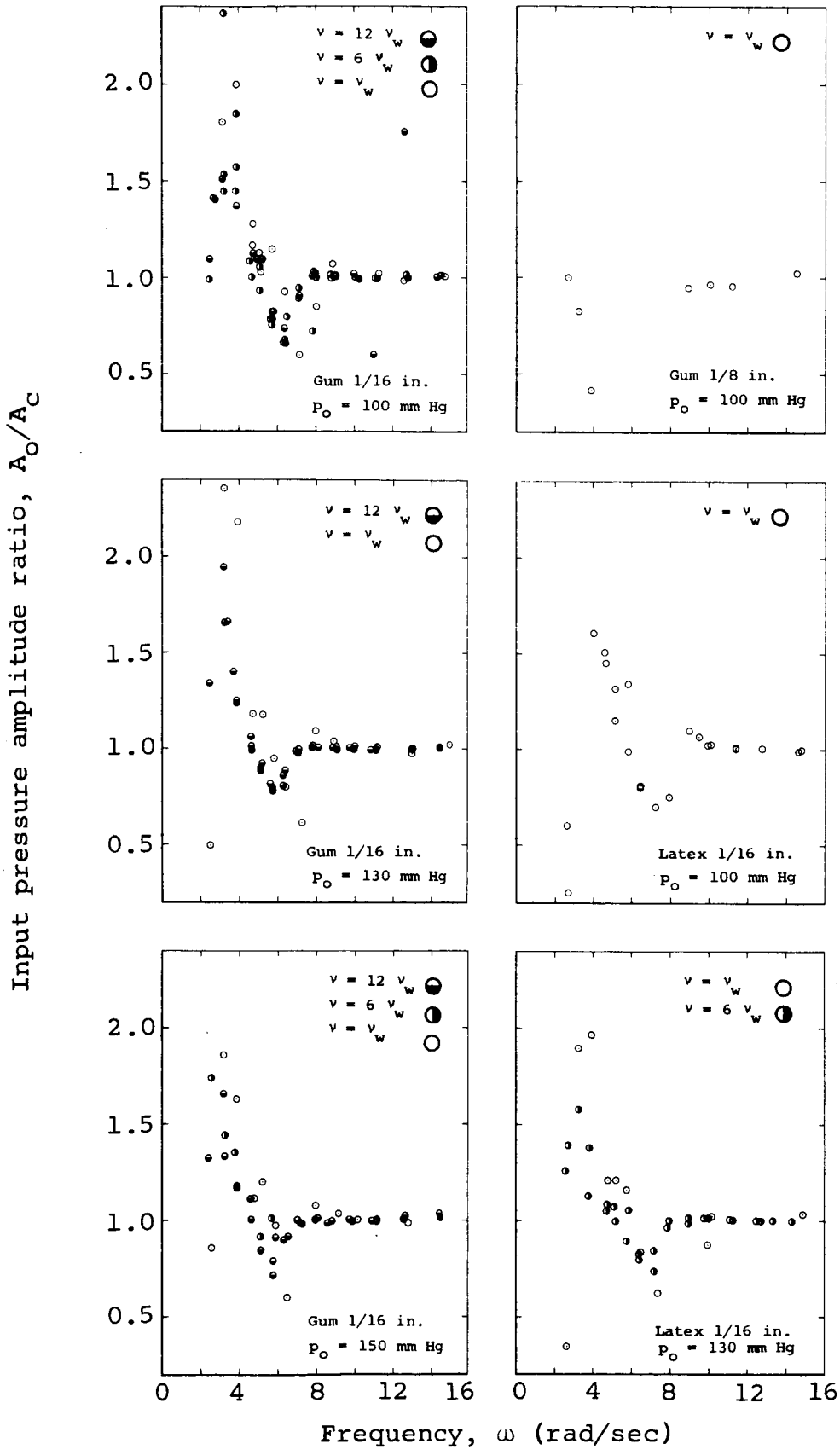

Figure 18.- Effect of artery occlusion on the amplitude of the pressure input by the pulse generator.

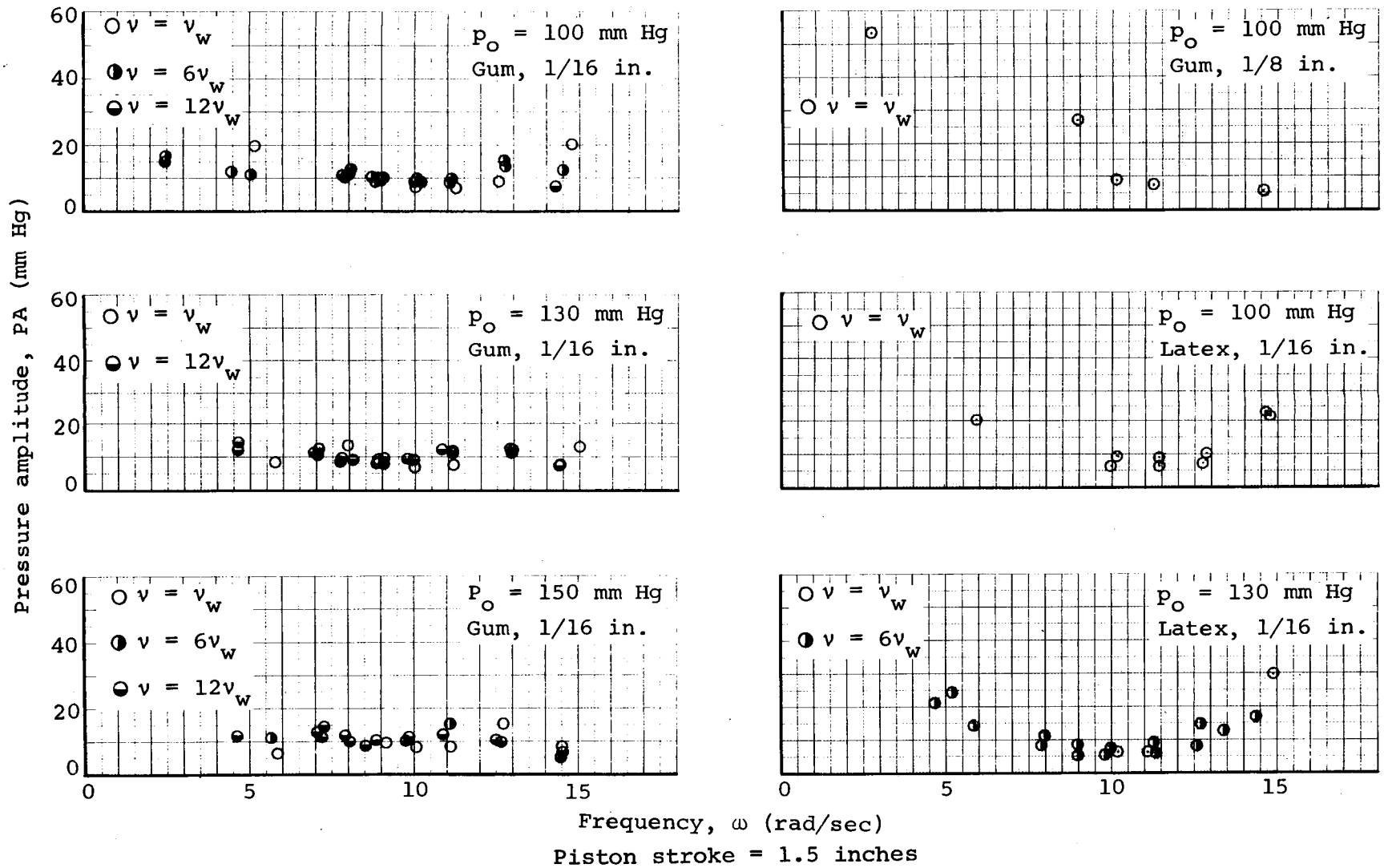

Figure 19.- Variation of pressure amplitude with frequency inside the simulated artery (Newtonian fluids).

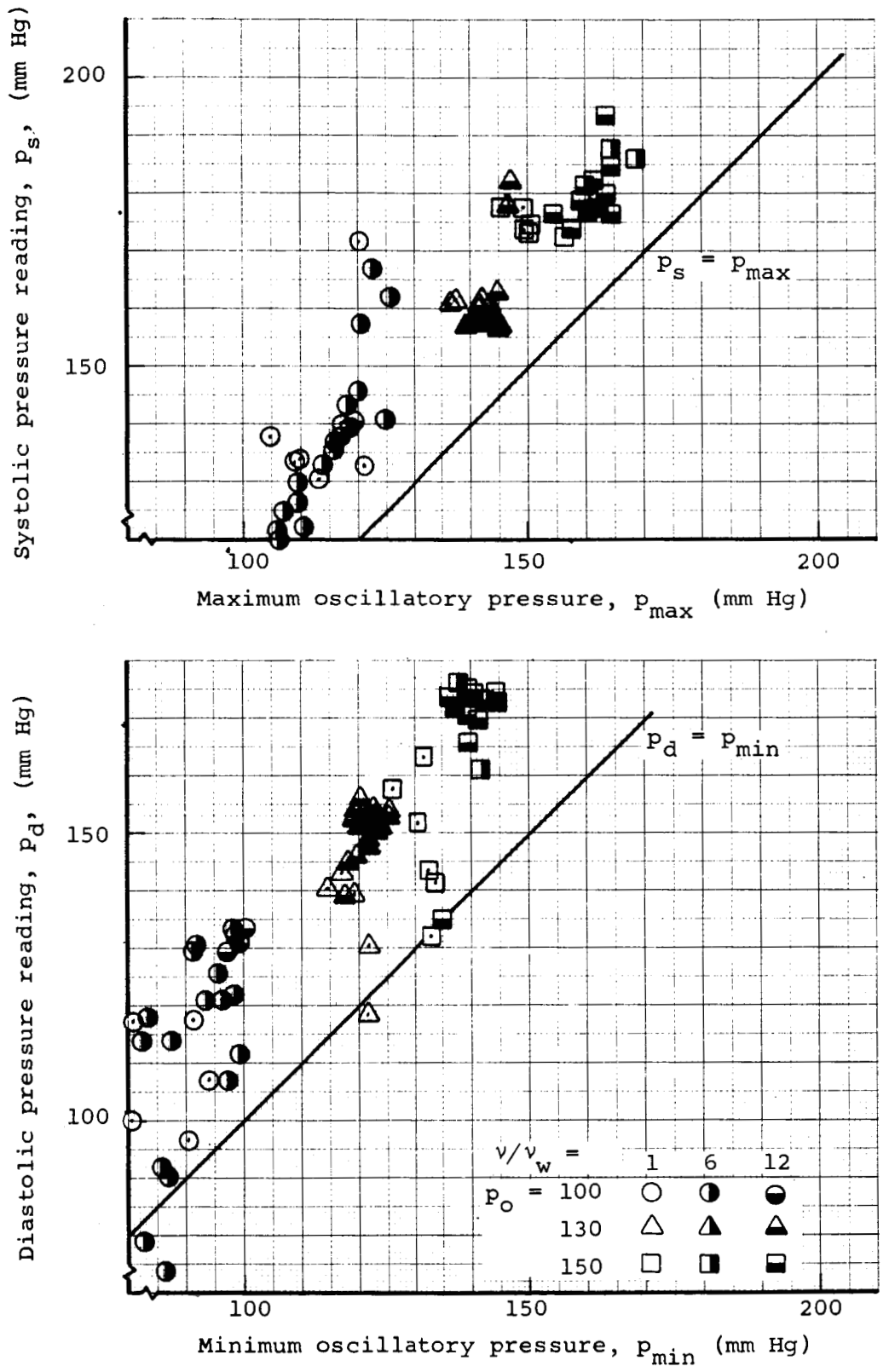

Figure 20.- Auscultatory versus direct pressure measurements for Newtonian fluids in 1/16-inch wall gum rubber tubing.

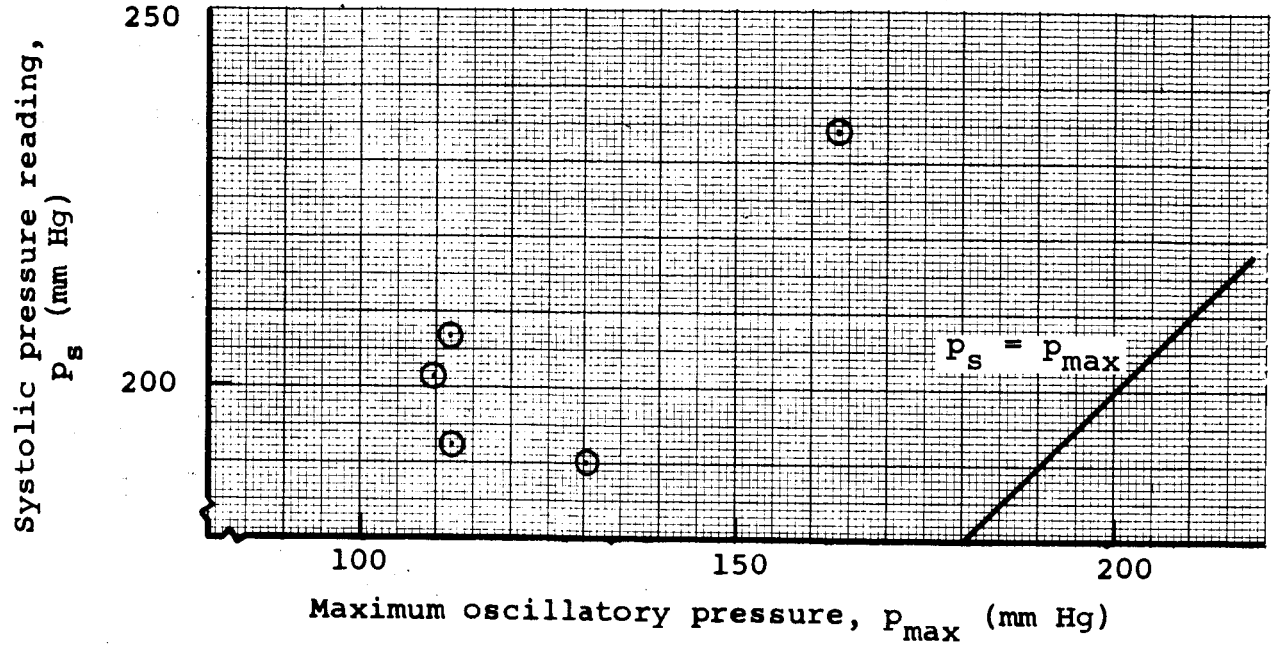

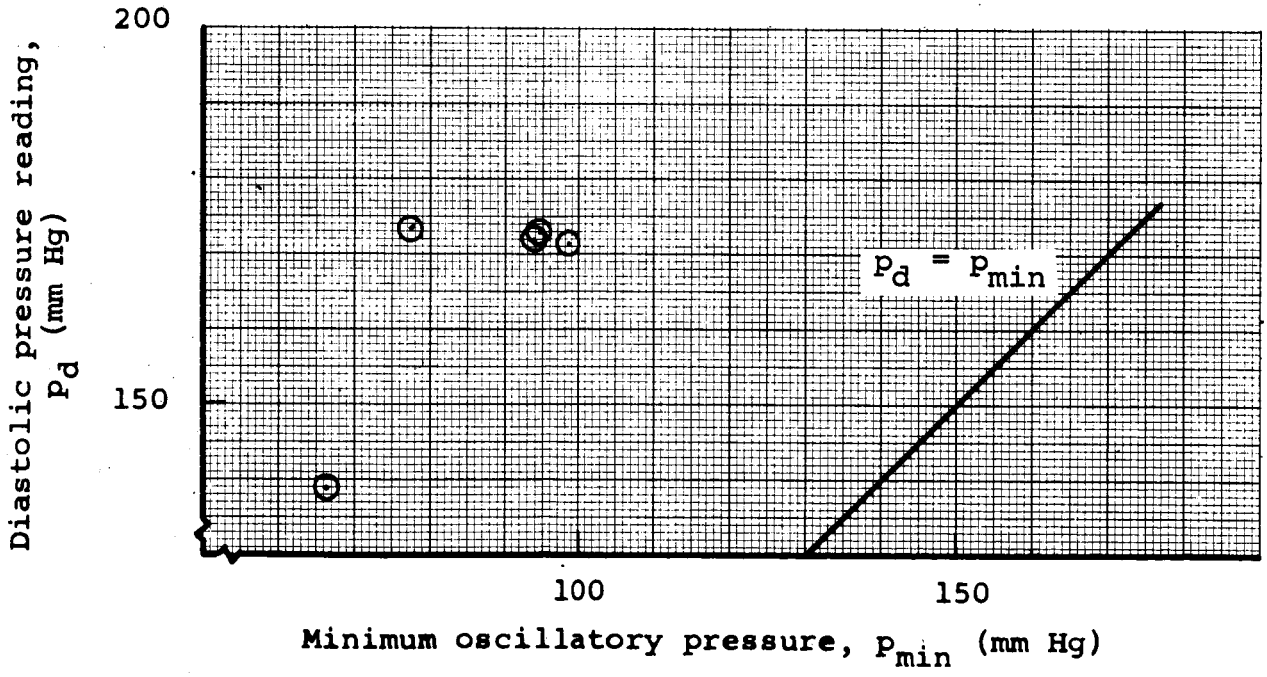

Figure 21.- Auscultatory versus direct pressure measurements for water in 1/8-inch wall gum rubber tubing (p_o = 100 mm H_2O).

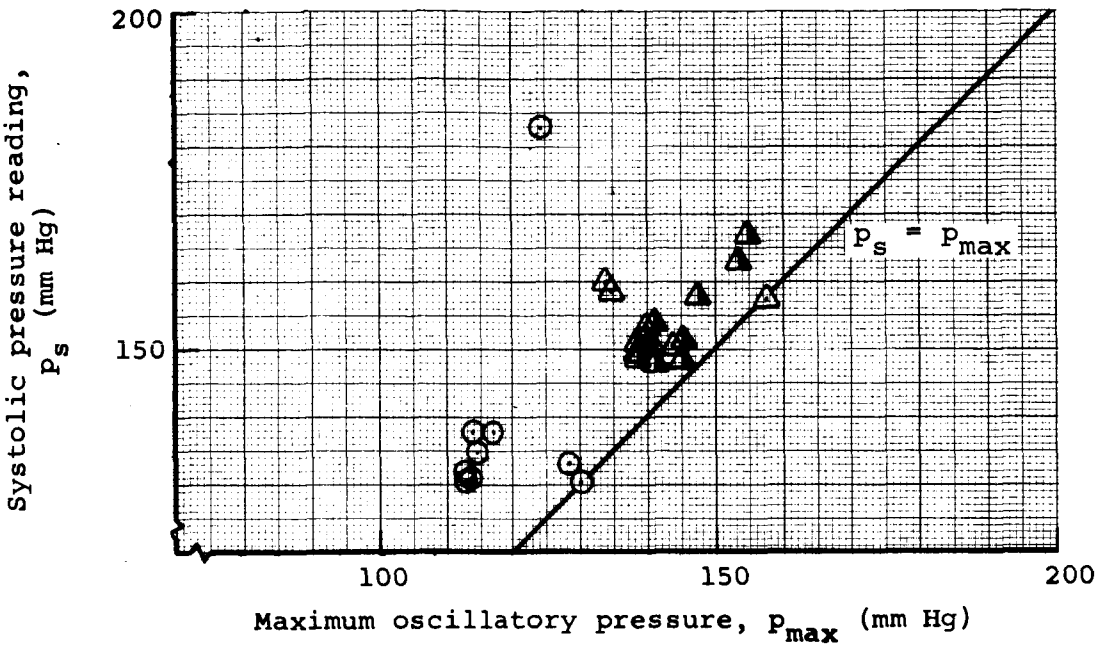

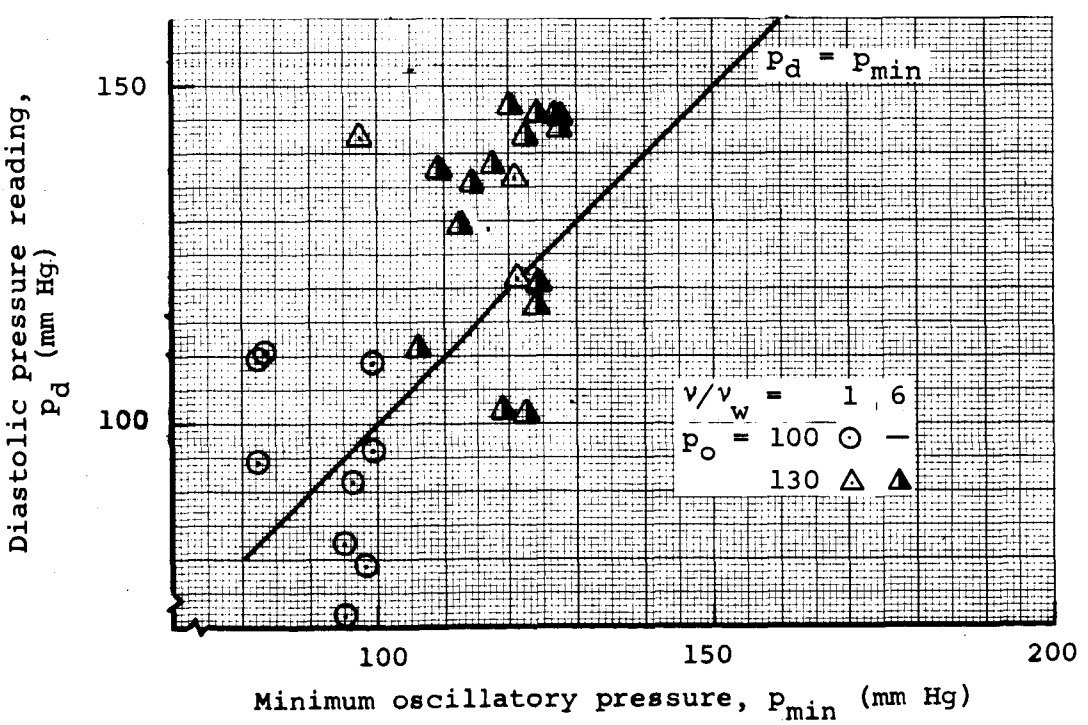

Figure 22.- Auscultatory versus direct pressure measurements for Newtonian fluids in 1/16-inch wall latex tubing.

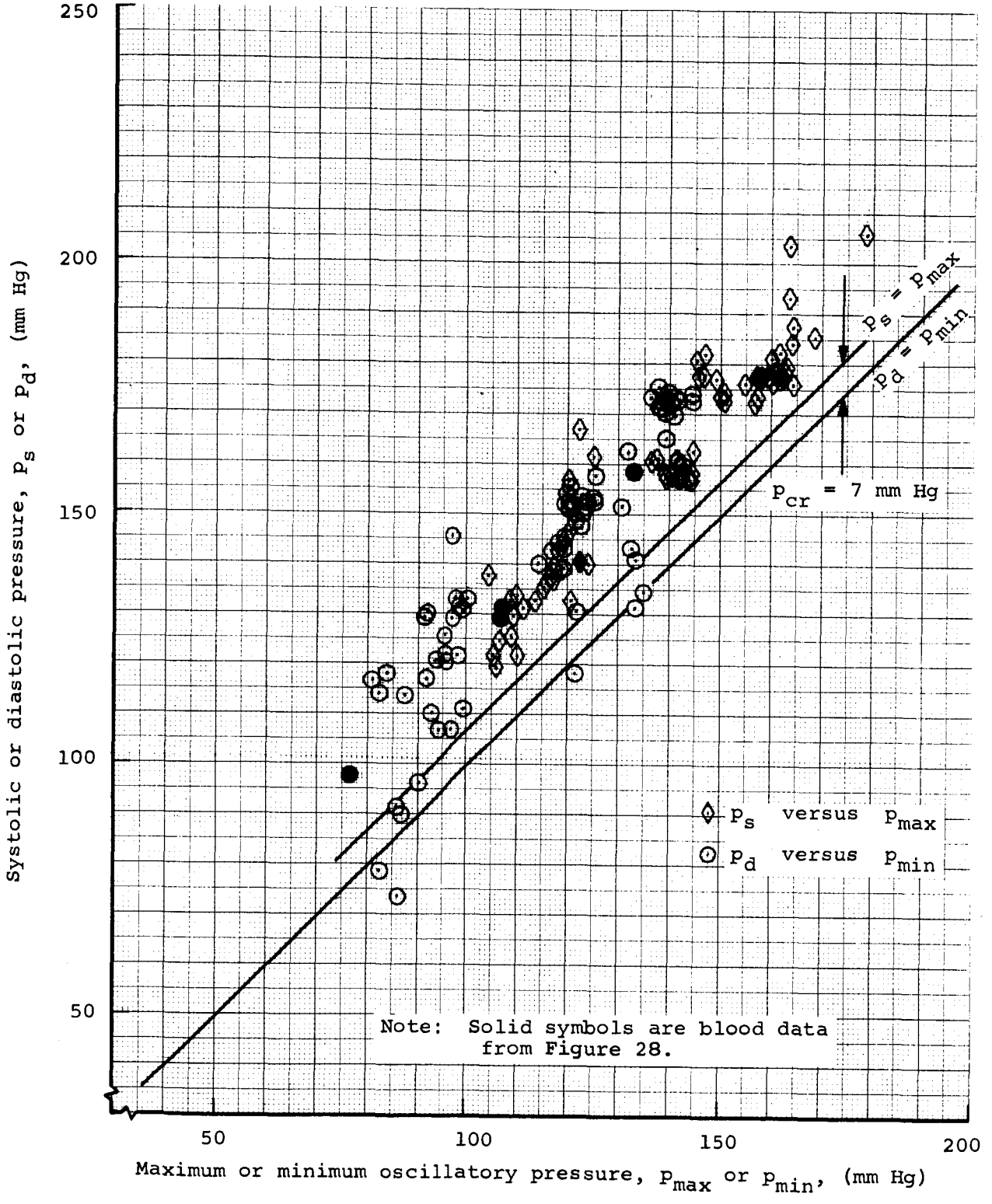

(a) 1/16-inch gum rubber tubing.

Figure 23.- Summary of auscultatory versus direct pressure measurements for Newtonian fluids in simulated arteries.

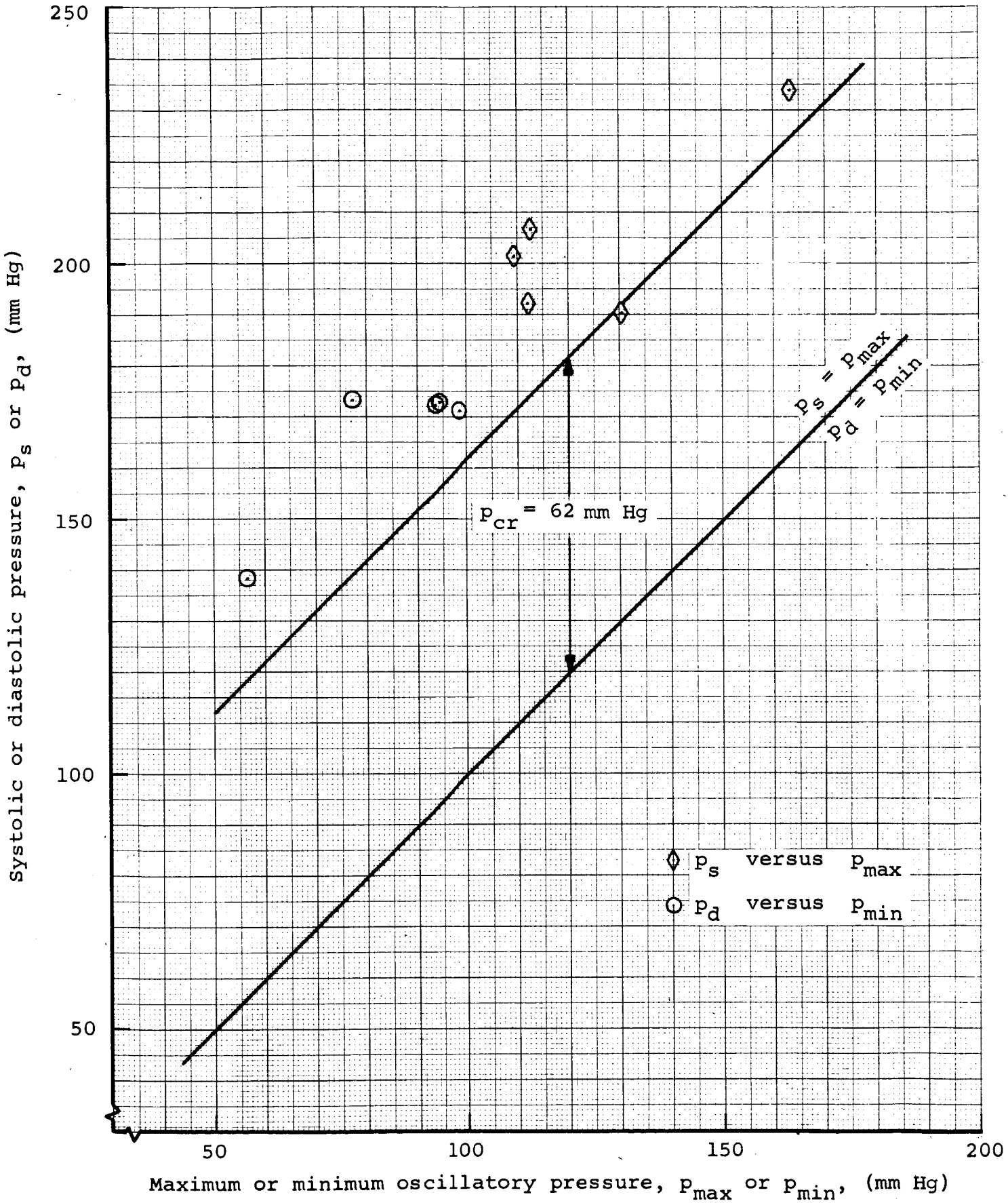

(b) 1/8-inch wall gum rubber tubing.

Figure 23.- Continued.

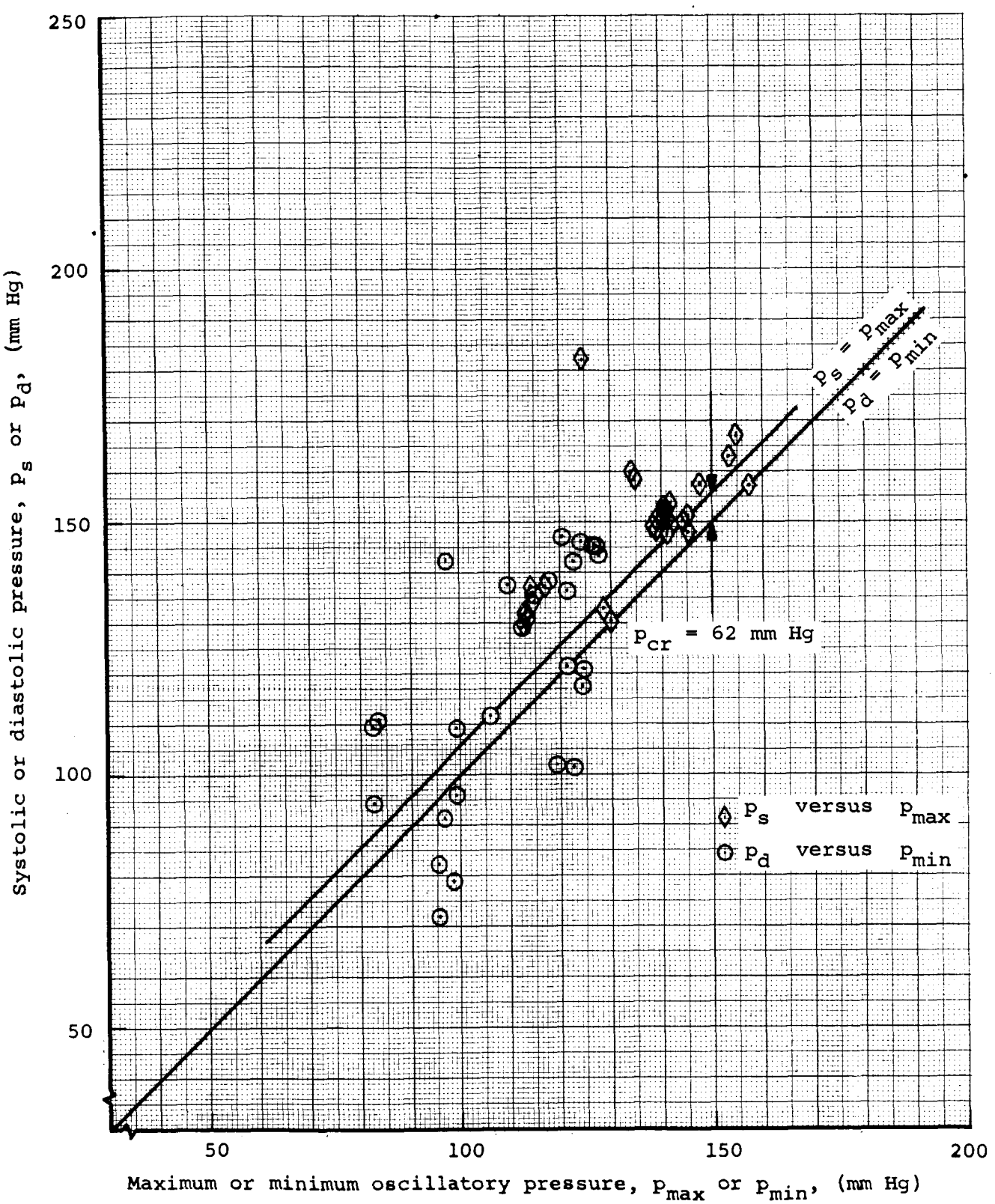

(c) 1/16-inch wall latex tubing.

Figure 23.- Concluded.

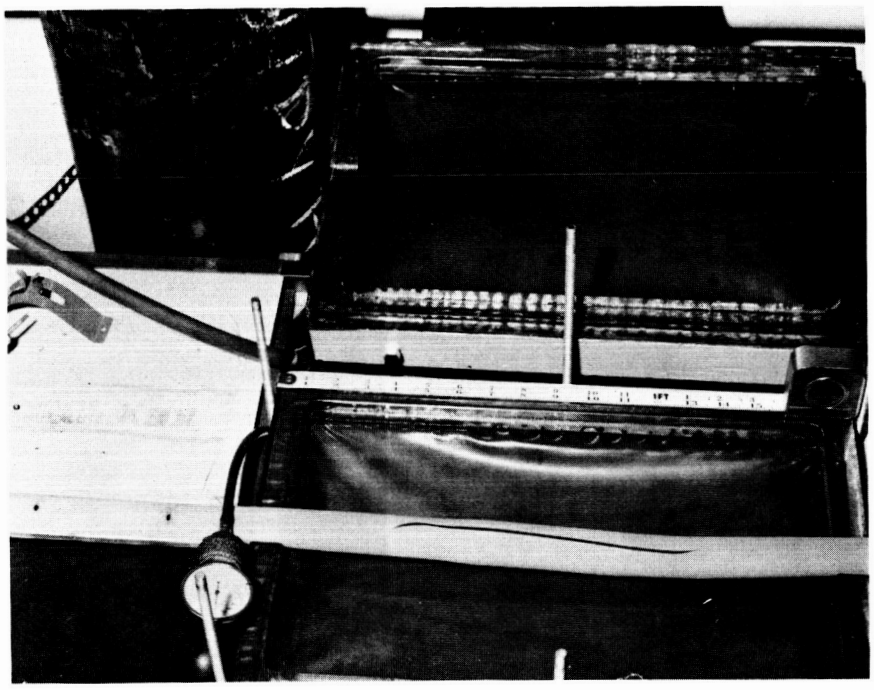

Figure 24.- 1/16-inch wall gum rubber tube showing longitudinal rupture.

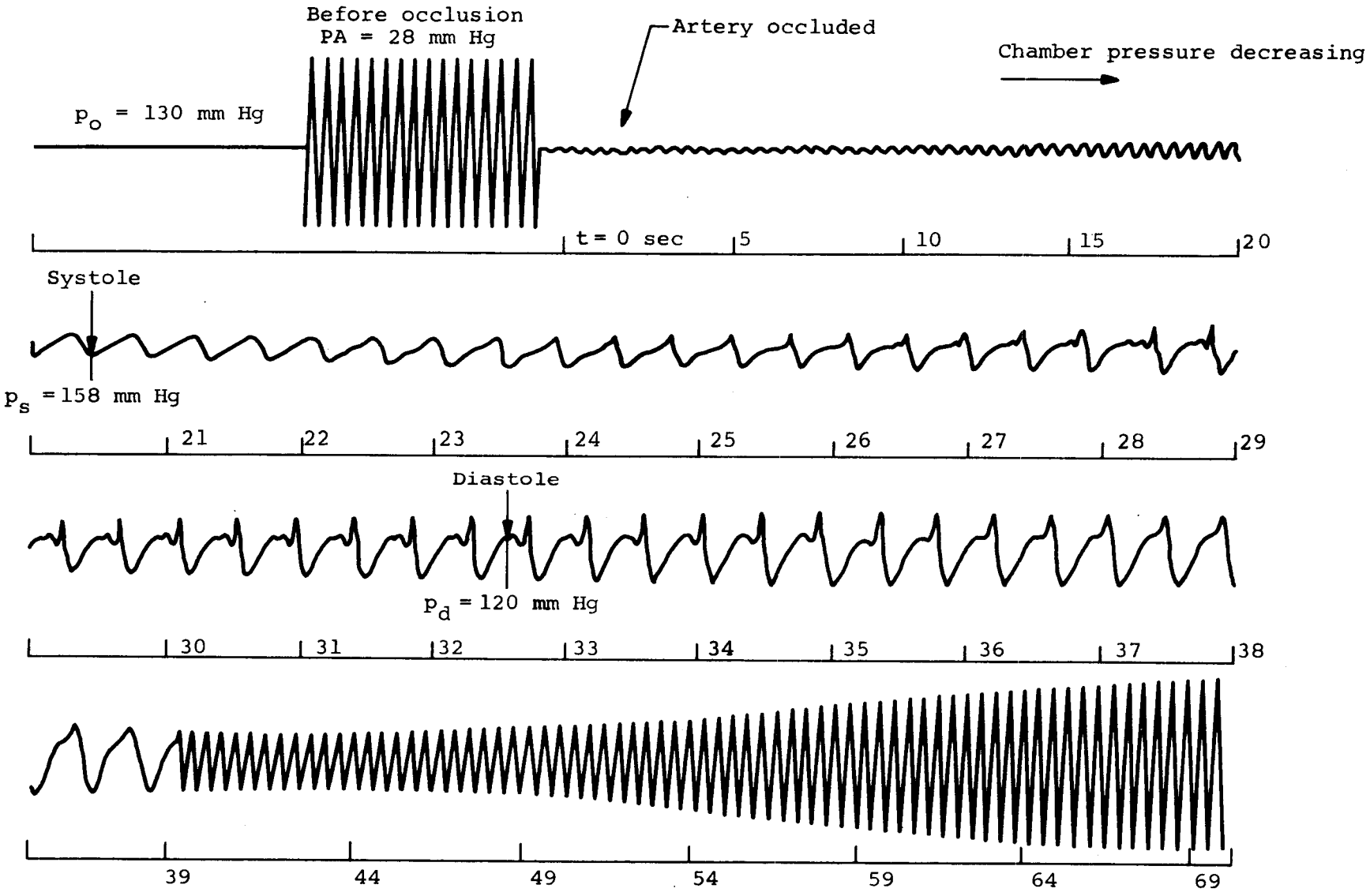

Figure 25.- Oscillograph record of static (lateral) pressure just distal to pressure chamber during decompression.

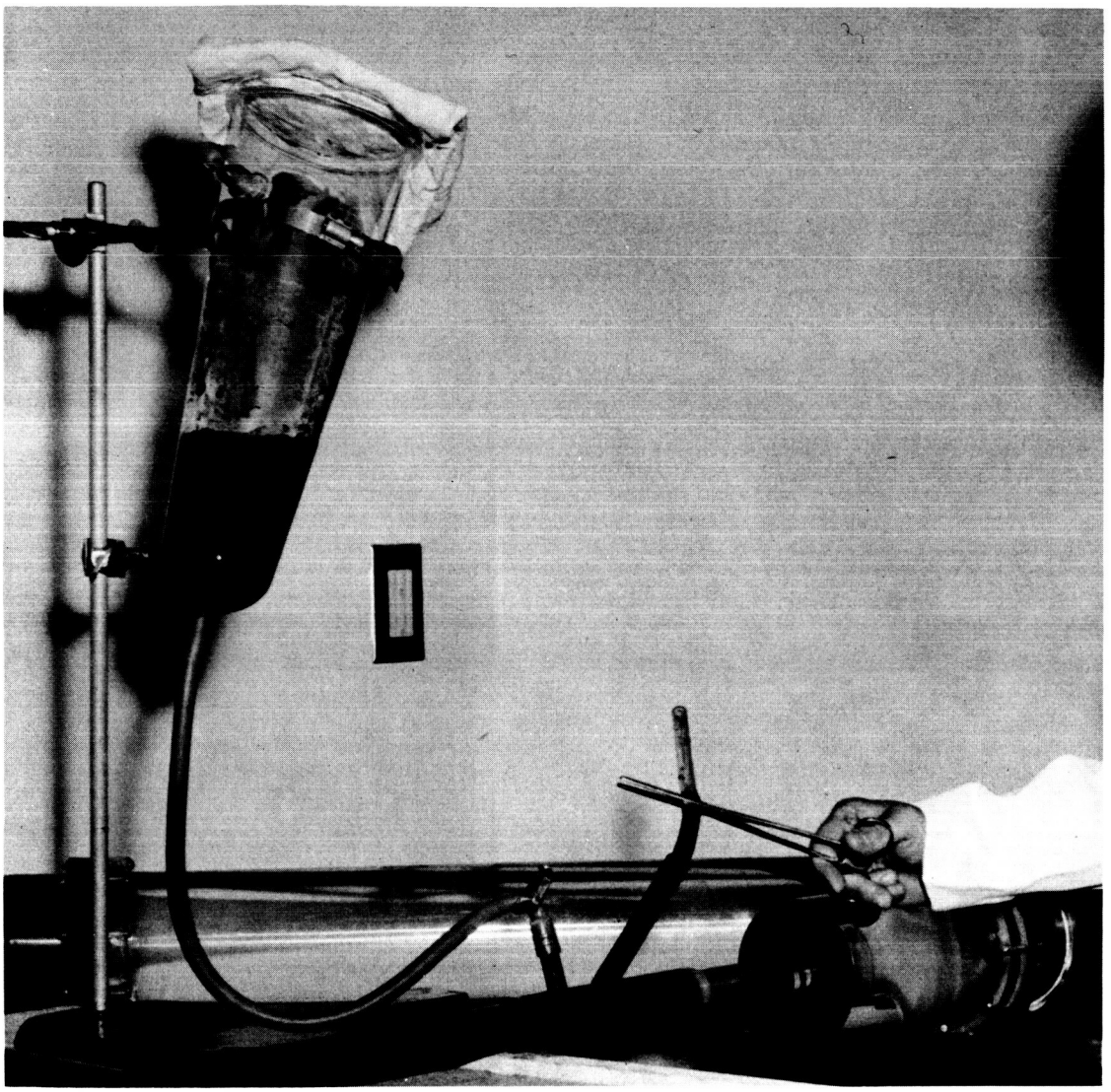

Figure 26.- Upstream end of 1-inch plastic tube showing blood inlet and balloon diaphragm.

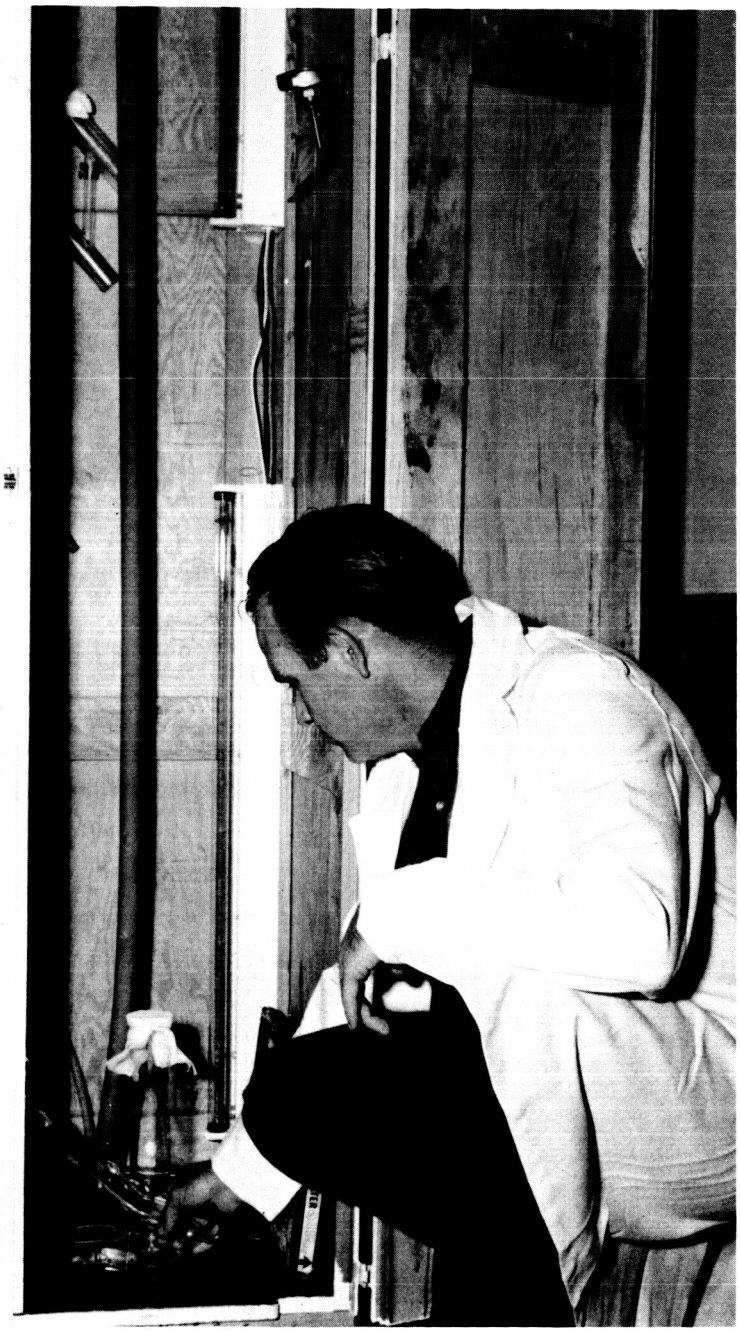

Figure 27.- Sterilization chamber.

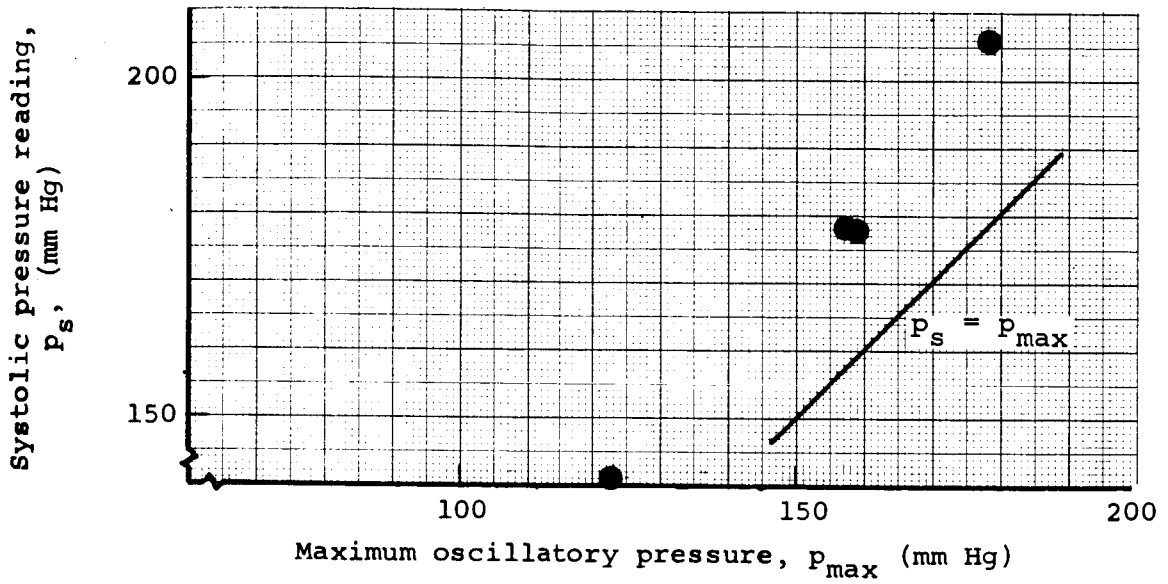

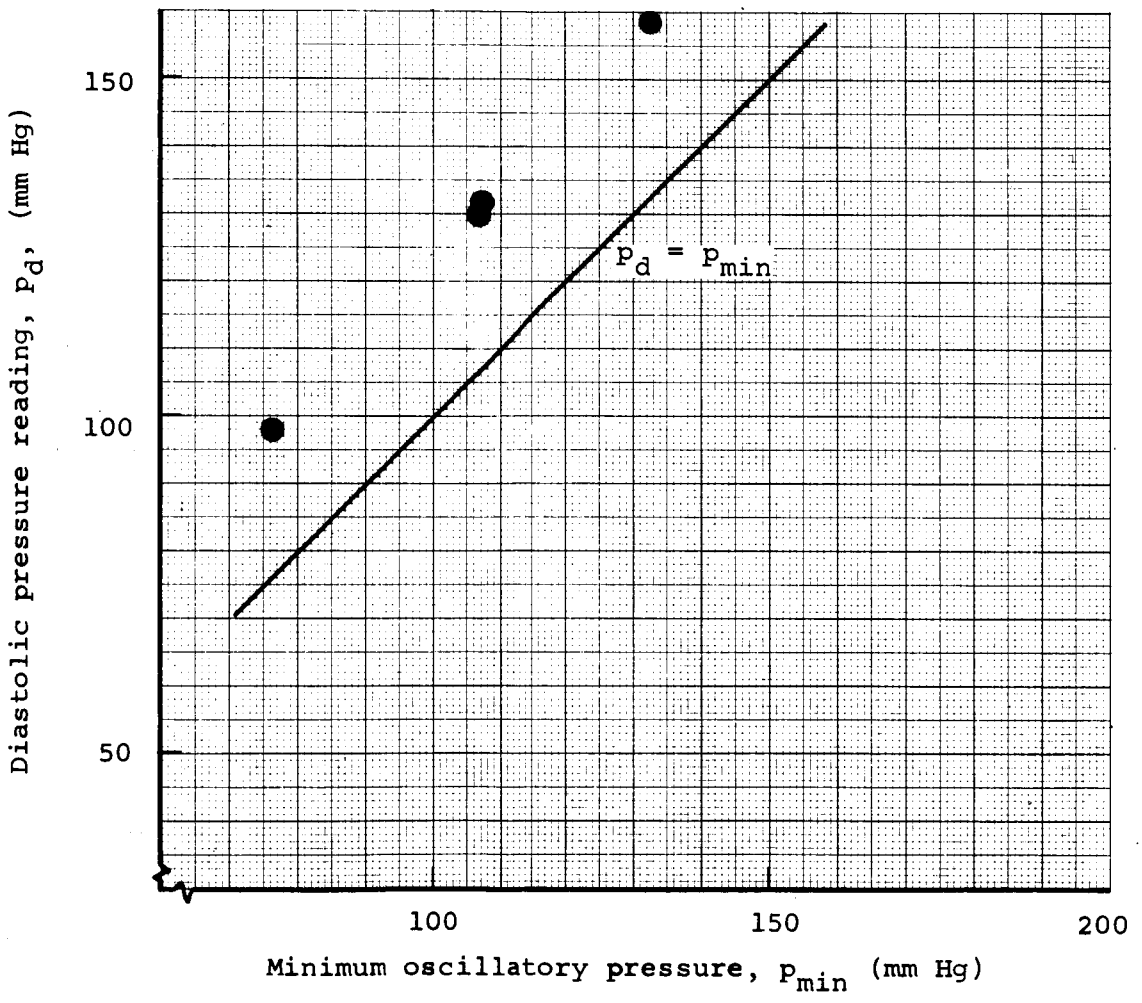

Figure 28.- Auscultatory versus direct pressure measurements for steer blood in 1/16-inch wall gum rubber tubing.

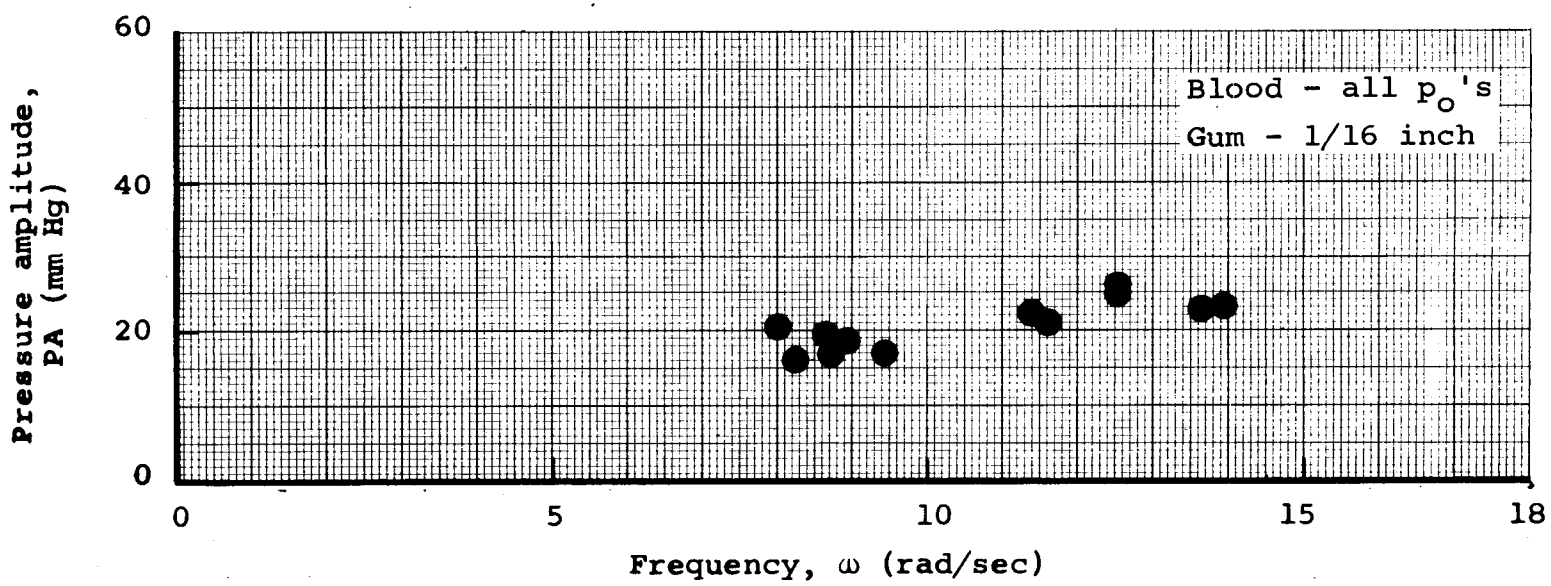

Figure 29.- Variation of pressure amplitude with frequency inside the simulated artery (steer blood).

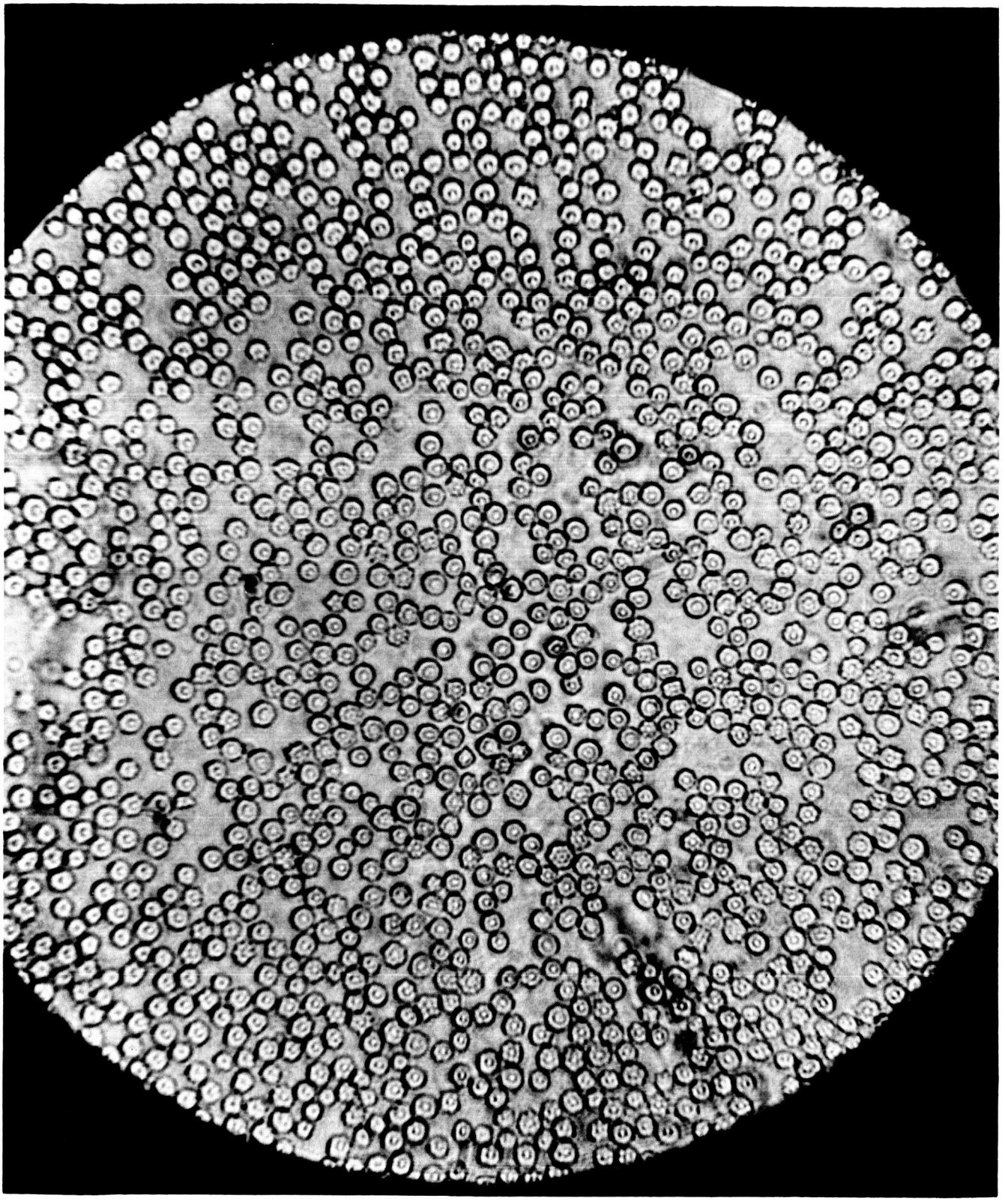

Figure 30.- Microphotograph of steer blood red cells (taken after use in tests). Magnification: 728 X

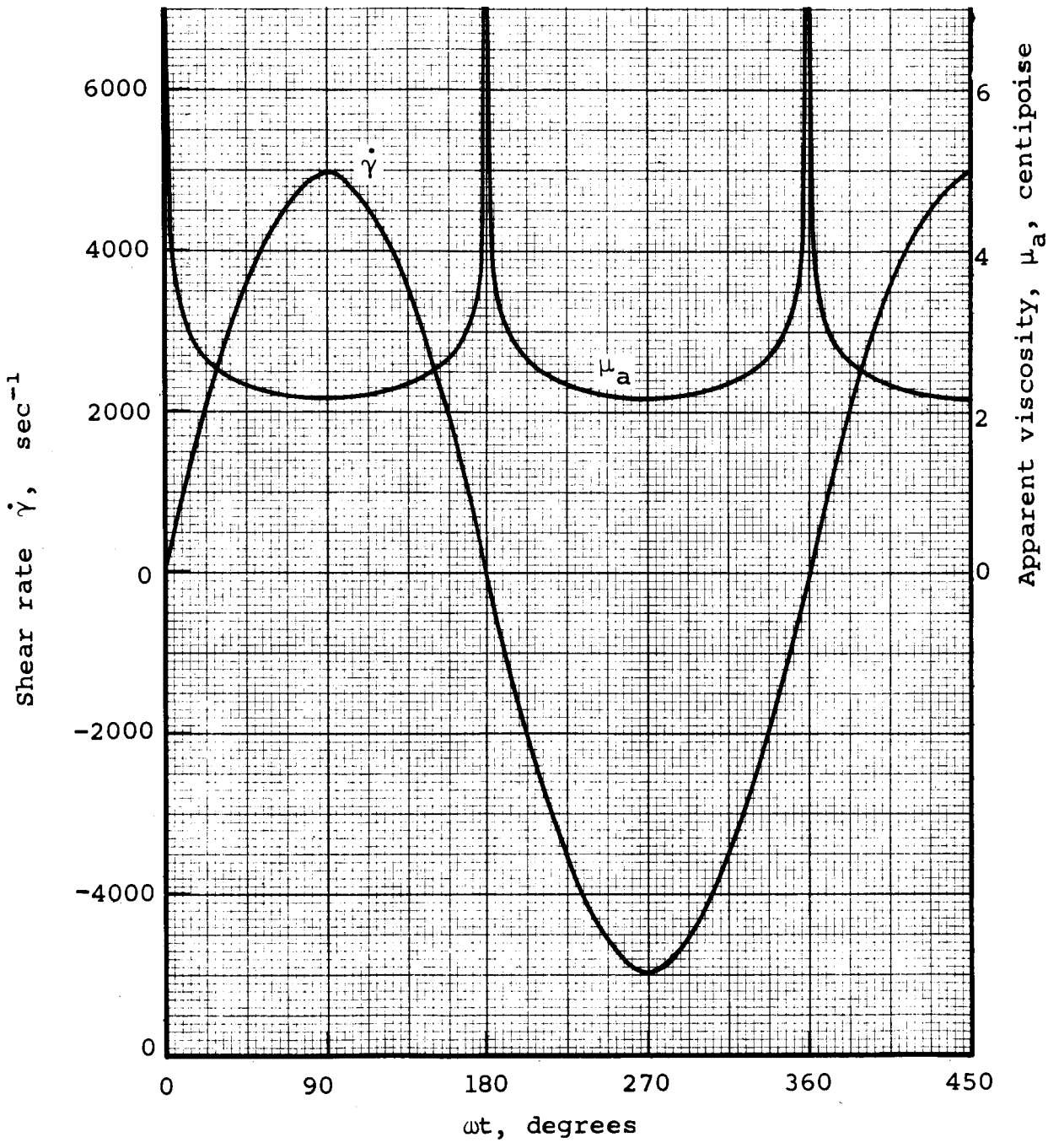

Figure 31.- Variation of viscosity for blood in oscillatory flow.

APPENDIX A

USE OF A CAPILLARY VISCOMETER AS A MEANS FOR DETERMINING VISCOSITY CHARACTERISTICS OF A PSEUDOPLASTIC FLUID

Wilkenson (Ref. 24) has shown that, for any fluid which satisfies the relation

$$\dot{\gamma} = f(\tau) \tag{A.1}$$

the steady-state flow rate Q in a capillary tube of radius R and length L is given by

$$\frac{Q}{\pi a^3} = \frac{1}{\tau_w^{\,3}} \int_0^{\tau_w} \tau^2 f(\tau)\, d\tau \tag{A.2}$$

Thus, the flow rate (Q) depends only upon the wall stress (τ_w), which is given by

$$\tau_w = \frac{a\Delta P}{2L} \tag{A.3}$$

where ΔP is the pressure loss over the length of the tube. Now, substituting the pseudoplastic equation

$$\dot{\gamma} = \left(\frac{\tau}{K}\right)^{1/n} \qquad n < 1 \tag{A.4}$$

into Equation (A.2) and integrating yields

$$\frac{Q}{\pi a^3} = \left(\frac{a\Delta P}{2L}\right)^{1/n} \frac{1}{K^{1/n}} \; \frac{n}{3n + 1} \tag{A.5}$$

or

$$\ln \frac{Q}{\pi a^3} = \frac{1}{n} \ln\left(\frac{a\Delta P}{2L}\right) + \ln\left[\frac{n}{(3n + 1)K^{1/n}}\right]$$

Therefore, a pseudoplastic fluid exhibits a linear relationship between the logarithms of $(Q/\pi a^3)$ and $(a\Delta P/2L)$, and the proportionality constant yields the pseudoplastic exponent n. One can now calculate the constant K from Equation (A.5) after determining the exponent n. Thus, the flow curve described by Equation (A.4) is completely determined.

If the pseudoplastic exponent is exactly equal to one (the value for a Newtonian fluid), then the constant K becomes the Newtonian coefficient of viscosity μ. Thus, Equation (A.5) yields the familiar Poisuelle equation

$$\mu = \pi \frac{(\Delta P/L)a^4}{8Q} \tag{A.6}$$